

**Centro de Investigación Científica y de Educación
Superior de Ensenada, Baja California**



**Doctorado en Ciencias
en Ecología Marina**

**$\delta^{15}\text{N}$ values of zooplankton groups to infer nitrogen sources in
the Gulf of Mexico's deep water zone**

Tesis

para cubrir parcialmente los requisitos necesarios para obtener el grado de
Doctor en Ciencias

Presenta:

Oscar Gabriel Hernández Sánchez

Ensenada, Baja California, México

2022

Tesis defendida por

Oscar Gabriel Hernández Sánchez

y aprobada por el siguiente comité

Dra. Sharon Zinah Herzka Llona
Co-directora de tesis

Dr. Víctor Froylan Camacho Ibar
Co-director de tesis

Dr. Juan Carlos Herguera Garcia

Dra. María Ana Fernández Álamo

Dr. Joao Marcos Azevedo Correia de Souza



Dr. Rafael Andrés Cabral Tena
Coordinador del posgrado en Ecología Marina

Dr. Pedro Negrete Regagnon
Director de Estudios de posgrado

Oscar Gabriel Hernández Sánchez © 2022

Queda prohibida la reproducción parcial o total de esta obra sin el permiso formal y explícito del autor y director de la tesis

Resumen de tesis que presenta Oscar Gabriel Hernández Sánchez como requisito parcial para obtención del grado de Doctor en Ciencias en Ecología Marina

Valores de $\delta^{15}\text{N}$ de distintos grupos del zooplancton para inferir fuentes de nitrógeno en la región de aguas profundas del Golfo de México

Resumen aprobado por

Dra. Sharon Zinah Herzka Llona

Co-directora de tesis

Dr. Víctor Froylan Camacho Ibar

Co-director de tesis

La fijación de N_2 es una fuente importante de N nuevo en aguas oligotróficas oceánicas, pero su contribución no ha sido cuantificada en el centro y sur del Golfo de México (GM), donde los remolinos de meso-escala anticiclónicos (ACE) y ciclónicos (CE) influyen en la disponibilidad de NO_3^- para el fitoplancton. Se investigó la variación temporal y espacial en los valores de $\delta^{15}\text{N}$ del zooplancton como un indicador de línea base las fuentes de nitrógeno y estimamos la contribución de la fijación y el nitrato sub-superficial a la producción secundaria. Además, se usaron *isoscapes* sinópticos de carbono y nitrógeno del zooplancton de todo el golfo de México como aproximación de la línea de base isotópica y las contribuciones regionales calculadas de las fuentes de N. Se recolectaron muestras de copépodos, eufáusidos y dos clases de tamaño de zooplancton de 0 a 200 m de profundidad durante cinco cruceros XIXIMI entre 2011 y 2016. Para los *isoscapes* sinópticos de todo el golfo, se tomaron muestras de zooplancton a 0-200 m de profundidad (si la profundidad lo permitió) durante el XIXIMI-06 y GOMECC-3 realizados durante el verano de 2017. Para estimar la contribución relativa de las posibles fuentes de nitrógeno, el golfo se dividió en seis regiones en función de la distribución espacial de la chl-a superficial, SST satelital y las posibles contribuciones de fuentes específicas de cada región: GM norte costero (NGMc), GM norte oceánico (NGMo), GM central (CGM), GM sur (SGM), Plataforma de Yucatán (YS) y región influenciada por la Corriente del Lazo (LC). Se utilizaron valores de composición isotópica de materia orgánica particulada (MOP) tomados de literatura para caracterizar los valores isotópicos de los *endmembers* específicos para cada región que se utilizaron para el modelo de mezcla de isótopos bayesiano. Los valores $\delta^{15}\text{N}$ de zooplancton fueron más altos durante el invierno debido a la profundización de la capa de mezcla impulsada por el viento, lo que refleja el transporte de NO_3^- hacia la superficie. Hubo una mayor contribución estimada de la fijación durante los meses de verano altamente estratificados. Los valores $\delta^{15}\text{N}$ del zooplancton dentro de ACE fueron significativamente más bajos comparados con CE, asociados con una profundización de la isopícnica 25.5 y una profundidad integrada más baja [NO_3^-]. La fijación contribuyó con el 60-80 % del N en los ACE. Algunas estaciones dentro de la Bahía de Campeche mostraron valores más altos de $\delta^{15}\text{N}$ debido al transporte de NO_3^- a la capa eufótica debido al CE semipermanente, surgencia regional y la descarga del río. Los resultados de los modelos de mezcla bayesianos indicaron que la fijación de nitrógeno es la más fuente importante (45-74 % de contribución) de nitrógeno nuevo en las regiones oceánicas del golfo (NGMo, CGM, CGM, LC) y YS, incluso considerando la entrada potencial de nitrato relativamente ligero que refleja la remineralización o excreción de nitrógeno ligero por heterótrofos. Los valores de $\delta^{15}\text{N}$ más altas se encontraron en el NGMc, asociadas principalmente a la contribución relativa de N desnitrificado (60%) y la escorrentías de los ríos Mississippi-Atchafalaya se asoció con valores relativamente altos de $\delta^{15}\text{N}$ que mostraron una contribución moderada (promedio de 17 %) solo para el NGMc, a pesar de que es la principal fuente de materia orgánica terrestre y nutrientes para el GM del norte. Mis resultados destacan la importancia del nitrógeno fijado en una extensa región del GM, especialmente en las aguas oligotróficas como la central y la región influenciada por LC.

Palabras clave: Mesozooplancton, Golfo de México, isótopos estables, fuentes de nitrógeno, remolinos de meso-escala.

Abstract of the thesis presented by Oscar Gabriel Hernández Sánchez as a partial requirement to obtain the Doctor of Science degree in Marine Ecology

$\delta^{15}\text{N}$ values of zooplankton groups to infer nitrogen sources in the Gulf of Mexico's deep water zone

Resumen aprobado por

Dra. Sharon Zinah Herzka Llona

Thesis co-advisor

Dr. Víctor Froylan Camacho Ibar

Thesis co-advisor

N_2 fixation is an important source of new N in oceanic oligotrophic waters, but its contribution has not been quantified in the central and southern Gulf of Mexico (GM), where mesoscale anticyclonic (ACE) and cyclonic eddies (CE) influence NO_3^- availability for phytoplankton. I investigated the temporal and spatial variation in zooplankton $\delta^{15}\text{N}$ values as a proxy for baseline nitrogen sources and estimated the contribution of N_2 fixation and subsurface nitrate to secondary production. Also, synoptic gulf-wide isoscapes of carbon and nitrogen in the Gulf of Mexico based on zooplankton were used as a proxy for the isotopic baseline and calculated regional contributions of N sources. Copepods, euphausiids, and two size classes of zooplankton were collected from 0-200 m during five XIXIMI cruises between 2011 and 2016. For the synoptic gulf-wide isoscapes, zooplankton were sampled at 0-200 m (depth permitting) during the XIXIMI-06 and GOMECC-3 cruises held during the summer 2017. To estimate the fractional contribution of potential nitrogen sources, the gulf was divided into six regions based on the spatial distribution of surface chl a, SST from remote sensing products and likely region-specific source contributions: coastal northern GM (NGMc), northern oceanic GM (NGMo), central GM (CGM), southern GM (SGM), Yucatan Shelf (YS) and region of influence of the Loop Current (LC). A literature survey of POM isotope ratios was used to characterize region-specific endpoint isotope ratios for use in a Bayesian isotope mixing model. Zooplankton $\delta^{15}\text{N}$ values were higher during winter due to wind-driven deepening of the mixed layer, reflecting NO_3^- transport toward the surface. There was a higher estimated contribution of N_2 fixation during the highly stratified summer months. Zooplankton $\delta^{15}\text{N}$ values from ACEs were significantly lower than in CE, associated with a deepening of the 25.5 isopycnal and lower depth-integrated $[\text{NO}_3^-]$. N_2 fixation contributed 60-80% of the N in ACEs. Some stations within the Bay of Campeche showed higher $\delta^{15}\text{N}$ values due to NO_3^- transport to the euphotic layer due to a semi-permanent CE, regional upwelling and river discharge. Regional differences in $\delta^{15}\text{N}$ values and the results of Bayesian mixing models indicated nitrogen fixation is an important source (45-74% contribution) of new nitrogen in the oceanic regions of the gulf (NGMo, CGM, CGM, LC), and YS, even considering the potential input of relatively light nitrate that reflects remineralization or excretion of light nitrogen by heterotrophs. The highest nitrogen isotope ratios were found in the NGMc, associated mainly by fractional denitrified N contribution (60%) and the inflow of the Mississippi-Atchafalaya river system was associated with relatively high $\delta^{15}\text{N}$ values showed moderate contribution (average 17%) only for the northern GM shelf, despite the fact is the major source of terrestrial organic matter and nutrients inputs to the northern GM. My results highlight the importance of fixed nitrogen over an extensive region of the GM, especially in the oligotrophic waters such as the central and the region influenced by Loop Current.

Key words: Mesozooplankton, Gulf of Mexico, stable isotopes, nitrogen sources, mesoscale eddies.

Dedication

Ésta tesis se te la dedico a ti papá y al Emilio favorito.

Acknowledgements

Al Centro de Investigación Científica y de Educación Superior de Ensenada (CICESE) y al posgrado en ecología marina por brindarme la oportunidad de realizar mi estudio doctoral y contribuir a mi formación profesional y académica. Además de proporcionarme financiamiento para terminar mi tesis doctoral.

Al Consejo Nacional de Ciencia y Tecnología (CONACYT) por el apoyo económico brindado para poder llevar a cabo esta tesis y mi estudio doctoral (CVU 405018).

Esta investigación ha sido financiada por el Fondo Sectorial CONACYT-SENER-Hidrocarburos, proyecto 201441. Esta es una contribución del Consorcio de Investigación del Golfo de México (CIGoM). Reconocemos a PEMEX por promover ante el Fondo la demanda específica sobre los derrames de hidrocarburos y el medio ambiente. Así mismo por brindarme financiamiento para terminar mi estudio doctoral.

A mis co-directores, la Dra. Sharon Herzka y el Dr. Víctor Camacho. Gracias por su apoyo incondicional en mi formación profesional y académica. Por enseñarme a trabajar duro y siempre dar lo mejor. Por enseñarme que siempre se puede mejorar. Por su soporte en los momentos duros, nunca lo voy a olvidar.

A los miembros de mi comité de tesis, la Dra. María Ana Fernández, al Dr. Joao Da Souza y al Dr. Juan Carlos Herguera que brindaron críticas que enriquecieron mi trabajo de tesis.

A la Dra. Leticia Barbero, de la Universidad de Miami quien fue jefe científico durante el crucero GOMECC-3 durante el cual se tomaron muestras de zooplancton y hacen parte de esta tesis.

Data reported in this work were partially collected under the auspices of the National Oceanic and Atmospheric Administration (NOAA)'s Ocean Acidification Program (OAP). We are grateful to the government of the United Mexican States for fishing licenses and research permission allowing us to conduct our research within their Exclusive Economic Zones during the GOMECC-3 cruise (PPFE/DGOPA-137/17, EG0082017).

A la tripulación que participaron durante los cruceros XIXIMIs a bordo del buque oceanográfico Justo Sierra y que ayudaron en la colecta de muestras que se utilizaron para el desarrollo de esta tesis.

Al personal administrativo de CICESE, en especial a Yadira Palma, Pilar Ensaldo, gracias por todo el apoyo realizado durante mi estancia doctoral.

Gracias a la M. en C. Carmen Rodríguez, técnica del laboratorio de ecología pesquera, por todo su apoyo durante estos años durante mis años como estudiante de doctorado.

A Reyna y Meliza por su ayuda con el procesado de muestras para análisis isotópico.

A Rigel Zaragoza por su apoyo durante la construcción de los mapas isotópicos.

A los integrantes del laboratorio de Ecología Pesquera I y II que me tocó convivir y seguimos conviviendo. Al Dr. Oscar Sosa por aceptarme y hacerme parte de su laboratorio. Masao, Luz, Emiliano, Zuri, Gonzalo, Kena, Jesús, Laurita, Reyna, Aurora, Ricardo, Gina, Meliza, Daniel, Mily, Elea, Frida, Christian, Salomé y Felipe, por su apoyo, por sus consejos, soporte moral.

Al Laboratorio CiNeMa del IIO. A Mari Carmen, Augusto, Cristian, Erika, Guillermo, Jorge, René, Jennifer, Paulina, Paula. Gracias por sus comentarios y retroalimentación durante nuestras reuniones maratónicas.

A mi familia. A Gricelda, que siempre estuvo apoyando incondicionalmente todos estos años. Por su amor y cariño siempre. Por sus regaños y llamadas de atención que me hicieron mejorar. Gracias mamá. A mis hermanos, Gabriela y Abel por siempre darme fortaleza y decir las palabras necesarias para seguir adelante a pesar de las dificultades. A mi mamá Magui y papá Tito, por su inmenso amor y sus sabios consejos. A mi tía Claudia y tío Jorge, por apoyarme y siempre estar al pendiente de mí.

A mi familia en Ensenada, Gera, Caro, Ana Luisa, Rafa. Por soportarme en mis malos ratos y por estar ahí en los momentos más difíciles pero sobre todo hacer que estos años fueran muy felices. Mil gracias.

A Erika, mi novia, por su apoyo a pesar de las dificultades y hacerme muy feliz estos últimos años.

A los pelicarrones, a los miembros que están y los que estuvieron. Por esas tarde de futbol, risas, enojos y pláticas únicas.

Table of content

Abstract in Spanish	iii
Anstract in English	iv
Dedication.....	v
Acknowledgements	vi
Figure list	x
Table list	xiv
Chapter 1. General introduction.....	1
1.1 Background	1
1.2 Justification	3
1.3 Objectives	3
1.3.1 General objective	3
1.3.2 Specific objetives.....	3
Chapter 2. Nitrogen sources (NO_3^- vs N_2 fixation) inferred from bulk $\delta^{15}\text{N}$ values of zooplankton from the deep water region of the Gulf of Mexico	5
2.1 Introduction	5
2.2 Methods	8
2.2.1 Study Area	8
2.2.2 Zooplankton sampling and isotope analysis	9
2.2.3 Hydrography and nutrient concentrations	11
2.2.4 Station classification based on mesoscale structures	13
2.2.5 Data Analysis.....	13
2.2.6 Two-source isotope mixing model	14
2.3 Results.....	15
2.3.1 Variability in isotopic composition.....	15
2.3.2 Oceanographic conditions	16
2.3.3 Isotopic composition of zooplankton and mesoscale eddies.....	17
2.3.4 Regional distribution of isotopic values.....	18
2.3.5 PC Analysis	19
2.3.6 Bayesian mixing models	20
2.4 Discussion.....	22

2.4.1	Temporal variability in zooplankton	22
2.4.2	Mechanisms for the incorporation of light nitrogen into lower trophic level consumers ...	23
2.4.3	Comparison of $\delta^{15}\text{N}$ values of copepods and euphausiids and size fractions.....	26
2.4.4	Isotopic composition of zooplankton relative to mesoscale eddies	28
2.4.5	Regional patterns in the isotopic composition of zooplankton	29
Chapter 3. A Gulf-wide synoptic isoscape of zooplankton isotopes ratios reflects regional nitrogen sources in the Gulf of Mexico		31
3.1	Introduction	31
3.2	Methods	35
3.2.1	Nitrogen and carbon sources in the Gulf of Mexico basin	35
3.2.2	Oceanographic surveys	36
3.2.3	Isoscapes.	37
3.2.4	Regionalization of the Gulf of Mexico.....	38
3.2.5	Data analysis	39
3.2.6	Application of Bayesian mixing models	40
3.2.7	Effect of the variation of the nitrate isotope composition on source contributions estimates.....	40
3.3	Results	41
3.3.1	Zooplankton, particulate organic matter isotope ratios and isoscapes	41
3.3.2	Bayesian mixing model	45
3.3.3	Effect of variations in $\delta^{15}\text{N-NO}_3$ in N source contribution calculations	48
3.4	Discussion.....	49
3.4.1	Regional patterns in zooplankton isoscapes.....	49
3.4.2	Regional source contributions	50
3.4.3	Variation in $\delta^{15}\text{N-NO}_3$	55
Chapter 4. General conclusions		60
Literature cited.....		62
Supplementary material		77

Figure list

Figure	Page
1	10
2	13
3	14
4	16
5	

1 Study region in the Gulf of Mexico. Schematic diagram of the main regions and mesoscale features that dominate the central and southern Gulf of Mexico. The black line marks the limit between the central and southern regions. The thick red lines indicate the Loop Current with various levels of intrusion into the gulf. Red and blue circles represent anticyclonic and cyclonic eddies, respectively. The black dotted arrow indicate the main pathway of Loop Current Eddie (LCEs). Grey thin lines are the 200 and 1000 m isobaths. Fixed stations for zooplankton and NO₃⁻ concentration sampling and CTD casts covered during the XIXIMI cruises are indicated by black dots. All stations are at depths > 1000m, except for some in the Yucatan Channel.....

2 SSHA (a,d,g) and nitrogen isotopic composition of nitrogen of copepods (b, e, h) and euphausiids (c, f, i) during XIXIMI-01 (a, b, c), XIXIMI-02 (d, e, f) and XIXIMI-03 (g, h, i). Red diamonds, blue circles and white stars represent stations influenced by anticyclonic, cyclonic and non-eddy structures, respectively. For XIXIMI-01, the stations were not classified to mesoscale eddies because the CTD malfunction did not allow for estimates of the depth of the 25.5 kg/m⁻³ isopycnal. Arrows represent geostrophic velocities. Numbers identify Loop Current eddies named by the Horizon Marine Group (www.horizonmarine.com): 1) Franklin, 2) Jumbo, 3) Icarus/Jumbo remnants.....

3 SSHA (a,d) and nitrogen isotopic composition of nitrogen of small (b, e) and large zooplankton fractions (c, f) during XIXIMI-04 (a, b, c) and XIXIMI-05 (d, e, f). Red diamonds, blue circles and white star symbols represent the ACE, CE and NE stations, respectively. Arrows represent geostrophic velocities. Numbers identify Loop Current eddies based on the nomenclature of the Horizon Marine Group (www.horizonmarine.com): 4) Nautilus remnant, 5) Olympus, 6) Olympus remnant, 7) Poseidon.....

4 Mean ± standard deviation (SD) of δ¹⁵N values of copepods and euphausiids and small (<1000 μm) and large (1000-2000 μm) size fractions of zooplankton caught during five cruises covering the deepwater region of the Gulf of Mexico. Significant differences between cruises (2-way ANOVA p-values < 0.05) are indicated by different letters (a,b). Significant interaction of δ¹⁵N values of copepods as function of mesoscale eddies and cruises, for more details, see Table 10.....

5 Mean ± standard deviation (SD) δ¹⁵N values of copepods and euphausiids (XIXIMI-02 and -03) and the small (<1000 μm) and large (1000-2000 μm) size fractions of zooplankton (XIXIMI-04 and -05) caught within anticyclonic eddies, cyclonic eddies, or outside of eddies in the deep water region of the Gulf of Mexico. Significant

	differences between mean values for each group (2-way ANOVAs P-values < 0.05) are indicated by different letters (a,b,c). Significant interaction of $\delta^{15}\text{N}$ values of copepods as function of mesoscale eddies and cruises, for more details, see Table 10.....	17
6	Mean \pm standard deviation (SD) $\delta^{15}\text{N}$ values of copepods and euphausiids (XIXIMI-02 and 03) and the small (<1000 μm) and large (1000-2000 μm) size fractions of zooplankton (XIXIMI-04 and 05) caught in the central Gulf of Mexico and Campeche Bay. Significant differences between regions for each group and cruise were evaluated with one-way ANOVAs. P-values < 0.05 are indicated with different letters (a,b). For more details, see text results.....	18
7	Principal component analysis of environmental variables and nitrogen isotope ratios of zooplankton. Biplot of the first two components (PC1 and PC2) show the sampling stations covered in XIXIMI-02 and -03 (left panel) and XIXIMI-04 and -05 (right panel). Circles indicate XIXIMI-02 (left) and XIXIMI-04 (right) and triangles indicate XIXIMI-03 (left) and XIXIMI-05 (right). For environmental and isotopic variables see table 1. Color red, blue and yellow indicate the categories of mesoscale structures ("ACE" anticyclonic eddies, "CE" cyclonic eddies and "NE" no eddies stations, respectively).....	20
8	Results (means \pm SD) of the Bayesian isotope mixing model estimating the contribution of N_2 fixation and NO_3^- to zooplankton. Estimates are based on the mean $\delta^{15}\text{N}$ values of copepods (left panel) and small zooplankton fraction (<1000 μm right panel). ACE: anticyclonic eddies; CE: cyclonic eddies, NE: non-eddies.....	21
9	Results (means \pm SD) of the Bayesian isotope mixing model estimating the contribution of N_2 fixation and NO_3^- to zooplankton collected at stations in Campeche Bay (CB) and the central Gulf of Mexico. Estimates are based on the $\delta^{15}\text{N}$ values of copepods (left panel) and small size fraction (<1000 μm) of zooplankton (right panel).....	22
10	Zooplankton sampling stations in the Gulf of Mexico during the XIXIMI-06 (X6) and GOMECC-03 (G3) cruises held during the summer of 2017. The six regions considered for which fractional contributions of different N sources were calculated are depicted.....	33
11	$\delta^{13}\text{C}$ and $\delta^{15}\text{N}$ isoscapes of zooplankton < 1000 μm sampled in the Gulf of Mexico during the summer of 2017. Dots indicate sampling stations. Maps adapted from Le-Alvarado et al. (2021).....	43
12	$\delta^{13}\text{C}$ and $\delta^{15}\text{N}$ isoscapes of surface layer POM sampled in the Gulf of Mexico during the XIXIMI-06 cruise during the summer of 2017. Dots indicate sampling stations.....	44

13	Correlation analysis between $\delta^{15}\text{N}$ -POM and $\delta^{15}\text{N}$ values of zooplankton (top) and nitrate concentration integrated between 0-200 m at XIXIMI-06 stations (bottom). Grey areas indicate confidence interval.....	46
14	Percent contribution of (A) N_2 fixation, (B) nitrate, (C) Mississippi-Atchafalaya River System "MARS", (D) denitrification, (E) Western Florida shelf "WFS" and (F) Grijalva-Usumacinta System "GUS" for different regions of in the Gulf of Mexico. Black dotted lines represent the isolines of fractional contributions and numbers show the percent contribution. White areas indicate a particular source was not considered important in the region and was thereby not included in isotope mixing models.....	47
15	Percent contribution of N sources calculated by varying the isotopic composition of nitrate. (A) Scenario 1: $\delta^{15}\text{N}\text{-NO}_3 = 4.0 \pm 0.3\text{‰}$ of subsurface waters for the western Atlantic, (B) Scenario 2: $\delta^{15}\text{N}\text{-NO}_3 = 3.5 \pm 1.1\text{‰}$ from Howe et al. (2020), (C) Scenario 3: $\delta^{15}\text{N}\text{-NO}_3 = 1.9 \pm 0.8\text{‰}$ from Holl et al. (2007). NGMc: Coastal Northern Gulf of Mexico; NGMo: Oceanic Northern Gulf of Mexico; CGM: Central Gulf of Mexico; SGM: Southern Gulf of Mexico, LC: Loop Current region; YS: Yucatan Shelf.....	48
16	Schematic of the isotopic composition of nitrate, dissolved inorganic nitrogen (DIN), phytoplankton, and zooplankton based on measurement of $\delta^{15}\text{N}\text{-NO}_3$ values within different regions of Gulf of Mexico. The $\delta^{15}\text{N}\text{-NO}_3$ values of 3.5‰ reported by Howe et al. (2020) for the northern Gulf of Mexico (A, B, C), and $\delta^{15}\text{N}\text{-NO}_3$ values of 2.0‰ reported by Holl et al. (2007) for the northwestern Gulf of Mexico(D, E, F). Scenarios when the subsurface nitrate is the major N source (A, D), scenarios when the subsurface nitrate fluxes are limited or absent (B, E), and scenarios with isotopic composition of particulate organic matter (phytoplankton) measured in this study (C, F). Arrows represent only flux direction.....	58
17	Sampling stations for zooplankton, NO_3^- concentration sampling and CTD cast are indicated by black dots. A) XIXIMI-01, November 2010; B) XIXIMI-02, July 2011; C) XIXIMI-03, Feb-Mar 2013; D) XIXIMI-04, August 2015; E) XIXIMI-05, July 2016. CTD data was no available for XIXIMI-01 due to equipment malfunction. All stations are at depths > 1000m, except for some in the Yucatan Channel.....	77
18	Pearson's correlation between the isotopic composition (in ‰) of copepods and euphausiids for XIXIMI-01, -02 and -03.....	78
19	Pearson's correlation between isotopic composition (in ‰) of small and large fraction for XIXIMI-04 and -05.....	78

20 SSHA for August 2017. The red circles and blue diamonds represents the GOMECC-3 and XIXIMI-06 station samples, respectively. Black line represents 200 m isobath. Arrows represent geostrophic velocities..... 79

Table list

Table	Page
1 Results of principal components analysis on a correlation matrix of environmental variables. Variables are sorted in order of decreasing correlations of the variables with PC1.....	21
2 Mean \pm SD carbon and nitrogen isotope ratios of source POM used as endpoints in isotope mixing models. The likely sources used to estimate source contributions varied regionally and are represented by X. NGMc: Coastal Northern Gulf of Mexico; NGMo: Oceanic Northern Gulf of Mexico; CGM: Central Gulf of Mexico; SGM: Southern Gulf of Mexico, LC: Loop Current region; YS: Yucatan Straight.....	39
3 Mean \pm SD carbon and nitrogen stable isotope ratios of zooplankton collected in six regions of the Gulf of Mexico during the summer of 2017.....	41
4 Wilcoxon signed-rank test post-hoc pairwise comparisons of the isotopic composition of zooplankton collected in different regions of the Gulf of Mexico. $\delta^{13}\text{C}$ in lower left and $\delta^{15}\text{N}$ in (upper right). Bold indicates significant differences. NGMc: Coastal Northern Gulf of Mexico; NGMo: Oceanic Northern Gulf of Mexico; CGM: Central Gulf of Mexico; SGM: Southern Gulf of Mexico, LC: Loop Current region; YS: Yucatan Shelf...	42
5 Dinitrogen fixation rates in oligotrophic waters and Gulf of Mexico.....	44
6 Summary of published stable isotope values of end members used for zooplankton in the upper water column.....	80
7 Published trophic enrichment factors (TEF) used for zooplankton.....	80
8 Mean \pm standard deviations (SD) of $\delta^{15}\text{N}$ values of zooplankton sampled during five cruises that covered the deep water region of the Gulf of Mexico. Ranges presented in parentheses. The n represents the number of stations covered in each cruise.....	81
9 Mean \pm standard deviation (SD) of $\delta^{15}\text{N}$ values of copepods, euphausiids, and the small fraction and large size fractions of zooplankton caught within anticyclonic eddies, cyclonic eddies, or outside of eddies during the XIXIMI-02, -03, -04 and -05 cruises in the deep water region of the Gulf of Mexico. The n represents the number of stations (and hence zooplankton samples) classified to each feature. The range of values are reported within parenthesis.....	81

10	Results of two-way ANOVAs of $\delta^{15}\text{N}$ values of copepods and euphausiids collected during XIXIMI cruises. ACE: Anticyclonic eddy, CE: Cyclonic eddy, NE: non-eddy.....	81
11	Mean \pm standard deviation (SD), minimum and maximum $\delta^{15}\text{N}$ values of copepods, euphausiids, small (<1000 μm) and large (1000-2000 μm) size fractions of zooplankton caught in the central Gulf of Mexico and the Bay of Campeche during the XIXIMI-01, -02, -03, -04 and -05 cruises in the deepwater region of the Gulf of Mexico. Samples were collected in the Yucatan Channel only during XIXIMI-04 and -05.....	82
12	Stable isotopes values for POM in the Gulf of Mexico collected at the euphotic layer....	83
13	Mean and SD Isotope ratios of carbon and nitrogen of particulate organic matter collected during XIXIMI-06 cruise at different depths.....	84

Chapter 1. General introduction

1.1 Background

Zooplankton play a fundamental role in the transfer of energy from phytoplankton to higher trophic levels, which gives zooplankton key ecological importance (Turner 2004). The most abundant groups in zooplankton samples are copepods and have very varied feeding habits (herbivores, omnivores, carnivores). Euphausiids are filter-feeding and an abundant group in zooplankton samples. Due to their abundance and ubiquitous distribution, both groups have been analyzed in isotopic studies to estimate the relative importance of different nitrogen sources (Banaru et al., 2014; Gorbatenko et al., 2014). Also, studies have been demonstrated to evaluate the isotopic composition of zooplankton based on size ranges, to infer food sources making the assumption that the smaller ones have a lower trophic level with herbivorous behavior (McClelland et al., 2003; Hannides et al., 2013; Banaru et al., 2014).

In oligotrophic regions, the N_2 fixation and subsurface nitrate are the main new N sources that support the food web. The N results from N_2 fixation in the ocean could have $\delta^{15}N \approx 0\text{‰}$ which is close to atmospheric N_2 , while, the subsurface nitrate would be $\sim 4\text{-}6\text{‰}$ in subtropical and tropical Atlantic subsurface waters (Sigman and Casciotti, 2001). Depleted $\delta^{15}N$ values have been observed in shallow, oligotrophic waters at low latitudes and related to N_2 fixation. Within the nitrogen cycle, different processes produce distinct degrees of isotopic discrimination. For example, N_2 fixation and remineralization processes are low ($0\text{-}2\text{‰}$), while the first step of nitrification ($\sim 15\text{‰}$) and denitrification process ($15\text{-}25\text{‰}$). In addition, the assimilation, is the process that degree of isotopic discrimination could be high $\delta^{15}N$ if the source is not limiting ($0\text{-}20\text{‰}$) (Sigman and Casciotti 2001, Sigman and Fripat, 2019).

Although isotopic composition from primary producers have been used to track N sources in the ocean (Martinetto et al., 2006), $\delta^{15}N$ values from zooplankton represent better water column conditions because zooplankton integrate isotope values from phytoplankton and smooth temporal variations by integrating their isotopic composition over time (Hue et al 2013). Also, the isotopic composition of N sources can be tracked through the food web due to the consistent isotopic difference between a consumer and food source, that usually have been used 3‰ but in zooplankton (mainly crustaceans) is approximately 2‰ (Henschke et al., 2015; Vanderklift and Ponsard, 2003).

The Gulf of Mexico is a semi-enclosed basin located in the northwestern Caribbean Sea. Muller-Karger et al. (2015) found the seasonal cycle in hydrographic conditions is marked by summer and winter in the deep

water zone. The SST during the months of April-August was warmer (29-30 ° C) than September-March (22-26 ° C), while the mixing layer depth shallowest during the summer (20-30 m) than winter (100-110 m) and found the mixing layer depth was associated with the wind patterns. However, net primary production is higher during the winter months and lower during the spring-summer months. Also, the deep water region (>1000 m) of the Gulf of Mexico is considered an oligotrophic region because the nutrients, mainly nitrate, are below the detection limit in the upper part of the water column (Biggs, 1992, Pasqueron De Fommervault et al., 2017).

The dynamics of the Gulf of Mexico are mainly influenced by the Loop Current and the Loop Current eddies (LCE) detached and from it and this eddies modify the physical-biological conditions in the first 800 to 1000 m depth (Hamilton et al. 2018). From the Loop Current, the LCEs are large anticyclonic eddies (ACE, ~200 km), and could appear with a periodicity of 6 to 11 months, move westward and could last for several months until they reach the continental shelf where they dissipate (Sturges and Leben, 2000). This ACE are characterized by convergence producing deepening the thermocline and nitracline and the mixing layer is deeper and the N availability of nutrients is lower in the upper layers, therefore primary production is limited (Klein and Lapeyre, 2009). While, a semipermanent cyclonic eddy has been reported in the western region of Bay of Campeche (Pérez-Brunius et al., 2013), and subsurface waters pumping with high NO₃ concentrations would be expected in the upper layer (Lévy, 2008). Also, the rivers inputs could be an important N sources for the coastal and shelf regions, especially in the delta of Mississippi and Atchafalaya rivers in the northern GM and Grijalva and Usumacinta rivers in the southern GM. These mesoscale structures, such as Loop Current, anticyclonic and cyclonic eddies modify the structure of the water column and in turn the availability of N that supports the trophic network.

In the GM, studies on the zooplankton community has been focused, with emphasis on the northern part of the basin (Biggs et al., 1997; Biggs and Ressler, 2001). Meanwhile, in the Mexican region, the sampling had been focused on the continental shelf (Súarez-Morales and López-Salgado, 1998; Zavala-García et al., 2016), but in the recent years, studies in the deep water region focused on the plankton community and ecology (Martinez et al., 2021; Ursella et al., 2021; Dauden-Bengoia et al., 2020; Hereu et al., 2020; Gaona-Hernández, 2019) as a part of a large-scale project that intend to generate a baseline for physical, chemistry and biota in the Mexican region of the GM.

1.2 Justification

Estimate the relative importance of different N sources (subsurface NO_3^- vs. N_2 fixation) and spatial and temporal variation in the deep water region of the Gulf of Mexico contributes to understanding the biogeochemical pathways of nitrogen and how these N sources support the primary and secondary production of this oligotrophic region.

1.3 Objectives

1.3.1 General objective

Evaluate the relative importance of different sources of reactive N (subsurface nitrate, N_2 fixation, rivers input contributions, denitrified N) in the surface layer of the Gulf of Mexico as a function of local oceanographic characteristics based on the isotopic composition of zooplankton as tracer of the geochemical and physical processes that influence the nitrogen cycle.

1.3.2 Specific objectives

- Examine the temporal variation in the isotopic composition of zooplankton
- Estimate the relative contribution of NO_3^- vs fixed N_2 to primary production based on the isotopic composition of zooplankton
- Evaluate the relationship between mesoscale features and nitrogen contributions
- Test for regional differences in the contribution of N sources.
- To apply the mixing models, isotopic endpoints were obtained based on literature-derived regional isotope ratios for POM.

- Estimate the fractional contribution of different N sources throughout the GM based on the $\delta^{13}\text{C}$ and $\delta^{15}\text{N}$ values of zooplankton reported by Le-Alvarado et al. (2021)
- Evaluate how the variation in the $\delta^{15}\text{N-NO}_3$ reported for the GM impact regional source contributions.

Chapter 2. Nitrogen sources (NO_3^- vs N_2 fixation) inferred from bulk $\delta^{15}\text{N}$ values of zooplankton from the deep water region of the Gulf of Mexico

2.1 Introduction

Dinitrogen (N_2) fixation is an important source of new N to the euphotic zone in the ocean and plays a crucial role in supporting food webs. In oligotrophic oceanic systems, N_2 fixation by diazotrophs can contribute up to 50% of the N fueling primary production (Capone *et al.*, 2005; Lévy, 2008; Klein and Lapeyre, 2009; Knapp *et al.*, 2018; Tang *et al.*, 2019). N_2 fixing organisms transform nitrogen gas to ammonia (NH_3) intracellularly, which is either assimilated or released and subsequently assimilated by other primary producers. Diazotroph-derived nitrogen (DDN) also includes dissolved organic nitrogen (DON) that can be consumed by phytoplankton or remineralized to dissolved inorganic nitrogen (DIN) in the water column (Mulholland *et al.*, 2006; Holl *et al.*, 2007).

The cyanobacteria *Trichodesmium* spp. is the most widely studied N_2 fixing organism, and can be responsible for up to half of the N supply that supports primary production in tropical and subtropical regions of the western Atlantic Ocean (McClelland and Montoya, 2002; Montoya *et al.*, 2002; McClelland *et al.*, 2003; Mompean *et al.*, 2016, Martínez-Pérez *et al.*, 2016). Unicellular cyanobacteria and heterotrophic picoplankton can also fix atmospheric nitrogen, contributing up to 30% of the fixed N in some regions of the western Atlantic Ocean (Zhang *et al.*, 2015; Martínez-Pérez *et al.*, 2016; Bombar *et al.*, 2016, Zehr and Capone, 2020). In oligotrophic oceans, the growth of picoplankton (i.e. *Prochlorococcus* and *Synechococcus*) may be largely supported by recycled N (urea and ammonium) fixed by the diazotrophic community (Casey *et al.*, 2007; Moisaner *et al.*, 2012).

Mesoscale cyclonic eddies (CE) can increase the vertical nitrogen flux from subsurface layers to the euphotic layer (Siegel *et al.*, 1999). Their divergent circulation causes a shallowing of the thermocline and drives subsurface water pumping, which increases the availability of new nitrogen (NO_3^-) in the euphotic zone and consequently increases primary production and chl a concentrations (Seki *et al.*, 2001). In turn, higher phytoplankton biomass supports greater zooplankton production (Dickey-Collas *et al.*, 1996, Strzelecki *et al.*, 2007, Venkataramana *et al.*, 2019). On the other hand, anticyclonic eddies (ACE) lead to convergence, causing a sinking of the thermocline with the consequent limitation of nutrients in the upper layers, which tends to be reflected in lower primary production (Biggs, 1992; Zimmerman and Biggs, 1999; Biggs and Ressler, 2001; Henschke *et al.*, 2015). Hence, mesoscale eddies play an important role in the

hydrographic structure of the upper ocean and can increase or limit the flux of NO_3^- to the euphotic layer; the depth of the mixed layer relative to that of the nitracline will determine whether subsurface nitrate reaches the euphotic surface layer (Muller-Karger *et al.*, 2015; Pasqueron De Fommervault *et al.*, 2017; Damien *et al.*, 2018).

The isotopic composition of nitrogen ($\delta^{15}\text{N}$) of autotrophs has been widely used to identify nutrient sources that support primary and secondary production (Anderson and Fourqurean, 2003; García-Sanz *et al.*, 2011, Bode *et al.*, 2015). In marine systems, $\delta^{15}\text{N}$ values measured in particulate organic matter (POM) can be used to infer energy sources supporting production and to trace its pathways through food webs (Montoya, 2002, Bănaru *et al.*, 2014). The isotope discrimination associated with nitrogen fixation is low, and consequently $\delta^{15}\text{N}$ values of N fixers is $\sim 0\text{‰}$, which is similar to that of atmospheric N_2 (Macko *et al.*, 1984; Montoya *et al.*, 2002). In contrast, due to denitrification, $\delta^{15}\text{N-NO}_3^-$ values are 4-6‰ in subtropical and tropical Atlantic subsurface waters (Altabet, 2005).

Although measurements of POM have been widely used as a proxy for the isotopic composition phytoplankton (Macko *et al.*, 1984; Martinetto *et al.*, 2006; Hou *et al.*, 2013), $\delta^{15}\text{N}$ values tend to be highly variable (Holl *et al.*, 2007; Hannides *et al.*, 2013). The isotopic composition of zooplankton tends to smooth the fine-scale temporal (hours/days) and spatial variation that is often observed in the isotopic composition of POM due to their lower rates of isotopic turnover (Waite *et al.*, 2007; Hou *et al.*, 2013). Since zooplankton play a fundamental role in the transfer of energy from phytoplankton to upper trophic levels (Roger, 1994; Turner, 2015; Steinberg and Landry, 2017), they provide a robust isotopic baseline for the estimation of trophic position in marine food webs (Olson *et al.*, 2010; El-Sabaawi *et al.*, 2013; Yang *et al.*, 2017).

The isotopic composition of zooplankton can lend insight into the importance of nitrogen source supporting food webs over several spatial scales. For example, a positive relationship between *Trichodesmium* abundance and low $\delta^{15}\text{N}$ values of zooplankton has been observed in the subtropical oligotrophic Atlantic, reflecting the assimilation of fixed nitrogen and its incorporation into the food web (Montoya *et al.*, 2002, McClelland *et al.*, 2003). Variability in $\delta^{15}\text{N}$ values of zooplankton has been linked to mesoscale eddies (Waite *et al.*, 2007; Dorado *et al.*, 2012; Henschke *et al.*, 2015; Wells *et al.*, 2017); higher values in CE compared with ACE indicates a greater contribution of subsurface NO_3^- vs. fixed nitrogen, respectively (Dorado *et al.*, 2012; Wells *et al.*, 2017).

Due to their abundance and ubiquitous distribution, the isotopic composition of copepods and euphausiids have been used to estimate the relative importance of nitrogen sources in plankton food webs (Hou *et al.*, 2013; Bănaru *et al.*, 2014). The Copepoda are diverse and abundant crustaceans. They are the dominant group in zooplanktonic communities in the pelagic realm (Boxshall and Halsey, 2004), showing various feeding strategies that primarily include herbivores, omnivores and filter feeders, but there are also carnivorous and parasitic species. Small copepods (<1 mm) that can contribute up to 50% of the abundance are mainly herbivores or omnivores (Turner, 2004). Euphausiids can constitute 20-40 % of zooplankton biomass in high productivity regions (Brinton *et al.*, 2000). They are generally filter-feeder herbivores (Gurney *et al.*, 2001), although omnivory, detritivory, and carnivory are also observed (Maucheline and Fisher, 1959). Hence, the isotopic composition of copepods and euphausiids corresponds to that of either primary or secondary consumers (Kinsey and Hopkins, 1994; Sogawa *et al.*, 2017).

Alternatively, studies have measured the isotopic composition of zooplankton of specific size ranges; this approach relies on the assumption that smaller organisms feed at a lower trophic level (McClelland *et al.*, 2003; Hanniades *et al.*, 2013), although some larger zooplankton such as filter-feeding salps occupy a low trophic level (Bănaru *et al.*, 2014). The selection of specific size fractions for isotopic analysis must consider that a sample encompasses organisms of varied feeding habits and trophic levels. Despite the uncertainty regarding the trophic level at which a multispecies group or size fraction of zooplankton feed, their relatively low position in the food web renders them useful for inferring nitrogen sources based on measurements of their isotopic composition.

The Gulf of Mexico (GM) is a semi-enclosed marginal sea that is connected with the Caribbean Sea through the Yucatan Channel and with the Atlantic Ocean by the Florida Straits. The mesoscale circulation in the central, deep GM is dominated by the Loop Current (LC), which enters through the Yucatan Channel and exits through the Florida Straits. When the LC exhibits a high level of intrusion into the gulf, it can detach Loop current anticyclonic eddies (LCEs; Sturges and Leben, 2000) that measure 200-400 km in diameter, reach depths of 800-1000 m, and move westward at speeds of 2-5 km day⁻¹ over a period of months (Oey *et al.*, 2005; Hamilton *et al.*, 2018). The mesoscale circulation in the Bay of Campeche (BC) in the southern GM is dominated by a semi-permanent cyclonic eddy (Pérez-Brunius *et al.*, 2013). LCEs and CE play a dominant role in the circulation and productivity throughout the central and southern gulf (Zimmerman and Biggs, 1999; Biggs and Ressler, 2001), and likely modulate the contribution of different nitrogen sources to the euphotic zone.

We examined the relative importance of nitrogen fixation and subsurface NO_3^- in supporting primary and secondary production throughout the deep water region of the Mexico's Exclusive Economic Zone (EEZ), including the Bay of Campeche. The aims of this study were four-fold: (1) examine the temporal variation in the isotopic composition of zooplankton, (2) estimate the relative contribution of NO_3^- vs fixed N_2 to primary production based on the isotopic composition of zooplankton, (3) evaluate the relationship between mesoscale features and nitrogen contributions, and (4) test for regional differences in the contribution of N sources. We hypothesized that temporal variation in the isotopic composition of zooplankton would be more limited than the spatial variation, that $\delta^{15}\text{N}$ values of zooplankton from the central gulf would reflect a greater contribution of N_2 fixation, and that the Bay of Campeche would reflect a greater contribution of subsurface NO_3^- .

2.2 Methods

2.2.1 Study Area

The Central region of the GM (22-25 °N) is considered oligotrophic and NO_3^- concentrations are near or below the detection limits to a depth of ~ 90 m in the region of influence of the LC (Biggs and Ressler 2001; Pasqueron De Fommervault *et al.*, 2017). During the winter, surface concentrations of chl a are higher than during the summer (Zavala-Hidalgo *et al.*, 2009). This has been attributed to seasonal variations in the mixed layer depth (MLD) as a deeper MLD in winter favors the transport of NO_3^- to the euphotic zone (Biggs and Ressler 2001; Muller-Karger *et al.*, 2015; Damien *et al.*, 2018).

The Bay of Campeche has been reported with a higher surface chl a concentration than in the central region in the late summer and autumn, and has a large contribution from the cross-shelf transport of chl a rich waters to the offshore (Martínez-López and Zavala-Hidalgo, 2009). Upwelling has been observed throughout the year along the western Campeche Bank (also known as the Yucatan Peninsula), and a maximum in surface chl a is observed in September (Zavala-Hidalgo *et al.*, 2006). Recently, Damien *et al.* (2018) used a coupled circulation and biogeochemical model to examine the patterns of variability of surface and depth-integrated chl a concentrations, and proposed a partition of open waters in the GM into a northern, central and southern regions. The central region includes our sampling stations between 22-25 °N and the southern region includes the stations in open waters of the Bay of Campeche south of 22 °N (Fig. 1).

2.2.2 Zooplankton sampling and isotope analysis

Five oceanographic cruises were conducted in the deep water region of Mexico's EEZ (>1000 m) between November 2010 and July 2016 (Figs. 1 and 17). Zooplankton samples were collected at some of 57 fixed stations: XIXIMI-01 (November 2010, n=35), XIXIMI-02 (July 2011, n=34), XIXIMI-03 (Feb-Mar 2013, n=20), XIXIMI-04 (August 2015, n=45) and XIXIMI-05 (July 2016, n=31; see sampling stations and oceanographic conditions in Figs. 2,3 and 17).

At each station, zooplankton samples were collected with double-oblique tows using a 60 cm diameter bongo equipped with 335 μm or 500 μm mesh nets. Tows were carried out to a depth of 200 m (except during XIXIMI-01, when they were performed to 150 m). Limited spatial coverage was achieved during XIXIMI-03 because of equipment loss and adverse weather conditions.

For XIXIMI-01, -02 and -03, a subsample of zooplankton (about 2-3 ml) was collected from the 500 μm mesh net using a sieve to concentrate zooplankton, stored in centrifuge tubes and frozen at -10 °C. For XIXIMI-04 and -05, a 20% by volume aliquot from the sample of the 335 μm mesh net was obtained with Hempel-Stempel pipette and frozen in Whirl-Pak bags at -10 °C. All zooplankton samples were defrosted and rinsed in distilled water in preparation for SIA.

For XIXIMI-01, -02, and -03, copepods and euphausiids were sorted with forceps under a stereomicroscope. For XIXIMI-04 and -05, zooplankton were analyzed based on size classes that were separated using Nitex mesh sieves (<1000 μm and 1000-2000 μm); these are subsequently referred to as the small and large size fractions (SF and LF, respectively). The components of the zooplankton community that analyzed differed between the first three and the last two cruises because we were unable to consistently obtain sufficient euphausiids at some stations due their low abundance, and since we considered that focusing on specific size fractions should yield a more consistent and integrative representation of the isotopic baseline than specific groups with variable feeding habits. Copepods nevertheless constitute the dominant group in both size fractions (Hopkins, 1982; Ortner *et al.*, 1989; Strezelecki *et al.*, 2007; Elliot *et al.*, 2012; Walsh and O'Neil, 2014), making their isotopic values roughly comparable to those obtained from the same group during the first three cruises.

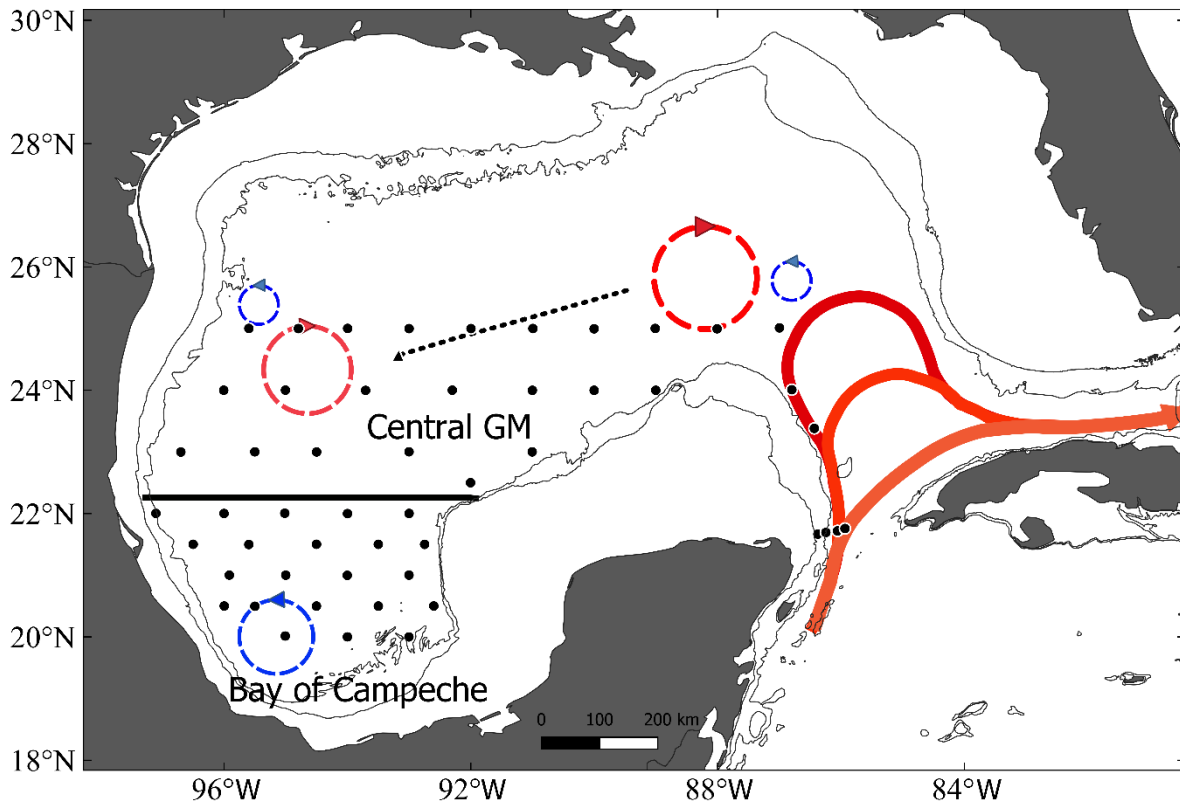


Figure 1. Study region in the Gulf of Mexico. Schematic diagram of the main regions and mesoscale features that dominate the central and southern Gulf of Mexico. The black line marks the limit between the central and southern regions. The thick red lines indicate the Loop Current with various levels of intrusion into the gulf. Red and blue circles represent anticyclonic and cyclonic eddies, respectively. The black dotted arrow indicate the main pathway of Loop Current Eddie (LCEs). Grey thin lines are the 200 and 1000 m isobaths. Fixed stations for zooplankton and NO₃ concentration sampling and CTD casts covered during the XIXIMI cruises are indicated by black dots. All stations are at depths > 1000m, except for some in the Yucatan Channel.

Sample processing included cleaning of surfaces and instruments with ethanol and distilled water to avoid cross contamination. Copepods, euphausiids and zooplankton size fractions were dried at 60 °C during 48 hours in pre-cleaned aluminum trays. Samples were then ground to a fine powder using an agate mortar and pestle. Dry sub-samples of 0.8-1.0 mg of weight were packed in 5x9 mm Costech® tin capsules and sent to the Stable Isotope Facility of the University of California at Davis. SIA samples were processed with an PDZ Europa ANCA-GSL elemental analyzer interfaced to a PDZ Europa 20-20 isotope ratio mass spectrometer. The standard deviation of internal standard materials (glutamic acid, bovine liver, enriched alanine, and nylon) ranged between 0.04 and 0.07 ‰ for $\delta^{13}\text{C}$ and 0.05 and 0.08‰ for $\delta^{15}\text{N}$.

Stable isotope values were reported in delta (δ) notation using the following equation:

$$(1) \delta X (\text{‰}) = \left[\frac{R_{\text{sample}}}{R_{\text{standard}}} - 1 \right] * 1000$$

Where X is ^{13}C or ^{15}N , and R_{sample} and R_{standard} are the relative abundance of the heavy to light isotopes ($^{13}\text{C}/^{12}\text{C}$ or $^{15}\text{N}/^{14}\text{N}$) in a sample and internal standard (Vienna Pee Dee Belemnite and atmospheric nitrogen for $\delta^{13}\text{C}$ and $\delta^{15}\text{N}$, respectively). Isotope ratios are reported in parts per thousand (‰).

The inverse Distance Weighted (IDW) interpolation method was used to generate isoscapes of the N isotopic composition of zooplankton. Search distance of five times the cell size of the output raster and a power adjustment of 2 were used. The maps of the $\delta^{15}\text{N}$ of zooplankton with this interpolation are for visual purposes.

2.2.3 Hydrography and nutrient concentrations

Environmental parameters at each sampling station were measured with a SeaBird 9plus conductivity-temperature-depth meter (CTD) equipped with temperature ($^{\circ}\text{C}$), salinity, pressure (dbar), oxygen (mL^{-1}) and chl a fluorescence sensors. Unfortunately, CTD data were not available for XIXIMI-01 due to equipment malfunction.

A 20 L rosette sampler with 20 L Niskin bottles was used to collect water for $\text{NO}_3^- + \text{NO}_2^-$ (hereinafter referred to as NO_3^-) measurements at 12 nominal depths (0, 10, 50, fluorescence maximum, 150, oxygen minimum, 600, 800, 1000, 1200, 2000, 2500 m and 20-40 m off the bottom). Immediately after collection, water samples for NO_3^- analyses that were collected from 0-200 m were filtered (GF/F 0.7 μm Whatman filters) and stored frozen in polyethylene vials at -10°C . Samples collected below 200 m were frozen without filtration. Samples from the XIXIMI-01, -02 and -03 cruises were analyzed for NO_3^- with a Skalar SANplus nutrient analyzer according to the protocols described in Gordon *et al.*, (1993). For these cruises, the precision and accuracy of nutrient analyses was determined by repeated measurements of a Seawater Certified Reference Material for Nutrients (MOOS-1 or MOOS-2; National Research Council Canada). Samples for the XIXIMI-04 and 05 cruises were analyzed with an AA-3 HR SEAL Analytical nutrient analyzer according to the protocols described in Hydes *et al.* (2010). Precision and accuracy were determined by repeated measurements of Certified Reference Material for Nutrients in seawater (lot CC with a calculated certified value for NO_3^- of $30.996 \pm 0.245 \mu\text{mol kg}^{-1}$, and lot CD with a calculated certified value for NO_3^- of $5.516 \pm 0.054 \mu\text{mol kg}^{-1}$, KANSO Technos, Japan www.kanso.co.jp). Continuous NO_3^- profiles were

constructed using a Pchip interpolation of discrete NO_3^- samples and integrated NO_3^- concentrations ($[\text{NO}_3^-]_{\text{int}}$) were calculated from the surface to 200 m at each station as a proxy of NO_3^- availability in the euphotic zone.

The MLD was calculated for each station using temperature and density profiles following Huang *et al.* (2018). The average temperature from the surface to 200 m depth and from the surface to the MLD was calculated, as well as the depth of the 25.5 kg m^{-3} isopycnal as a proxy for the presence of ACE and CE. For each station and cruise, sea surface temperature (SST), sea surface chl a (CHL), and sea surface height anomalies (SSHA) were obtained from Marine Lab Copernicus (<https://marine.copernicus.eu/>). Non-steric sea surface heights (SSH) were calculated subtracting the average SSH value for the GM to SSH data (Chambers *et al.*, 2004).

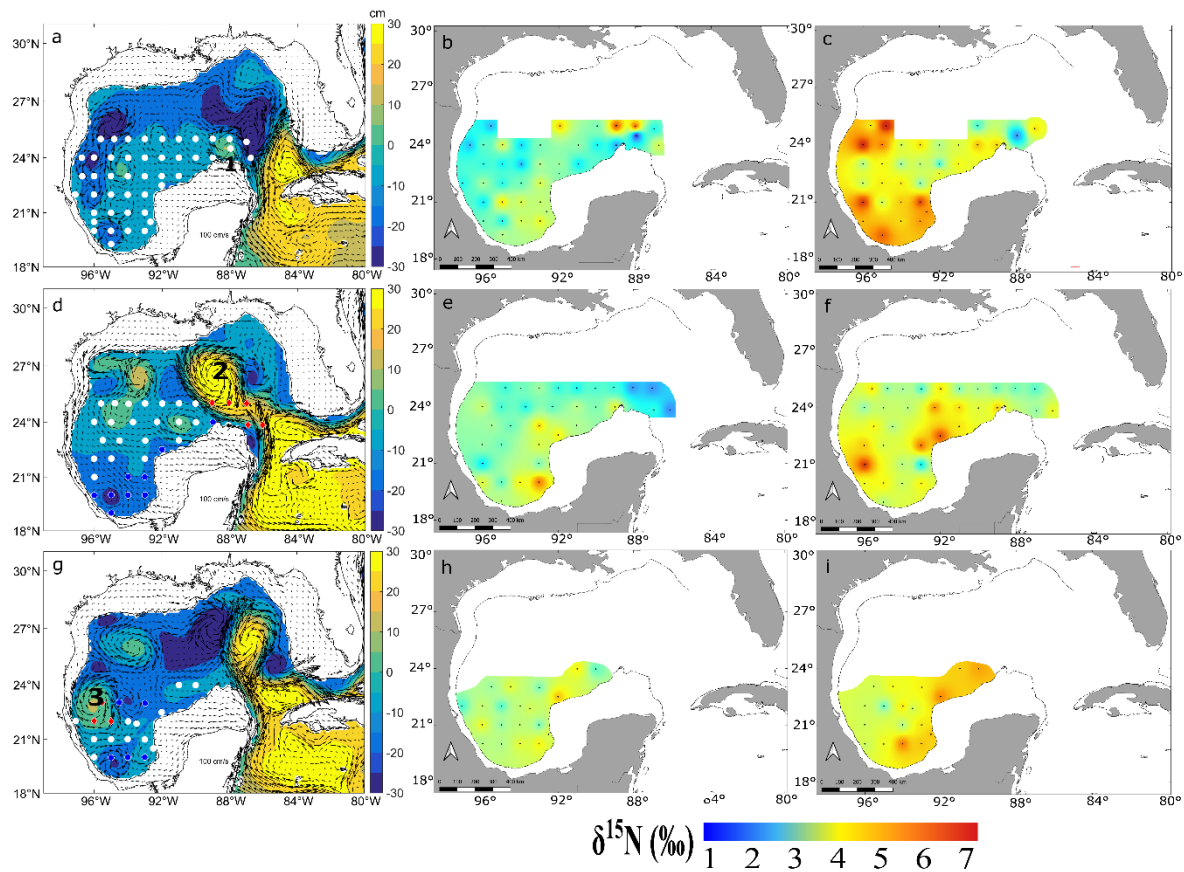


Figure 2. SSHA (a,d,g) and nitrogen isotopic composition of nitrogen of copepods (b, e, h) and euphausiids (c, f, i) during XIXIMI-01 (a, b, c), XIXIMI-02 (d, e, f) and XIXIMI-03 (g, h, i). Red diamonds, blue circles and white stars represent stations influenced by anticyclonic, cyclonic and non-eddy structures, respectively. For XIXIMI-01, the stations were not classified to mesoscale eddies because the CTD malfunction did not allow for estimates of the depth of the 25.5 kg/m^{-3} isopycnal. Arrows represent geostrophic velocities. Numbers identify Loop Current eddies named by the Horizon Marine Group (www.horizonmarine.com): 1) Franklin, 2) Jumbo, 3) Icarus/Jumbo remnants

2.2.4 Station classification based on mesoscale structures

Stations were classified to one of three categories: anticyclonic eddy, cyclonic eddy or no eddy (NE) based on geostrophic currents, SSHA (Hamilton *et al.*, 2018) and the depth of the 25.5 kg m⁻³ isopycnal as a proxy for the depth of the nitracline (Linacre *et al.*, 2015, Pasqueron de Fommervault *et al.*, 2018). First, we used the geostrophic currents (Marine Lab Copernicus) to identify stations that clearly fell within mesoscale eddies. We then categorized stations as ACE when the depth of the 25.5 kg m⁻³ isopycnal > 100 m and SSHA > 9 cm, as CE when isopycnal 25.5 kg m⁻³ < 80 m and SSHA < -4 cm, and as NE when the depth of the 25.5 kg m⁻³ isopycnal < 100 m but >80 and SSHA < 9 but >-4 cm. We were unable to calculate the depth of the 25.5 kg m⁻³ isopycnal for XIXIMI-01 because of the absence of reliable CTD data and hence the classification was applied to XIXIMI-02 through -05.

2.2.5 Data Analysis

A paired t-test was used to compare the differences in $\delta^{15}\text{N}$ values of copepods vs euphausiids, and differences in small vs large fraction for each cruise. Regression analyses were used to determine whether higher $\delta^{15}\text{N}$ values of copepods and the small size fraction were reflected in higher values of euphausiids and the large size fraction, respectively which would be indicative of the trophic coupling within the food web. One-way analysis of variance (ANOVA) was used to test for differences in $\delta^{15}\text{N}$ values of zooplankton collected in the stations of the central region (22-25 N) and the Bay of Campeche (south of 22 N) for each cruise. Also, two-way ANOVA was used to test for differences in $\delta^{15}\text{N}$ values of zooplankton between mesoscale structures and cruises. Data for copepods and euphausiids (XIXIMI-02 and -03) and size-fractionated subsamples (XIXIMI-04 and -05) were analyzed separately. Post-hoc comparisons were performed using a Tukey HSD test with an α of 0.05. Normality and homoscedasticity were evaluated using the Shapiro-Wilk and Bartlett test, respectively. Statistical analyses were performed in RStudio version 3.4.1.

Principal component analysis (PCA) of oceanographic variables and the isotopic composition of zooplankton was applied to examine associations between $\delta^{15}\text{N}$ values and station classifications. When two variables were correlated at $r > 0.7$ (Pearson's correlation) one was removed prior to PCA. For XIXIMI-02 and -03, the analysis included MLD, CHL, depth of the 25.5 kg m⁻³ isopycnal, SST, SSH, $[\text{NO}_3^-]_{\text{int}}$, and $\delta^{15}\text{N}$ values of copepods and euphausiids. For XIXIMI-04 and -05, the PCA included MLD, CHL, depth of the 25.5

kg m^{-3} isopycnal, $[\text{NO}_3^-]_{\text{int}}$, and the $\delta^{15}\text{N}$ and of SF ($<1000 \mu\text{m}$). LF data were excluded due to a high correlation with SF.

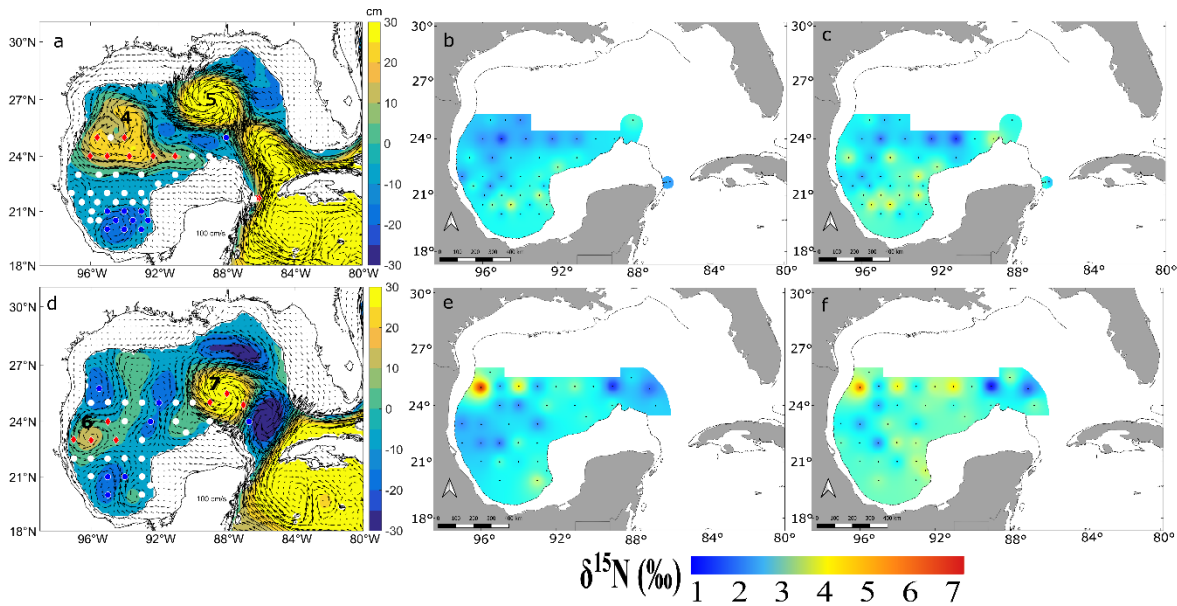


Figure 3. SSHA (a,d) and nitrogen isotopic composition of nitrogen of small (b, e) and large zooplankton fractions (c, f) during XIXIMI-04 (a, b, c) and XIXIMI-05 (d, e, f). Red diamonds, blue circles and white star symbols represent the ACE, CE and NE stations, respectively. Arrows represent geostrophic velocities. Numbers identify Loop Current eddies based on the nomenclature of the Horizon Marine Group (www.horizonmarine.com): 4) Nautilus remnant, 5) Olympus, 6) Olympus remnant, 7) Poseidon.

2.2.6 Two-source isotope mixing model

To estimate the contribution of N_2 fixation vs NO_3^- to zooplankton, a two-source Bayesian mixing model was applied using package SIMMR in R (Parnell *et al.*, 2010). The model was applied with the data from each cruise to obtain seasonal estimates of source contributions. The inputs for the mixing model were the $\delta^{15}\text{N}$ values of zooplankton, the mean ($\pm\text{SD}$) values of the sources (NO_3^- and N_2), and the mean ($\pm\text{SD}$) trophic discrimination factor (TDF) for zooplankton. Based on a literature survey, we used $5.0 \pm 0.2\text{‰}$ and $-1.3 \pm 0.6\text{‰}$ as $\delta^{15}\text{N}-\text{NO}_3^-$ and N_2 fixation end-member values (Table 6). The $\delta^{15}\text{N}-\text{NO}_3^-$ end-member reflects the isotopic composition of NO_3^- in intermediate waters (600-1000 m depth) in the Atlantic Ocean and the Gulf of Mexico (Sigman *et al.*, 2000, Knapp *et al.*, 2005; Knapp *et al.*, 2008; Table 6). Thus, in the model we assume that NO_3^- isotope ratios are not modified by processes occurring in the upper layer when transport to the euphotic layer occurs. The surface waters (upper 50 m) of the deep basin of the GM are oligotrophic, with $[\text{NO}_3^-]$ close to or below the limit of detection (Damien *et al.*, 2018; Howe *et al.*, 2020). Hence, any available nitrogen in these waters will be quickly assimilated by phytoplankton, which renders the surface

water a closed system, and we therefore assume that isotopic discrimination during the assimilation of N by phytoplankton was 0‰. For N₂ fixation, we used -1.3 ± 0.6 ‰ based on reports of the isotopic composition of *Hemiaulus/Richelina* and *Trichodesmium*, the most studied of diazotrophic organisms (Montoya *et al.*, 2002, McClelland *et al.*, 2003, Sigman and Casciotti, 2001; Table 6). The isotopic trophic enrichment factor (TEF) in crustaceans has been reported as ~2‰ (Davenport and Bax, 2002; Vanderklift and Ponsard, 2003; Henschke *et al.*, 2015; McCutchan *et al.*, 2003; Table 7). Therefore, a value of 2‰ (± 0.5 ‰) for zooplankton was assumed. The mixing model was only applied to copepods and SF considering that small copepods are mostly herbivores, and hence primary consumers (Turner, 2004). The model inputs for SIMMR excluded concentration dependence, and was run with 100,000 iterations and 10,000 burnins.

2.3 Results

2.3.1 Variability in isotopic composition

There was a significant interaction between isotopic composition of copepods as a function of cruise and mesoscale eddy classifications ($F=3.4$, $p<0.001$; Table 10). The mean $\delta^{15}\text{N}$ value of copepods was significantly lower in ACEs during the XIXIMI-02 summer cruise than for the other mesoscale features sampled as well as during the winter cruise (XIXIMI-03), suggesting a higher contribution of nitrogen fixation. The isotopic composition of euphausiids differed by 0.4‰ between XIXIMI-02 and XIXIMI-03 and means were significantly different (Fig. 4; $F=6.062$, $p=0.0145$). On the other hand, SF and LF did not show differences between XIXIMI-04 and -05 (Fig. 4; $F=1.138$ $p=0.611$).

The mean $\delta^{15}\text{N}$ value of copepods was significantly lower by ~1‰ than that of euphausiids during XIXIMI-01, XIXIMI-02 and XIXIMI-03 (paired t test = -8.2961 , $p \leq 0.002$ for all cruises), indicating they were feeding at a lower trophic level. The mean $\delta^{15}\text{N}$ values of the SF in XIXIMI-04 and -05 were similar (2.7 and 2.9‰, respectively, Fig. 4) and had overlapping ranges (Table 8) which suggests similar nitrogen source contributions. The LF had average values that were about 0.5‰ higher, and differed significantly from SF (paired t test= -6.684 , $p<0.001$). The $\delta^{15}\text{N}$ values of copepods and euphausiids showed a low but significant positive correlation ($R=0.32$, $p=0.0033$; Fig. 18), while the small and large fractions showed a highly significant positive correlation indicating consistent feeding at a higher trophic level in the LF ($R=0.79$, $p<0.001$; Fig. 19).

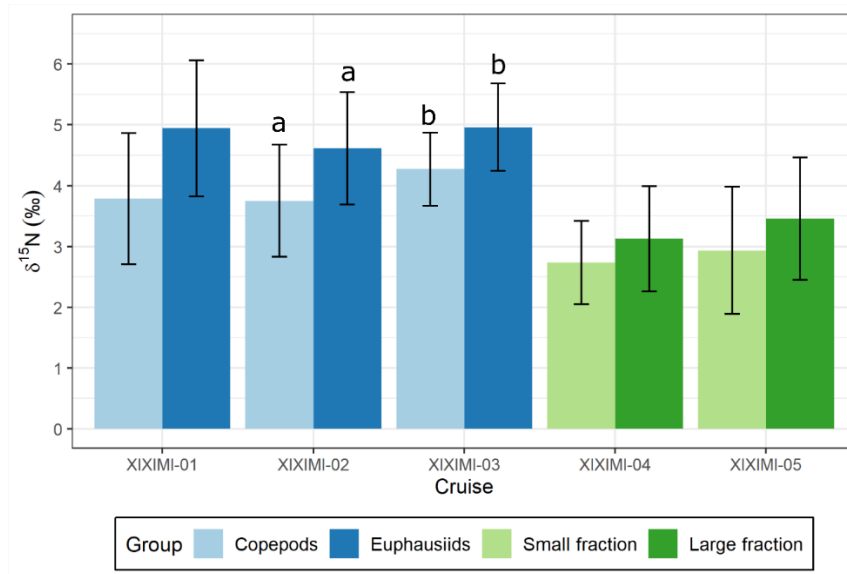


Figure 4. Mean \pm standard deviation (SD) of $\delta^{15}\text{N}$ values of copepods and euphausiids and small (<1000 μm) and large (1000-2000 μm) size fractions of zooplankton caught during five cruises covering the deepwater region of the Gulf of Mexico. Significant differences between cruises (2-way ANOVA p-values < 0.05) are indicated by different letters (a,b). For more details, see Table 10.

2.3.2 Oceanographic conditions

The location and size of mesoscale structures varied between cruises, reflecting the dynamic nature of the gulf's deep water region. The map of SSH anomalies for XIXIMI-01 (Fig. 2a) indicates that two weak anticyclonic structures were present; LCE Franklin and an additional one in the western gulf. The semi-permanent cyclonic eddy of the Bay of Campeche was in its southwestern region. During XIXIMI-02, the Loop Current had recently generated a LCE (Icarus) and BC's cyclone was relatively small (Fig. 2d). During XIXIMI-03, a LCE (remnants of Icarus/Jumbo) and a ACE were present in the western gulf and there were two cyclones: the semi-permanent CE in the Bay of Campeche and another one located east of the remnants of LCE (Fig. 2g).

During XIXIMI-04 the Loop Current had recently released a LCE (Olympus), similar to what was observed during XIXIMI-02. A large anticyclonic feature was observed in the western of GM (the remnant of LCE Nautilus), while cyclonic structures were found in the Bay of Campeche and close to the LC (Fig. 3a). During XIXIMI-05 an ACE had recently detached from the LC (Poseidon), and the remnant of LCE Olympus was

present in the western GM. With regard to cyclonic structures, one was observed in BC and another in the central gulf (Fig. 3d).

2.3.3 Isotopic composition of zooplankton and mesoscale eddies

Average $\delta^{15}\text{N}$ values of copepods from ACE were significantly lower than copepods from CE and NE by ~ 1.2 and 0.4‰ , respectively (Fig. 5; $F=10.63$, $p<0.001$), which would be consistent with a great contribution of fixed nitrogen in ACE. Euphausiids of CEs were 0.7‰ higher than in ACEs (Fig. 5; $F=3.625$, $p=0.035$). The $\delta^{15}\text{N}$ values of SF of zooplankton collected in XIXIMI-04 and -05 were also lower in ACE than in CE and NE stations (Fig. 5; $F=18.53$, $p<0.001$) by 1.2 and 0.8‰ , respectively. On the other hand, the LF values were lower in ACE than CE and NE by 1.4 and 1.0‰ , respectively (Fig. 5; Table 9; $F=10.591$, $p<0.001$).

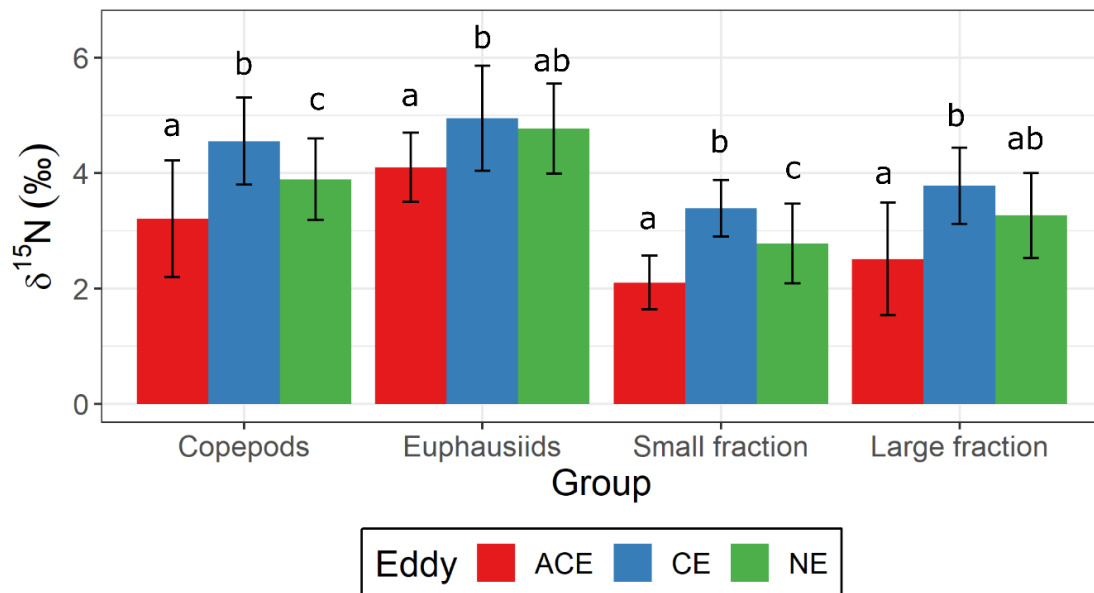


Figure 5. Mean \pm standard deviation (SD) $\delta^{15}\text{N}$ values of copepods and euphausiids (XIXIMI-02 and -03) and the small ($<1000\ \mu\text{m}$) and large ($1000\text{-}2000\ \mu\text{m}$) size fractions of zooplankton (XIXIMI-04 and -05) caught within anticyclonic eddies, cyclonic eddies, or outside of eddies in the deep water region of the Gulf of Mexico. Significant differences between mean values for each group (2-way ANOVAs P -values < 0.05) are indicated by different letters (a,b,c). Significant interaction of $\delta^{15}\text{N}$ values of copepods as function of mesoscale eddies and cruises, for more details, see Table 10.

2.3.4 Regional distribution of isotopic values

For XIXIMI-01 and -02, the $\delta^{15}\text{N}$ values of copepods showed significantly lower values at stations from the central region ($3.6\pm 1.2\text{‰}$ and $3.5\pm 0.8\text{‰}$, respectively), which is indicative of a higher contribution of fixed nitrogen, compared with those from BC ($4.7\pm 0.9\text{‰}$ and $4.2\pm 0.9\text{‰}$, respectively Fig. 6; Table 11; $F=18.51$, $p<0.001$). The euphausiids also showed slightly higher mean $\delta^{15}\text{N}$ values in BC than in the central region, but the difference was not statistically significant. Copepods showed the lowest $\delta^{15}\text{N}$ values during XIXIMI-02 at three stations influenced by the LC (A9, A10, B19; mean $2\pm 0.1\text{‰}$). During XIXIMI-03, the $\delta^{15}\text{N}$ values of copepods and euphausiids did not show a clear spatial pattern, and mean $\delta^{15}\text{N}$ values did not differ significantly between regions. However, this cruise had the most limited coverage in the central region.

The SF showed significantly lower $\delta^{15}\text{N}$ values in the central region ($2.5\pm 0.7\text{‰}$) and the Yucatan channel ($2.2\pm 0.3\text{‰}$) than in BC ($3.0\pm 0.6\text{‰}$, Fig. 3b and 6; $F=6.07$, $p=0.0185$) during XIXIMI-04, while isotope ratios of the LF did not differ significantly. For XIXIMI-05, the $\delta^{15}\text{N}$ values of both the SF and the LF were similar when comparing the central region (2.9 ± 1.2 and $3.4\pm 1.2\text{‰}$, respectively) with BC ($2.9\pm 0.7\text{‰}$ and $3.6\pm 0.7\text{‰}$, respectively; Fig. 6).

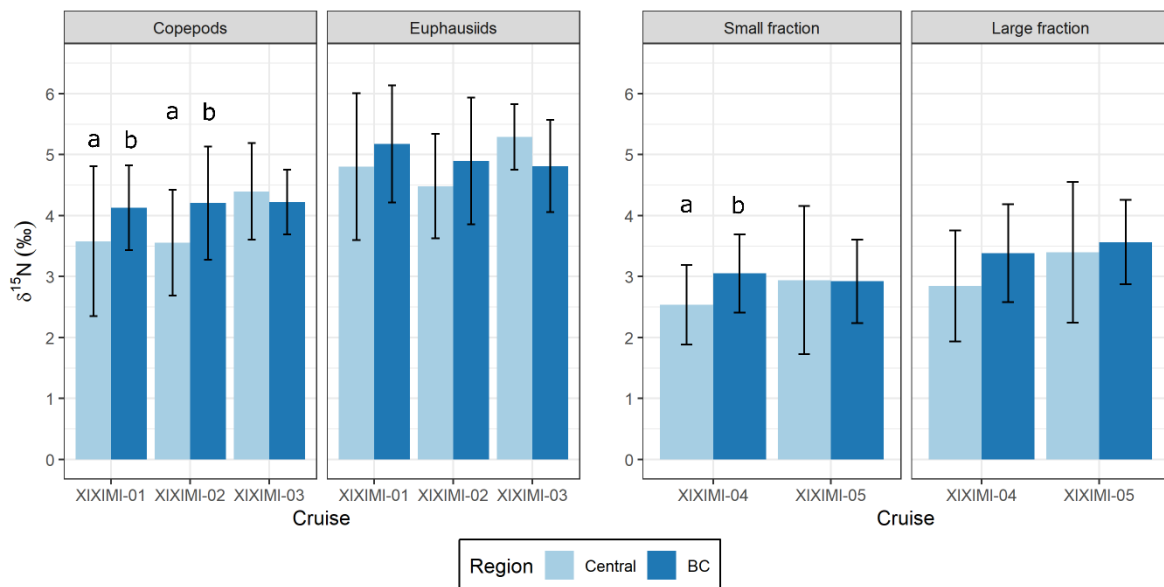


Figure 6. Mean \pm standard deviation (SD) $\delta^{15}\text{N}$ values of copepods and euphausiids (XIXIMI-02 and 03) and the small (<1000 μm) and large (1000-2000 μm) size fractions of zooplankton (XIXIMI-04 and 05) caught in the central Gulf of Mexico and Campeche Bay. Significant differences between regions for each group and cruise were evaluated with one-way ANOVAs. P-values < 0.05 are indicated with different letters (a,b). For more details, see text results.

2.3.5 PC Analysis

PC analysis of oceanographic variables and $\delta^{15}\text{N}$ values for XIXIMI-02 and -03 indicated that components 1 and 2 explained 64.5% of the variability (Fig. 7). The PCA grouped stations classified as anticyclonic and cyclonic eddies; stations that fell outside of mesoscale structures were positioned in between. There was a medium to strong ($r > 0.3$) positive correlation between PC1, integrated NO_3^- concentration, $\delta^{15}\text{N}$ values of copepods and euphausiids and chl a, and weak ($r < 0.15$) negative correlations with the depth of the 25.5 isopycnal, MLD and SST (Table 1).

Table 1. Results of principal components analysis on a correlation matrix of environmental variables. Variables are sorted in order of decreasing correlations of the variables with PC1.

XIXIMI-02,-03		
Variables	Eigenvectors	
	PC1	PC2
Integrated NO_3^- concentration	0.5108	-0.1001
Copepods (cope)	0.5086	0.0821
Depth of the 25.5 kg/m^{-3} isopycnal	-0.4559	0.3636
Euphausiids (Euph)	0.3571	0.1625
Surface chlorophyll a concentration (chl-a)	0.3173	0.3222
Mixing Layer Depth (MLD)	-0.1490	0.5483
SST	-0.1489	-0.6483
XIXIMI-04,-05		
Variables	Eigenvectors	
	PC1	PC2
Integrated NO_3^- concentration	0.5631	0.0892
Depth of the 25.5 kg/m^{-3} isopycnal	-0.5474	-0.1610
Small zooplankton (Small)	0.4410	-0.1470
Surface chlorophyll a concentration (chl-a)	0.4318	-0.2436
SST	0.0487	0.6597
Mixing Layer Depth (MLD)	0.0007	-0.6708

For XIXIMI-04 and XIXIMI-05, PC 1 and 2 explained 67.6% of the variability. The PCA also grouped stations classified as ACEs and CEs (Fig. 7). The integrated NO_3^- concentration, chl a and isotopic composition of the small size fraction were positively correlated with PC1, and the depth of the 25.5 isopycnal was negatively correlated with this component. Again, higher $\delta^{15}\text{N}$ values were found under conditions consistent with CE. For both sets of data, PC2 had a low correlation with the isotopic composition of zooplankton ($r < 0.17$), although higher values were found at low SSTs and great MLD in both models.

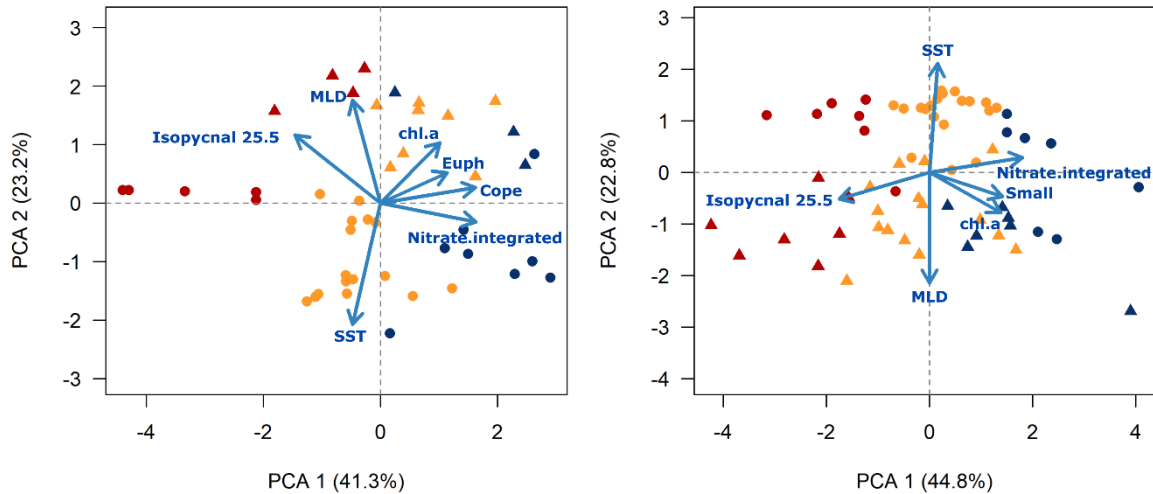


Figure 7. Principal component analysis of environmental variables and nitrogen isotope ratios of zooplankton. Biplot of the first two components (PC1 and PC2) show the sampling stations covered in XIXIMI-02 and -03 (left panel) and XIXIMI-04 and -05 (right panel). Circles indicate XIXIMI-02 (left) and XIXIMI-04 (right) and triangles indicate XIXIMI-03 (left) and XIXIMI-05 (right). For environmental and isotopic variables see table 1. Color red, blue and yellow indicate the categories of mesoscale structures (“ACE” anticyclonic eddies, “CE” cyclonic eddies and “NE” no eddies stations, respectively).

2.3.6 Bayesian mixing models

Results of the two-source Bayesian mixing model indicated that N_2 fixation was the dominant source of nitrogen ($60.4 \pm 6.7\%$, mean and SD) for copepods at stations within ACEs, while NO_3^- was the dominant source ($65.3 \pm 4.6\%$) at stations in cyclonic eddies. Likewise, for the smaller size fraction of zooplankton, N_2 fixation was most important for stations within ACEs ($77.3 \pm 2.4\%$; Fig. 8), although in CE and NE its contribution was also dominant (64.8% and 59.3% , respectively). The contribution of NO_3^- was highest at stations within CE ($40.7 \pm 2.2\%$ of the N).

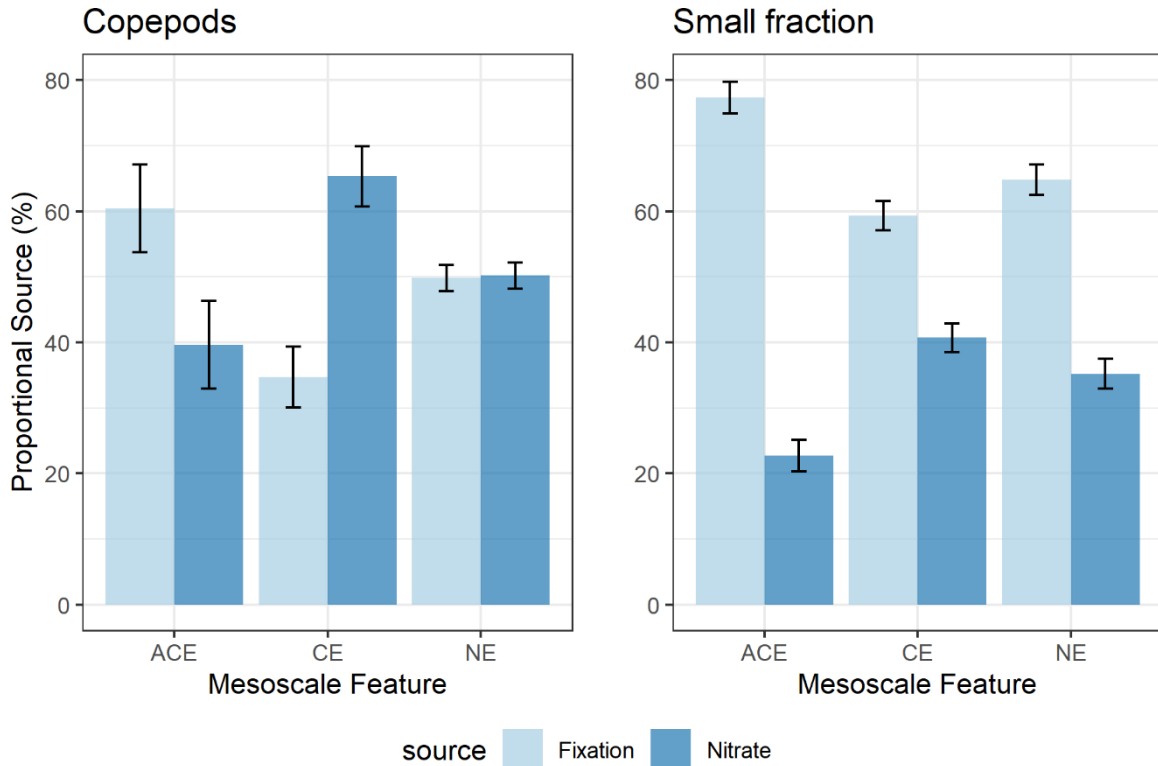


Figure 8. Results (means \pm SD) of the Bayesian isotope mixing model estimating the contribution of N_2 fixation and NO_3^- to zooplankton. Estimates are based on the mean $\delta^{15}N$ values of copepods (left panel) and small zooplankton fraction ($<1000 \mu m$ right panel). ACE: anticyclonic eddies; CE: cyclonic eddies, NE: non-eddies.

The mixing model based on copepod isotope ratios indicated that for the central region both sources had a similar contribution, although N_2 fixation ($53.1 \pm 2.4\%$) was slightly more important than NO_3^- ($46.9 \pm 2.4\%$). In contrast, for BC, NO_3^- was the dominant source ($55.3 \pm 1.8\%$ vs $44.7 \pm 1.8\%$ for nitrogen fixation; Fig. 9). The model based on the small zooplankton size fraction indicated that N_2 fixation predominated in the central region ($67.2\% \pm 2.7$) and BC (63.5 ± 1.8 , Fig. 9).

NO_3^- contributed $57.9 \pm 3.9\%$ of the nitrogen during winter (XIXIMI-03) and $47.9 \pm 3.4\%$ and $47.4 \pm 3.4\%$ during summer (XIXIMI-01 and -02). The calculations based on the small size fraction sampled during the summer months (XIXIMI-04 and -05), indicated a 31.4% contribution of nitrate.

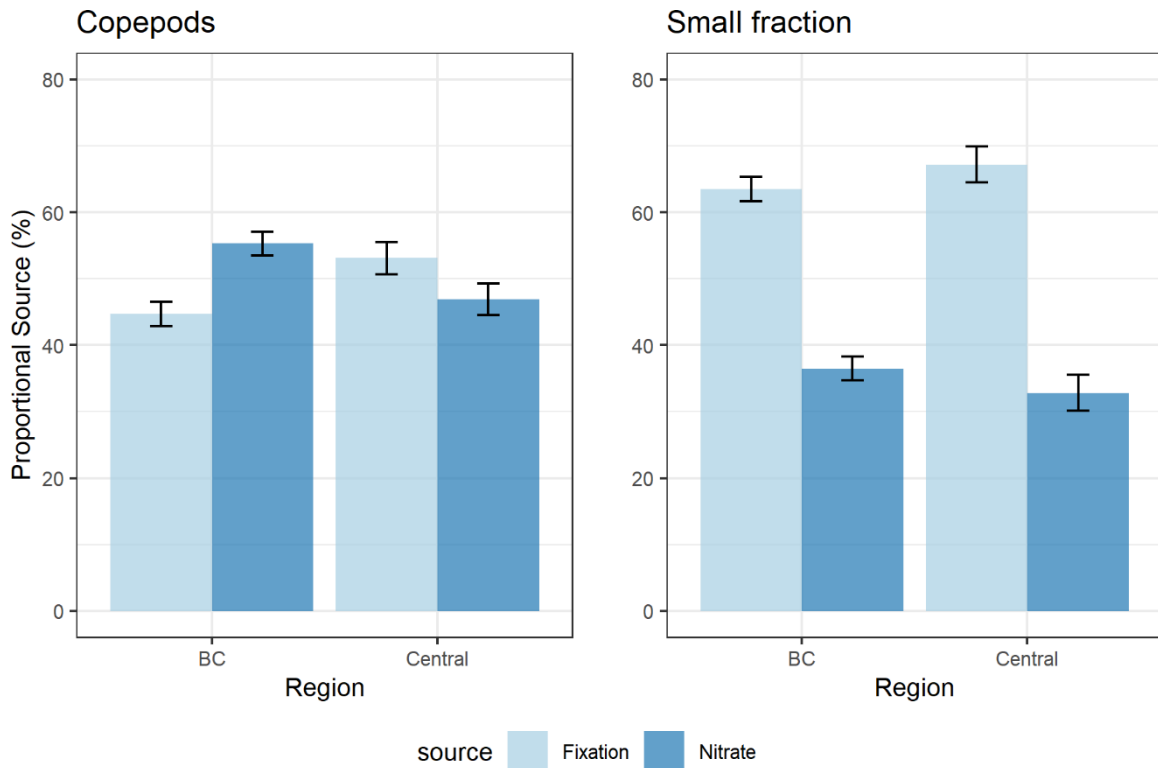


Figure 9. Results (means \pm SD) of the Bayesian isotope mixing model estimating the contribution of N_2 fixation and NO_3^- to zooplankton collected at stations in Campeche Bay (CB) and the central Gulf of Mexico. Estimates are based on the $\delta^{15}N$ values of copepods (left panel) and small size fraction ($<1000 \mu m$) of zooplankton (right panel).

2.4 Discussion

2.4.1 Temporal variability in zooplankton

Copepods and euphausiids showed significant albeit small (up to 0.6 and 0.4‰, respectively) differences in mean $\delta^{15}N$ values between cruises, with higher values during the winter cruise (XIXIMI-03) reflecting a higher availability of NO_3^- for primary production. Muller-Karger *et al.* (2015) examined the seasonal and spatial variability of hydrographic conditions in the deep water region of the GM between 1975 and 2012, and found that seasonal differences in the wind velocity and near-surface warming led to a deeper MLD during winter (~ 100 m) than in summer (20-30 m). They estimated a higher net primary production during the winter months, which was likely fueled by an increased influx of nutrients into the euphotic zone due to the deepening of the mixed layer (Muller-Karger *et al.*, 1991). Likewise, Damien *et al.* (2018) reported that the MLD in the central region of the GM could reach the nitracline (defined by the depth of the 1

mmol m⁻³ NO₃⁻ concentration) during the winter months, although integrated primary production was not higher.

Regardless of the impact on primary production, there appears to be higher supply of NO₃⁻ from the subsurface to the euphotic layer during the winter, leading to the higher δ¹⁵N values of zooplankton. Indeed, results from the mixing model indicate that close to 60% of the N assimilated by zooplankton in winter was derived from NO₃⁻. This high contribution could be associated with the injection of subsurface nitrate during the due to increased mixing, as well as a higher winter availability of picoplankton biomass living around the nitracline (with presumably higher δ¹⁵N), compared with the lower picoplankton biomass found in the gulf during the summer (Linacre *et al.*, 2015; 2019).

On the other hand, size-fractionated zooplankton did not show differences in isotopic composition between the two summer cruises, when the GM exhibits strong stratification of the upper layer due to surface heating and weaker winds. Under these conditions, the vertical flux of NO₃⁻ into the euphotic zone is absent or limited (Muller-Karger *et al.*, 2015, Damien *et al.*, 2018). The low (2.8±0.7‰ in the SF) δ¹⁵N values of zooplankton during the summer indicate N₂ fixation by diazotrophs is an important source of N for the upper layer.

2.4.2 Mechanisms for the incorporation of light nitrogen into lower trophic level consumers

Our mixing model indicated a higher contribution of N₂ fixation of 50-70% during the summer, which is similar to previous reports of diazotroph contribution for the west-central Atlantic Ocean and some regions of the GM (McClelland *et al.*, 2003; Mulholland *et al.*, 2006; Holl *et al.*, 2007; Landrum *et al.*, 2011). In addition to bulk analysis of isotopic composition, compound-specific stable isotope analysis (CSIA) of individual amino acids (AAs) has become a powerful tool in trophic ecology in the last decade because the AAs that show little or no trophic enrichment. The so-called source AA, such as phenylalanine (Phe), reflect the isotopic baseline since their isotopic composition changes little with trophic position (McClelland and Montoya, 2002; McMahon *et al.* 2016). Hence, δ¹⁵N_{Phe} values are complementary to bulk isotope ratios in terms of establishing source contributions. For the tropical Atlantic, measurements of both bulk δ¹⁵N and δ¹⁵N_{Phe} of zooplankton indicated that *Trichodesmium* was responsible for increasing N availability and supporting the food web, as reflected in the relatively low isotopic composition of the 1000-2000 μm size fraction (McClelland and Montoya, 2002; McClelland *et al.*, 2003). Recently, a study in the Baltic Sea using

$\delta^{15}\text{N}_{\text{bulk}}$ and $\delta^{15}\text{N}_{\text{Phe}}$ values of POM and zooplankton found that N_2 fixation by cyanobacteria contributed up to 84 and 65% of the N in small (100-300 μm) and large (>300 μm) zooplankton, respectively, during the season with high water column stratification (Loick-Wilde *et al.*, 2018). Stratification was also associated with a lower subsurface transport of new NO_3^- to surface waters.

While N_2 fixation rates have not been reported for the central and southern GM, the few studies available for the northern gulf indicate that *Trichodesmium* can be a significant source of new N. Mulholland *et al.* (2006) reported that on the West Florida Shelf *Trichodesmium* fixation rates (2.8-17.1 nmol N colony⁻¹ d⁻¹) were within the range reported for other oceanic regions where N_2 fixation is relatively important. They also reported that *Trichodesmium* is more abundant in the summer, with an average density of 20 colonies L⁻¹ and >1000 colonies L⁻¹ during blooms, than in autumn/winter, when an average abundance of 0.75 colonies L⁻¹ was observed. Higher nitrogen fixation in summer is consistent with the lower isotopic composition of zooplankton that we found during that season. Holl *et al.* (2007) found a gradient in *Trichodesmium* N_2 fixation from the continental shelf to the open ocean in the northwestern GM; deeper, more oligotrophic waters showed higher fixation rates that were reflected in lower $\delta^{15}\text{N}$ values of zooplankton and a higher (60%) estimated contribution of N fixation. On the other hand, Aldeco *et al.* (2009) reported the presence of *Trichodesmium* in the Bay of Campeche (1.5 to 175 trichomes L⁻¹). Although these abundances were lower than those reported by Holl *et al.* (2007) for the northwestern gulf, they indicate the presence of *Trichodesmium* and hence occurrence of N fixation within the bay.

Studies focused on unicellular cyanobacteria and heterotrophic picoplankton as sources of new N in the GM are still lacking, despite their importance in many oceanic regions (Zehr and Capone, 2020) including the northwestern Atlantic (Martínez-Pérez *et al.*, 2016). Mulholland *et al.* (2016) reported that, for the eastern GM, unicellular diazotrophs fixation rates were similar to those of *Trichodesmium* under background (low) abundance, but did not evaluate the fate of fixed N_2 and its contribution to the dissolved N pool or higher trophic levels. The isotopic composition of zooplankton in our study shows that N_2 fixation in the central (and southern) GM could be the most important source of new N, especially during the summer.

Several pathways may link the low $\delta^{15}\text{N}$ values of diazotrophs with those of zooplankton. Mulholland *et al.* (2006) found that *Trichodesmium* blooms could release 52% of the fixed N to the dissolved pool, providing the necessary N to support blooms of *Karenia brevis*, a red tide-forming dinoflagellate. A study in the New Caledonia lagoon in the south Pacific reported that a lineage of unicellular diazotrophic cyanobacteria (UCYN-C) released about 21% of diazotroph-derived nitrogen (DDN) as DON and NH_4 , which

was later assimilated by picophytoplankton and diatoms (Bonnet *et al.*, 2016). Studies suggest that *Trichodesmium* is more efficient in transferring DDN to non-diazotrophs compared with UCYN-C, and that DDN is quickly assimilated by non-diazotrophic plankton such as diatoms as well as bacteria, while DON accumulates in the dissolved pool (Berthelot *et al.*, 2016). Another potential source of light N to the dissolved pool is decaying *Trichodesmium* blooms (Berman-Frank *et al.*, 2004, Mulholland, 2004), which can release high amounts of DDN as NH_4 that is subsequently assimilated by picophytoplankton, bacteria and diatoms (Bonnet *et al.*, 2018).

In oligotrophic regions such as the GM the microbial loop has an important role in N cycling, and *Prochlorococcus* is the most important taxa of picophytoplankton with more than 60% of biomass that may be responsible for about half of photosynthetic biomass supporting secondary production (Linacre *et al.*, 2015; 2019). Protozoans could be feeding on *Prochlorococcus*, thus acting as an intermediate trophic step between phytoplankton and zooplankton that would increase $\delta^{15}\text{N}$ values of zooplankton due trophic isotope discrimination. However, but Gutiérrez-Rodríguez *et al.*, (2014) analyzed $\delta^{15}\text{N}$ values of bulk samples and of algae and protozoan consumers, and CSIA and reported that TEFs were very low or negligible in controlled experiment. Therefore, microzooplankton feeding on protozoans would reflect the isotopically light DDN assimilated by *Prochlorococcus*.

Another pathway for the incorporation of isotopically light nitrogen into consumers is through zooplankton grazing directly on diazotrophs. In the western tropical North Atlantic, grazing of diatom-diazotroph associations and of *Trichodesmium* by calanoid and harpacticoid copepods has been documented using molecular analysis of gut contents (Conroy *et al.*, 2017). Likewise, in the western South Pacific, 25-70% of zooplankton biomass may be supported by fixed nitrogen (Hunt *et al.*, 2016). Those authors reported zooplankton grazing directly on UCYN-C aggregations 100-500 μm in size, as well as feeding on *Trichodesmium* and *Richelia* associated with the diatom *Rhizosolenia*, leading to low $\delta^{15}\text{N}$ values of zooplankton. Studies that document zooplankton grazing on *Trichodesmium* colonies are scarce, but in the eastern Indian Ocean, low $\delta^{15}\text{N}$ values of zooplankton have been associated with zooplankton grazing on these diazotrophs (Raes *et al.*, 2014). However, some harpacticoid copepods may be able to graze on *Trichodesmium* (O'Neil and Roman, 1994), although for some copepod taxa it may be toxic (Hawser *et al.*, 1992). Therefore, feeding on diazotrophs could also be a mechanism for the incorporation of low $\delta^{15}\text{N}$ values into zooplankton in the GM.

2.4.3 Comparison of $\delta^{15}\text{N}$ values of copepods and euphausiids and size fractions

The $\delta^{15}\text{N}$ values of copepods were lower than those of euphausiids during the three cruises in which these groups were sampled. The mean difference in $\delta^{15}\text{N}$ values was 1.0 ($\pm 0.9\text{‰}$), which is roughly one half of a trophic level based on empirical TEFs for zooplankton of ca. 2‰ (Vanderklift and Ponsard, 2003; Henschke *et al.*, 2015; Schwamborn and Giarrizzo, 2015). There was a significant but low correlation ($R=0.32$) between the isotopic composition of both groups, which suggests that N source contributions found in copepods are also reflected in euphausiids. Although we did not analyze the feeding preferences of copepods and euphausiids, small copepods (<1 mm) that were abundant in all samples play an important role as grazers of phytoplankton and also feed on bacterioplankton and protists (Turner, 2004), which likely reflects their lower trophic level. However, differences between euphausiids and copepods $\delta^{15}\text{N}$ values at each station mostly ranged from -1 to 3‰ (Fig. 18), which implies that at some stations euphausiids may be feeding at similar trophic levels as copepods or up one trophic level higher.

The $\delta^{15}\text{N}$ values of euphausiids and copepods will depend on the baseline isotopic composition as well as the feeding strategies of individual taxa. Some studies indicate that large carnivorous copepod species have similar $\delta^{15}\text{N}$ values than some euphausiid taxa, while smaller omnivorous or herbivorous copepods can have lower $\delta^{15}\text{N}$ values (Bănaru *et al.*, 2014; Henschke *et al.*, 2015). Other authors found that the trophic position of euphausiids was similar or lower than that of carnivorous copepod species, although omnivorous or herbivorous copepods showed lower trophic levels (Gorbatenko *et al.*, 2015; Kürten *et al.*, 2016).

A recent study of community composition in the deep water region of the GM using molecular tools reported that the dominant families of calanoids were *Calanidae*, *Subeucalanae*, *Metridinidae*, and *Euphausiidae* in the case of euphausiids (Gaona-Hernández 2019, Martínez *et al.*, 2021, Herzka 2021). Also, studies in the deep water of the GM indicate that the most abundant genera of copepods are *Farranula*, *Undinula*, *Clausocalanus*, *Euchaeta*, *Pleuromamma*, which have various feeding habits that include herbivory, omnivory and carnivory (Hopkins 1982; Benedeti *et al.*, 2016). The more abundant species of euphausiids are *Stylocheiron carinatum*, *S. suhmi*, *Euphausia tenera* and *E. americana*, at least during late spring and summer (Castellanos and Gasca 1999; Gasca *et al.*, 2001). Gut content analyses of euphausiids collected from the deep water region of the eastern GM indicate they exhibit a variety of feeding strategies; larger species feed on copepods and other crustaceans, while smaller-sized species feed on small crustaceans, phytoplankton, protozoa, and detritus (Kinsey and Hopkins, 1994). Given that we analyzed copepods and euphausiids as a group, the isotopic values integrate the variability due to

differences in feeding habits between species. While future studies could focus on a single species or groups of species with similar and narrow prey preferences, the challenge will be obtaining sufficient material for analysis.

The well-characterized diel vertical migration of euphausiids (Castellanos and Gasca 1999; Biggs and Ressler 2001) could contribute to their higher $\delta^{15}\text{N}$ values compared with that of copepods. The $\delta^{15}\text{N}$ values of particulate organic matter have been reported to increase with depth in oligotrophic waters due to changes in the composition of POM (Hannides *et al.*, 2013) or remineralization of organic matter below the mixed layer (Landrum *et al.*, 2011). Ursella *et al.*, (2021) evaluated diel vertical migration in the western GM using acoustic backscatter data collected throughout the water column, and found clear evidence of migration between mesopelagic depths and the surface layer that was likely attributed to the migration of euphausiids and mesopelagic fishes. Some species of euphausiids avoid high temperatures in the upper layer during the summer months, and feed on copepods that are found below the thermocline (Buchholz and Buchholz 2013). Feeding at depth on organic matter enriched in ^{15}N would therefore increase the $\delta^{15}\text{N}$ values of zooplankton.

The mean difference between the small and large size fractions of zooplankton was $\sim 0.5\text{‰}$, which may be attributed to differences in the species composition between size fractions, with larger individuals in the larger size fraction feeding at higher trophic levels. Bănaru *et al.*, (2014) reported similar differences between LF and SF ($\sim 0.5\text{‰}$) in the coastal Mediterranean Sea during the summer. In the western GM, Holl *et al.*, (2007) reported $\delta^{15}\text{N}$ values of size-fractionated zooplankton collected in the deep water region, and the difference between the 500-1000 μm and 1000-2000 μm size fractions was around 1.5‰, indicating that larger zooplankton fed at a higher trophic level. In contrast, Figueiredo *et al.*, (2021) reported no significant differences between the 500-1000 and 1000-2000 μm size fractions in oceanic waters off northeastern Brazil. This was attributed to a high taxonomic richness in the 1000-2000 μm size fraction, which included chaetognaths, fish larvae, euphausiids and salps, some of which are filter feeders while the rest are carnivorous predators.

In our study, the estimates of the source contribution based on zooplankton groups (copepods and euphausiids) are not directly comparable to those based on size fractions (SF and LF), although both are likely reflecting feeding by primary and secondary consumers. The higher correlation in the isotopic composition of the small and large size fractions of zooplankton compared with that of copepods vs euphausiids suggests that size fractions may better reflect the trophic transfer of N at the base of the food

web. Specifically, the small size fractions appeared to be more sensitive to differences in source contribution, and may be a better indicator of baseline isotope ratios.

2.4.4 Isotopic composition of zooplankton relative to mesoscale eddies

The $\delta^{15}\text{N}$ values of zooplankton collected in ACEs were significantly lower than in CE and NE (by an average of 1.2 and 0.7‰, respectively). In our PCA, the ^{15}N depleted zooplankton collected at ACE stations was associated with deeper 25.5 kg m⁻³ isopycnals and lower integrated NO_3^- concentrations. The deepening of the isopycnals leads to an extension of NO_3^- -depleted waters throughout the euphotic zone, and therefore N_2 fixation becomes the dominant source of N supporting primary production.

Moreover, our mixing model results indicate N_2 fixation was the most important N source for copepods (~60% contribution) and the SF (~78%) at ACE stations. Holl *et al.*, (2007) also estimated a similar *Trichodesmium* contribution (60%) in the oceanic oligotrophic waters of the western GM. Similar differences in the isotopic composition of POM and zooplankton sampled in ACE and CE in the GM and other seas have been reported previously (Waite *et al.*, 2007; Dorado *et al.*, 2012; Wells *et al.*, 2017; Waite *et al.*, 2019). For example, Dorado *et al.*, (2012) reported that the low $\delta^{15}\text{N}$ values of zooplankton in ACE and oceanic waters (2.6‰) were associated with the presence of *Trichodesmium*, compared with those in neritic waters (5.4‰) influenced by the Mississippi River. Wells *et al.*, (2017) found lower $\delta^{15}\text{N}$ values of zooplankton in an ACE compared with a CE, and suggested the 1.7-2.8‰ difference is due to the presence of diazotrophs and the higher vertical flux of NO_3^- into the euphotic layer in CE.

CE stations showed higher integrated NO_3^- concentrations ($1731 \pm 316 \text{ mmol m}^{-2}$) compared with NE ($1055 \pm 337 \text{ mmol m}^{-2}$) and ACE ($412 \pm 224 \text{ mmol m}^{-2}$), and NO_3^- contributed ~65% of N to copepods and ~41% to the SF. Results of the PCA indicate the isotopic composition of zooplankton had a positive correlation with the integrated NO_3^- and surface chl a concentrations, and a negative correlation with the depth of the 25.5 isopycnal. This suggests that the shallowing of the nitracline in CE leads to an increased availability in subsurface NO_3^- in the euphotic zone, probably higher primary production and higher nitrogen isotope ratios in the food web. Higher phytoplankton biomass in CE than in ACE have been reported (Wormuth *et al.*, 2000; Linacre *et al.*, 2015; Wells *et al.*, 2017), which has been attributed to a higher vertical flux of nutrients to the upper layer (Biggs and Ressler 2001).

The presence of mesoscale eddies and local upwelling can lead to fine-scale (tens of km) differences in nitrogen sources and hence the isotopic composition of zooplankton. For example, stations in the northeastern reaches of our study area (stations A8, A9 and A9-A, Fig. 17) that were within the region of influence of the LC showed large differences of up to 5‰ in $\delta^{15}\text{N}$ values during XIXIMI-01 (Fig. 2a, 2b and 2c). Zooplankton from station A9-A that was located in the center of the LC ACE Franklin showed low $\delta^{15}\text{N}$ values (1.5 ‰), while A8 and A9 (classified as NE) fell along the edge of the eddy and showed the highest $\delta^{15}\text{N}$ values (6.2-6.4‰). Those stations fell in regions of shear between counter-rotating eddies, which favors upwelling of water richer in NO_3^- with higher $\delta^{15}\text{N}$ values from below the nitracline to the euphotic zone, a known mechanisms leading to the increase in primary producer biomass along their perimeter (Zimmerman and Biggs, 1999; Wormuth *et al.*, 2001; Kürten *et al.*, 2016; Waite *et al.*, 2007). Also, the transport of upwelled water due to the interaction of the Loop Current with the Yucatan Channel has been reported for this region and is observed as a high chlorophyll plume that extends into the gulf (Otis *et al.*, 2019), and could lead to high $\delta^{15}\text{N}$ values in zooplankton.

2.4.5 Regional patterns in the isotopic composition of zooplankton

The $\delta^{15}\text{N}$ values of copepods and SF were lower in the central gulf during XIXIMI-01, -02 and -04 than in the Bay of Campeche, indicating a limited regional difference in the relative contribution of N sources. The copepod-based mixing model indicated that on average N_2 fixation was slightly more important in the central region (~53%), while NO_3^- was more important in BC (~56%). Le-Alvarado *et al.*, (2021) also reported lower $\delta^{15}\text{N}$ values of small zooplankton (335-1000 μm) for the central gulf and higher $\delta^{15}\text{N}$ values for the Bay of Campeche during summer, especially at stations in the southern reaches. However, the $\delta^{15}\text{N}$ values of zooplankton did not show differences between regions during XIXIMI-03, -05.

The lack of a clear difference in the mean regional contribution of fixed N or NO_3^- may be due to strong influence of mesoscale eddies, which influence the density structure of the water column and generate spatial variability in the supply of NO_3^- to the euphotic layer. During XIXIMI-05, for example, the Loop Current eddy Poseidon had recently detached from the LC, there were three CE in the central GM, and the remnants of Olympus was in the western GM at ~22-24° N.

However, some stations in the western, southern and eastern reaches of BC did exhibit higher (3.5-6.0‰) $\delta^{15}\text{N}$ values of zooplankton, which is probably due to the increased importance of subsurface NO_3^- . For

example, applying the mixing model to stations along the eastern margin of BC indicates that NO_3^- contributed 70-80% of the N. BC is characterized by a semi-permanent cyclonic eddy (Pérez-Brunius *et al.*, 2013), in which divergent circulation and a shallowing of the pycnocline inject NO_3^- into the euphotic zone (Salas de León *et al.*, 2004; Durán-Campos *et al.*, 2017). Additionally, upwelling occurs during May to August over the Yucatan Shelf (also known as the Campeche Bank) and along the Veracruz-Tabasco shelves, and the prevailing circulation transports nutrient-rich water to the deep water region (Zavala-Hidalgo *et al.*, 2003; 2006; Martínez-López and Zavala-Hidalgo, 2009). Also, the high discharge of the Papaloapan, Coatzacoalcos and Grijalva-Usumacinta river systems during June-October could lead to higher $\delta^{15}\text{N}$ values due to nutrient inputs that are transported to the deep water region by convergent circulation over the shelf that generates offshore transport (Salmerón-García and Zavala-Hidalgo, 2011).

Chapter 3. A Gulf-wide synoptic isoscape of zooplankton isotopes ratios reflects regional nitrogen sources in the Gulf of Mexico

3.1 Introduction

Stable isotope analysis (SIA) of carbon ($\delta^{13}\text{C}$) and nitrogen ($\delta^{15}\text{N}$) in organic matter, including organisms, is an ecological and biogeochemical tool that provides information on food web trophic structure, sources of primary production and nutrient inputs (Post, 2002; Layman et al., 2012; Sigman and Fripiat, 2019). $\delta^{13}\text{C}$ values can be used to track carbon sources in the ocean, allowing for discrimination between phytoplankton, macroalgae and terrestrial C3 and C4 plants due to differences in photosynthetic pathways and the isotopic composition of the inorganic carbon pool, as well as growth rates (Fry and Sherr, 1984; Yamamuro et al., 1995; Ohkouchi et al., 2015 and references therein).

Variations in the isotopic composition of dissolved inorganic nitrogen (DIN) result from differences in the extent of isotope discrimination that take place during assimilation, nitrification, denitrification, N_2 fixation and remineralization (Sigman and Fripiat, 2019), and can also vary due to the mixing of water masses (Marconi et al., 2014). Nitrate (NO_3^-) from subsurface waters, or new nitrogen, has a global mean isotopic composition ($\delta^{15}\text{N-NO}_3$) of ca. 5‰ (Sigman and Casciotti, 2001), and is enriched in ^{15}N compared with fixed N_2 (-2 to 0‰; Carpenter et al., 1999, Montoya et al., 2002). Riverine DIN discharged in coastal areas has $\delta^{15}\text{N}$ values around 5‰ due to denitrification and inputs of waste waters and manure, but can occasionally be higher (Wissel and Fry, 2003; BryantMason et al., 2013). Denitrification, which predominates in waters with low oxygen concentrations, has a high isotope discrimination ($\sim 15\text{-}25\%$) that leads to residual nitrate enriched in ^{15}N compared with subsurface NO_3^- (Kritee et al., 2012). The assimilation of NO_3^- by primary producers has an isotope discrimination of $\sim 5\%$; when only part of the NO_3^- pool is assimilated, and the residual nitrate is enriched in ^{15}N . However, when all of the NO_3^- is assimilated, as is the case in the euphotic layer of oligotrophic systems (Somes et al., 2010), the water column behaves like a closed system and the isotopic composition of primary producers will reflect that of the DIN pool. Remineralization of organic matter leads to lower $\delta^{15}\text{N-NO}_3$ values than the isotopic composition of particulate organic matter ($\delta^{15}\text{N-POM}$), with an isotope discrimination of around 3‰ (Sigman and Fripiat, 2019).

Differences in the isotopic composition of the dissolved inorganic nitrogen (DIN) sources are reflected in primary producers (Sigman and Fripiat, 2019). In marine systems, the $\delta^{15}\text{N-POM}$ has been used to infer sources and geochemical processes underlying the nutrient pool supporting primary and secondary production, and is considered a proxy for phytoplankton (Waite et al. 2007; Kolasinki et al. 2012). However,

POM isotopic composition varies over small spatial and temporal scales due to changes in phytoplankton community composition, the rapid assimilation of pulsed nutrient inputs and rapid isotope turnover rates of small organisms, with isotope integration times of the order of days (Kürten et al., 2013; Llorrain et al., 2015). This implies frequent sampling is necessary for its adequate characterization of carbon and nitrogen sources at the base of the food web.

In comparison, mesozooplankton integrate the isotopic composition of their food sources through time, smoothing the variation in POM (Hou et al., 2013). Zooplankton consume phytoplankton and microzooplankton, and hence feed at the base of the food web (Turner, 2015). The $\delta^{13}\text{C}$ and $\delta^{15}\text{N}$ values of zooplankton can serve as a proxy for the isotopic baseline since they integrate the isotopic composition over longer time periods (weeks) than POM (Gorovkhova and Hansson, 1999; Schmidt et al., 2004). However, estimating source contributions based on zooplankton SIA requires estimates of the trophic discrimination factor (TDF), which is an empirically derived quantitative estimate of the isotope discrimination between consumers and their food sources. TDFs are consistently small ($\sim 1\%$) in the case of $\delta^{13}\text{C}$ values; carbon sources can thus be tracked through the food web (Post, 2002). On the other hand $\delta^{15}\text{N}$ values can be used to track N sources as well as for estimating trophic level, given TDFs of around 2-4‰ (Post, 2002, Vanderklitf and Ponsard, 2003, McCutchan et al., 2003). The trophic enrichment in the heavy isotope observed in consumer tissues implies that the nitrogen excreted by heterotrophs is lighter (Vanderklitf and Ponsard, 2003).

The $\delta^{13}\text{C}$ and $\delta^{15}\text{N}$ values of zooplankton have been successfully used to infer nitrogen sources and estimate their fractional contribution to secondary production using mixing models (Hernández-Sanchez et al., 2022; Chen et al., 2018; Le-Alvarado et al., 2021). They have also been used to establish regional and latitudinal patterns in the biogeochemical processes that dominate nitrogen cycling (McMahon et al., 2013), examine seasonal changes in N sources (El-Sabaawi et al., 2013; Kurle and McWhorter, 2017; Troina et al., 2020) and evaluating the importance of N derived from N_2 fixation vs. subsurface nitrogen (Landrum et al., 2011). For example, copepods have higher $\delta^{13}\text{C}$ values onshore compared with offshore, which has been linked to differences in the community composition of phytoplankton (Perry et al., 1999). In the Red Sea, high $\delta^{13}\text{C}$ and low $\delta^{15}\text{N}$ values of zooplankton in the northern region are associated with the presence of the nitrogen fixing *Trichodesmium*, whereas lower $\delta^{13}\text{C}$ and higher $\delta^{15}\text{N}$ values are associated with N fluxes of subsurface NO_3^- toward the south (Kürten et al., 2016). Differences in zooplankton $\delta^{15}\text{N}$ values have been found between anticyclonic and cyclonic eddies, which have been attributed to whether subsurface DIN reaches the euphotic layer and the contribution of N from N_2 fixation (Waite et al., 2007; Henschke et al., 2015).

The Gulf of Mexico (GM) is a marginal ocean basin surrounded by Mexico, the United States, and Cuba. The circulation and hydrography of the central gulf's upper waters (0-1000 m) are strongly influenced by the Loop Current (LC), which forms from the Yucatan Current and transports water from Caribbean Sea through the Yucatan channel and which exits the gulf through the Straits of Florida (Hamilton et al., 2018). The LC detaches anticyclonic mesoscale eddies periodically, and Loop Current eddies (LCEs) transport water masses into the central and western GM that mix with gulf waters when they dissipate (Oey et al., 2005; Cervantes-Diaz et al. 2021). During the summer, high SST and weaker winds lead to stratification and a shallow mixed layer, preventing vertical fluxes of subsurface the NO_3^- in the central GM (Muller-Karger et al., 2015, Pasqueron De Fommervault et al., 2017). Within the Bay of Campeche in the southern gulf, there is a semi-permanent cyclonic eddy that pumps subsurface water to the euphotic zone due to a shallowing of the pycnocline (Klein and Lapeyre, 2009; Pérez-Brunius et al., 2013; Durán-Campos et al., 2017).

Some studies indicate N_2 fixation may be the most important source of new N supporting secondary production in the oceanic GM, particularly during the summer months or during blooms of diazotrophs such as *Trichodesmium* (Mulholland et al., 2006; Holl et al., 2007; Landrum et al., 2011; Hunt et al., 2016). Over the Yucatan shelf, positive anomalies of chl *a* has been reported for the inner shelf during the summer months (Zavala-Hidalgo et al., 2006), upwelled water produced these positive anomalies due to interaction between Loop Current and topography in the eastern Yucatan shelf then was transported across the shelf (Merino, 1997; Jouanno et al., 2018). Along the shelves, nutrient inputs from rivers, in particular the Mississippi-Atchafalaya river system in the north and the Grijalva-Usumacinta in the south, can lead to high inputs of terrestrial carbon and inorganic nitrogen from various sources that include manure, waste water treatment, and fertilizers (Alexander et al., 2008). In the Mississippi-Atchafalaya rivers, high nutrient inputs have led to phytoplankton blooms and high water column respiration, which coupled with water column stratification leads to decreases dissolved oxygen concentrations in the subsurface and sediments that favors denitrification (Rabalais et al., 2002).

Isoscapes, or maps that reflect the spatial distribution of the isotopic baseline, can reveal geochemical gradients that allow for inferences regarding nutrient cycling, migration patterns of large organisms and the detection of isotopic baseline shifts due to changes in nutrient sources (Hobson et al., 2010; McMahon et al., 2013; Rabadaugh, et al. 2013). For example, zooplankton sampled in the Southern Ocean showed a latitudinal gradient, with low $\delta^{15}\text{N}$ values in the north compared with the south that was associated with a productivity gradient due to iron limitation (Brault et al., 2018). McMahon et al. (2013) generated isoscapes for the Atlantic Ocean basin based on the $\delta^{13}\text{C}$ and $\delta^{15}\text{N}$ values of zooplankton, and found low

(~0-2‰) $\delta^{15}\text{N}$ values in the subtropical western Atlantic and the Caribbean Sea that were attributed to inputs of fixed nitrogen. Recently, Le-Alvarado et al. (2021) used basin-wide isoscapes for the GM based on $\delta^{13}\text{C}$ and $\delta^{15}\text{N}$ values of zooplankton collected during the summer of 2017 to infer the foraging habitat and trophic position of migratory yellowfin tuna caught in the southern GM. They found a pronounced latitudinal gradient in the $\delta^{15}\text{N}$ values of zooplankton, with the highest $\delta^{15}\text{N}$ values in the northern gulf associated with the region of influence of the Mississippi-Atchafalaya Rivers, and lower values in the central oligotrophic gulf, which were presumably attributed to nitrogen fixation. However, studies to date in the GM have yet to examine regional N source contributions.

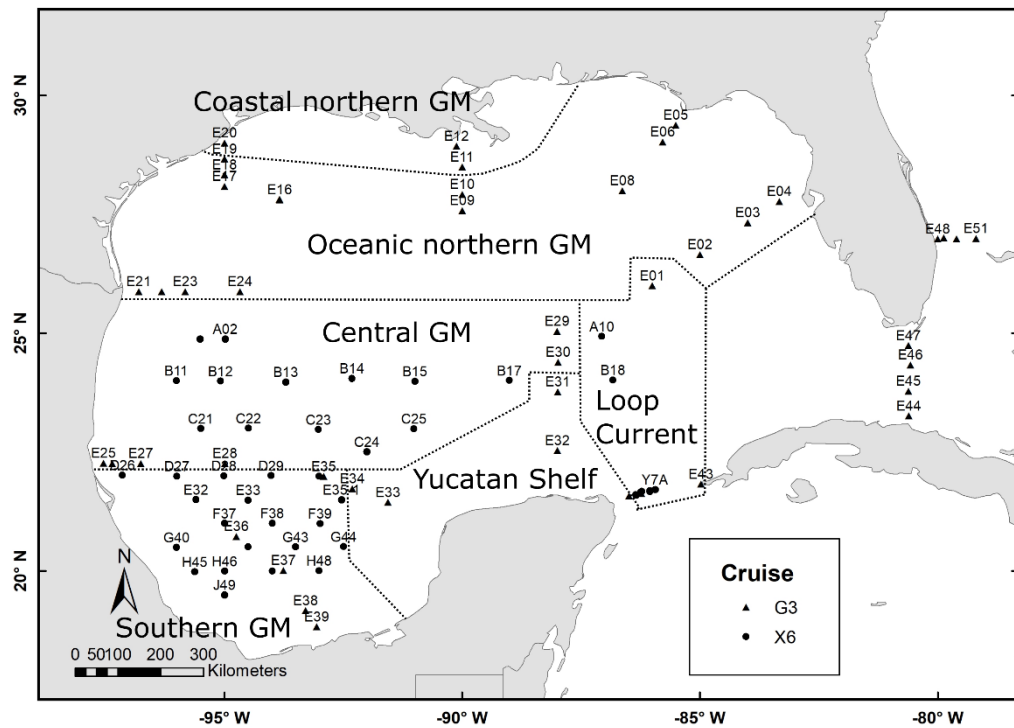


Figure 10. Zooplankton sampling stations in the Gulf of Mexico during the XIXIMI-06 (X6) and GOMECC-03 (G3) cruises held during the summer of 2017. The six regions considered for which fractional contributions of different N sources were calculated are depicted.

Here, I estimate the fractional contribution of different N sources throughout the GM based on the $\delta^{13}\text{C}$ and $\delta^{15}\text{N}$ values of zooplankton reported by Le-Alvarado et al. (2021) for the summer of 2017. I subdivided the GM into regions based on likely N sources, the known predominant circulation patterns, and chl *a* concentration variability, and calculated the relative importance of each N source using Bayesian isotope mixing models. To apply the mixing models, isotopic endpoints were obtained based on literature-derived

regional isotope ratios for POM. Given that variations in the $\delta^{15}\text{N-NO}_3^-$ have been reported for the GM, I also evaluate how these differences impact regional source contributions. I hypothesized that in the northern Gulf of Mexico denitrification is the most important source due to the inputs of the Mississippi-Atchafalaya River systems, while in the central GM and in the region of influence of the Loop Current, N_2 fixation is the most important source. In contrast, in the Bay of Campeche NO_3^- is the predominant source due to the presence of regional upwelling, cross-shelf transport and the presence of the semi-permanent cyclonic eddy. Lastly, I examine whether isotope ratios of zooplankton reflect those of POM based on samples collected at the same stations in which zooplankton were sampled.

3.2 Methods

3.2.1 Nitrogen and carbon sources in the Gulf of Mexico basin

Low $\delta^{15}\text{N}$ values of zooplankton (1.8‰ to 4‰) have been associated with high N_2 fixation rates measured in GM during the summer (Holl et al., 2007), and Dorado et al. (2012) reported low $\delta^{15}\text{N}$ values of zooplankton in the northern oceanic GM ($2.8 \pm 1.4\text{‰}$) suggesting that N_2 fixation by *Trichodesmium* is an important N source in the LC and in LCE. In contrast, Knapp et al. (2021) and Kelly et al. (2021), based on indirect estimates, reported low N_2 fixation rates in the GM suggesting that N_2 fixation is too small to be considered as a relevant N source; these authors also suggested that the low $\delta^{15}\text{N}$ values of POM were due to remineralization of primary producer supported by subsurface nitrate (Knapp et al., 2021; Kelly et al., 2021). On the other hand, cyclonic eddies with divergent conditions at their core lead to a shallower nitracline and pumping of subsurface NO_3^- to the euphotic zone (Durán-Campos et al., 2017), while transport of NO_3^- toward the surface can also occur due to a deepening of the mixed layer in winter (Muller-Karger et al., 2015; Damien et al., 2018). Important inputs of N into the gulf also occur through the discharge of the Mississippi-Atchafalaya river system, which is the major source of terrestrial organic matter and nutrients to the northern GM shelf. Low $\delta^{13}\text{C}$ values of POM have been reported compared with the reported in the open ocean of the northern shelf GM (Bianchi et al., 2007; Dorado et al., 2012; Cai et al., 2015; Wells et al., 2017). In the northern GM shelf, a shift from terrestrial to marine sources has been reported with lower $\delta^{13}\text{C}$ values of POC close to the shore and higher $\delta^{13}\text{C}$ values of POC with increased salinity (Cai et al., 2012); low $\delta^{13}\text{C}$ values near shore have been associated with the contribution of terrestrial C_3 plants (Bianchi et al., 2007; Cai et al., 2015). On the other hand, the higher $\delta^{15}\text{N}$ values from the Mississippi-Atchafalaya River have been associated with different sources including manure,

waste water, and agriculture occurring in the upper Mississippi River and tributaries, and denitrification in the lower basin (Chang et al., 2002; BryantMason et al., 2013). Hypoxic conditions have been reported for the Mississippi-Atchafalaya River delta during the spring and summer (Rabalais et al., 2002; 2001; Bianchi et al., 2010), which are attributed to high riverine nutrient and organic matter loads leading to intense phytoplankton blooms and high water column respiration, in combination with stratification of the water column leading to a decrease in dissolved oxygen concentrations in the subsurface (Rabalais et al., 2002). Hypoxia favors denitrification in the sediments, which increases the $\delta^{15}\text{N}$ values of the remnant NO_3^- pool since this process has an isotope discrimination against ^{15}N as high as $\sim 30\text{-}35\text{‰}$ (Heaton, 1986). In the Mississippi Sound, $\delta^{15}\text{N}$ values of between 8.2‰ and 11.1‰ have been reported for phytoplankton and POM (Chanton and Lewis, 1999; Moncreiff and Sullivan 2001). On the western Florida Shelf, a latitudinal pattern in $\delta^{15}\text{N}$ values of POM has been documented, with higher values on the northernmost samples ($\sim 6\text{-}7\text{‰}$) compared with those from the south ($\sim 3\text{-}5\text{‰}$) and $\delta^{13}\text{C}$ values with a nearshore-offshore pattern with higher values ($\sim 26\text{‰}$) in the coastal samples compared with oceanic samples ($\sim 24\text{‰}$; Radabaugh et al., 2013). In the southern GM, the Grijalva-Usumacinta River system represents the most important source of land-derived freshwater and nutrients and a mean $\delta^{15}\text{N}$ value of POM = $4.6 \pm 0.5\text{‰}$ in the lower river region has been reported (Sepulveda-Lozada et al., 2015).

3.2.2 Oceanographic surveys

Two oceanographic cruises, XIXIMI-06 and GOMECC-3, were conducted concurrently during August and September 2017. A total of 93 zooplankton samples were collected throughout GM with oblique tows using a 60 cm diameter bongo equipped with $335\ \mu\text{m}$ mesh nets (Fig. 10). Tows were deployed to a depth of 200 m except for shallower shelf stations where tows were done to about 20 m off the bottom. Once on board, 20% by volume of the sample was subsampled with a Hempel-Stempel pipette and frozen in Whirl-Pak bags at $-10\ \text{°C}$. Water samples for the measurement of the isotopic composition of POM were collected during XIXIMI-06 as a proxy for phytoplankton. Water was obtained at each of three depths (10, 20 and 50 m or at 10, 50 and maximum of fluorescence) with Niskin bottles mounted on a Sea Bird rosette. Samples from each depth were pooled (7-29 L total) and filtered onto pre-combusted ($500\ \text{°C}$ for 4 h) GF/F filters and frozen at $-20\ \text{°C}$.

Zooplankton samples were prepared for SIA as described in Le-Alvarado et al. (2021). Briefly, zooplankton samples were defrosted and rinsed in distilled water to remove dissolved inorganic carbon. Zooplankton

<1000 μm were separated using nitex mesh sieves cleaned with ethanol, dried, ground and placed in tin capsules to be sent to the Stable Isotope Facility at the University of California, Davis. SIA samples were processed with a PDZ Europa ANCA-GSL elemental analyzer interfaced to a PDZ Europa 20-20 isotope ratio mass spectrometer. The standard deviation of internal standards (glutamic acid, bovine liver, enriched alanine, and nylon) was between 0.04‰ and 0.07‰ for $\delta^{13}\text{C}$, and 0.05‰, 0.08‰, for $\delta^{15}\text{N}$, respectively. For POM samples, filters were cut in half to analyze carbon and nitrogen isotope ratios separately. Samples destined for $\delta^{13}\text{C}$ were treated with acid by fuming (1 M HCl treatment) to eliminate carbonates. All the samples were lyophilized. Isotope ratios of POM were analyzed with an elemental analyzer interfaced to a DELTA V isotope ratio mass spectrometer at CICESE. The standard deviation of the internal standard (glutamic acid and calcium carbonate) was 0.05‰ for $\delta^{13}\text{C}$ and 0.06‰ for $\delta^{15}\text{N}$, respectively. Isotope ratios are reported in delta (δ) notation calculated relative to Vienna Pee Dee Belemnite for $\delta^{13}\text{C}$ and atmospheric nitrogen for $\delta^{15}\text{N}$, using the following equation:

$$\delta X = \left[\frac{R_{\text{sample}}}{R_{\text{standard}}} - 1 \right] * 1000$$

where X is ^{13}C or ^{15}N , and R_{sample} and R_{standard} are the relative abundance of heavy to light isotope ratio ($^{13}\text{C}/^{12}\text{C}$ or $^{15}\text{N}/^{14}\text{N}$) for the sample and the standard, respectively. $\delta^{13}\text{C}$ and $\delta^{15}\text{N}$ values are reported in parts per thousand (‰).

3.2.3 Isoscapes.

We used the $\delta^{13}\text{C}$ and $\delta^{15}\text{N}$ values of zooplankton to create isoscapes that allowed for spatially explicit visualization of the isotopic baseline during the summer. Data from both cruises were pooled because sampling occurred concurrently. Zooplankton isoscapes were generated using ArcMap version 10.1 using an ordinary point kriging interpolation and tetraspherical semivariogram model. The $\delta^{13}\text{C}$ and $\delta^{15}\text{N}$ values of POM from samples of the XIXIMI-06 campaign were used to create an isoscape for the Mexican deep water region. These isoscapes were generated with QGIS version 3.16.6 using IWD interpolation.

3.2.4 Regionalization of the Gulf of Mexico

The GM has been regionalized based on the spatial distribution of surface chlorophyll-a and SST from remote sensing products. Most studies coincide in differentiating the shelf of the northern and southern GM from the oligotrophic central and southern (Bay of Campeche) oceanic regions (Salmerón-García and Zavala-Hidalgo, 2011; Callejas-Jiménez et al., 2012; Damien et al., 2018). The deep water region of the central GM is generally considered oligotrophic because NO_3^- concentrations are below the detection limit in the euphotic zone and chl-a concentration is low, with values around $0.1\text{-}0.7 \text{ mg m}^{-3}$ between 50 and 80 m depth at the deep chlorophyll maximum (Biggs, 1992; Salas-de-León et al., 2004; Pasqueron de Fommervault et al., 2017).

Table 2. Mean \pm SD carbon and nitrogen isotope ratios of source POM used as endpoints in isotope mixing models. The likely sources used to estimate source contributions varied regionally and are represented by X. NGMc: Coastal Northern Gulf of Mexico; NGMo: Oceanic Northern Gulf of Mexico; CGM: Central Gulf of Mexico; SGM: Southern Gulf of Mexico, LC: Loop Current region; YS: Yucatan Straight.

Source	Region to which specific sources were applied						$\delta^{13}\text{C}$ (‰)	$\delta^{15}\text{N}$ (‰)
	NGMc	NGMo	CGM	SGM	LC	YS		
N_2 Fixation	X	X	X	X	X	X	-21.9 ± 3.1	-0.9 ± 2.0
Subsurface NO_3^-	X	X	X	X	X	X	-21.0 ± 1.1	4.0 ± 0.3
Mississippi-Atchafalaya River System nitrogen	X	X					-23.1 ± 1.8	7.1 ± 0.4
Denitrification	X	X					-24.3 ± 2.5	9.8 ± 0.2
Western Florida Shelf nitrogen	X	X					-26.1 ± 2.7	5.4 ± 1.5
Grijalva-Usumacinta River System nitrogen				X			-24.4 ± 2.8	4.6 ± 0.6

Taking into account the previous considerations, in this study I divided the GM into 6 regions based on likely region-specific source contributions and also considering similarities in the spatial distribution of zooplankton isotope ratios, in order to estimate endpoint isotope ratios to apply the mixing model (Fig. 10). The regionalization was based on the premise that while some sources may play an important role in supporting primary and secondary production throughout the gulf, on a basin-wide scale other sources reflect regional contributions, as it is assumed that similarity in zooplankton isotope ratios reflect similar source contributions. Two sources were considered as contributing N gulf-wide: N_2 fixation and subsurface

NO_3^- . Inputs from the Mississippi-Atchafalaya river system, rivers that drain onto western Florida shelf, N from denitrification in the hypoxic region of the northern shelf, and the Grijalva-Usumacinta River were considered as regional sources with limited spatial extent. Although studies indicate that river inputs can reach the central GM under certain conditions, such as when LCE's interact with the gulf's northern slope (Otis et al., 2019) and during the fall in the Bay of Campeche due to the convergence of currents over the continental shelf (Martínez-López and Zavala-Hidalgo, 2009), our approach considers these inputs to be limited on a regional scale.

The regional source contributions were calculated based on published literature of values of the isotopic composition of POM. The northern GM (north of 26° N) was divided into the coastal (NGMc) and oceanic northern Gulf of Mexico (NGMo; [Table 2](#)). The likely N sources in these two regions are the Mississippi-Atchafalaya river system, river inputs to the western Florida shelf, denitrified N from the hypoxic region and the two Gulf-wide sources (fixed N_2 and subsurface nitrate). For the southern GM (SGM), the Grijalva-Usumacinta river system (GUS) and the two gulf-wide sources were included in the model. Finally, for the central GM (CGM), the Yucatan Shelf (YS) and the region of influence of the Loop Current (LC), only the Gulf-wide sources were included ([Table 2](#)).

The mean $\delta^{13}\text{C}$ and $\delta^{15}\text{N}$ values of POM for each of region was obtained from a literature review of reports for the GM (see [Table S1](#) and references therein). Data were available for Mississippi-Atchafalaya river system inputs (Macko et al., 1984; Wissel and Fry, 2005; Bianchi et al., 2007; Dorado et al., 2012), POM in regions with high inputs of denitrified N (Chanton and Lewis, 1999; Moncreiff and Sullivan, 2001), the West Florida shelf (Gu et al., 2001; Radabaugh et al., 2013), the Grijalva-Usumacitna river system (Sepulveda-Lozada et al., 2015), POM that reflects subsurface NO_3^- (Dorado et al., 2012), and POM linked to N_2 fixation (Holl et al., 2007; Wells and Rooker, 2006; Dorado et al., 2012). Isotope ratios presented in figures were extracted using Plot Digitizer software.

3.2.5 Data analysis

To test for differences in $\delta^{13}\text{C}$ and $\delta^{15}\text{N}$ values of zooplankton between regions, the Shapiro and Levene's tests were performed to assess normality and homoscedasticity of the data, respectively. Since the data did not meet the assumptions required for parametric analysis, a Kruskal-Wallis test was used. A Wilcoxon test post-hoc analysis was applied to find differences between groups. Sampling stations in the Florida

Strait and east Florida shelf from the GOMECC-3 cruise were not included in the analyses as they lie outside of the gulf six regions. The relationships between $\delta^{15}\text{N}$ values of zooplankton and POM were evaluated using linear regression analysis.

3.2.6 Application of Bayesian mixing models

Bayesian mixing models were applied to estimate the contribution of different N sources to zooplankton using the SIMMR package in R (Parnell et al., 2010). The model inputs were (1) the $\delta^{15}\text{N}$ and $\delta^{13}\text{C}$ values of zooplankton, (2) the isotope ratios of POM (mean and SD values, see [Table 2](#)) of the potential N sources for each region collected from the euphotic zone, and (3) the trophic discrimination factor for crustacean zooplankton of $\delta^{13}\text{C} = 1.0 \pm 0.6\text{‰}$, $\delta^{15}\text{N} = 2.0 \pm 0.5\text{‰}$ (Davenport and Bax, 2002; Vanderklift and Ponsard, 2003; Henschke et al., 2015). To estimate the contribution of each source, the model was applied to the zooplankton isotope ratios for all stations within each region. Model inputs for SIMMR did not include concentration dependence. The models were run with 100,000 iterations and 10,000 burnins (Phillips et al., 2014). Subsequently, maps with the fractional contribution for each source and stations within a region were generated using the IDW (Inverse Distance Weighting) interpolation method in QGIS version 3.16.6 for visualization purposes.

3.2.7 Effect of the variation of the nitrate isotope composition on source contributions estimates

To evaluate the potential effect of variations in the isotopic composition of nitrate reaching the euphotic layer on source contribution estimates, the Bayesian mixing model was applied using $\delta^{15}\text{N}$ -POM that reflects $\delta^{15}\text{N}$ - NO_3 values of subsurface nitrate reported for the western Atlantic Ocean between 400 to 600 m (scenario 1; $4.0 \pm 0.3\text{‰}$, [Table S1](#)), a value of $3.5 \pm 1.1\text{‰}$ corresponding to water samples collected in the northern GM at 26°N and $\sim 91\text{-}92^\circ\text{W}$ and at depths of 100-200 m (scenario 2; Howe et al., 2020) and $1.9 \pm 0.8\text{‰}$ reported for the western GM ($26\text{-}27^\circ\text{N}$ and $95\text{-}96^\circ\text{W}$) for samples collected at $\sim 200\text{ m}$ depth (scenario 3; Holl et al., 2007).

Table 3. Mean \pm SD carbon and nitrogen stable isotope ratios of zooplankton collected in six regions of the Gulf of Mexico during the summer of 2017.

Region	$\delta^{13}\text{C}$ (‰)	$\delta^{15}\text{N}$ (‰)
Coast and shelf of the northern Gulf of Mexico	-21.7 ± 1.1	10.4 ± 1.2
Oceanic northern Gulf of Mexico	-20.9 ± 1.0	5.0 ± 2.2
Central Gulf of Mexico	-20.1 ± 0.9	1.9 ± 0.5
Southern Gulf of Mexico	-20.4 ± 0.6	3.1 ± 0.9
Yucatan Shelf	-19.9 ± 1.0	3.8 ± 0.8
Region of influence of the Loop Current	-19.6 ± 0.4	2.3 ± 0.6

3.3 Results

3.3.1 Zooplankton, particulate organic matter isotope ratios and isoscapes

Average carbon isotope ratios of zooplankton exhibited a limited variability spanning 2.1‰ and were indicative of phytoplankton-derived primary production. Mean $\delta^{13}\text{C}$ values were lowest (-21.7 ‰) in the NGMc, ranging from -22.7 to 20.2 ‰, followed by NGMo with a mean of -20.9 ‰ (range -22.5 to -19.4 ‰). Relatively low values ~ -21.3 ‰ were observed in the SGM, especially at stations close to Grijalva-Usumacinta river (stations E38, E39 G44 and H48). The highest mean values were in stations of the Straits of Florida (-14.7 ‰) and the East Florida shelf (-17.8 ‰), which are regions close to extensive seagrass beds and macroalgae (Lamb and Swart, 2008; Dawes et al., 2004). Higher $\delta^{13}\text{C}$ values (-17.3 to -18.4 ‰) were found in the CGM, this could be possible due to contribution of remineralization of C from macroalgae rafts or *Trichodesmium* that is reported has a high $\delta^{13}\text{C}$ values compared with phytoplankton.

Mean $\delta^{13}\text{C}$ values of zooplankton varied significantly among regions (KW, $\chi^2 = 23.887$, $df = 5$, p -value < 0.001). However, post-hoc pairwise comparisons indicated that only zooplankton from the LC region had $\delta^{13}\text{C}$ values that were significantly higher than of those in the NGMo and SGM (1.3 and 0.8‰, respectively); all other comparisons did not differ statistically (Table 4). The $\delta^{13}\text{C}$ values including their limited range and lack of statistical differences among regions indicate that phytoplankton is the dominant carbon source throughout the GM.

Table 4. Wilcoxon signed-rank test post-hoc pairwise comparisons of the isotopic composition of zooplankton collected in different regions of the Gulf of Mexico. $\Delta^{13}\text{C}$ in lower left and $\delta^{15}\text{N}$ in (upper right). Bold indicates significant differences. NGMc: Coastal Northern Gulf of Mexico; NGMo: Oceanic Northern Gulf of Mexico; CGM: Central Gulf of Mexico; SGM: Southern Gulf of Mexico, LC: Loop Current region; YS: Yucatan Shelf.

	NGMc	NGMo	CGM	SGM	YS	LC
NGMc	-	0.00525	0.00525	0.00453	0.01984	0.00359
NGMo	0.9761	-	0.00048	0.01665	0.43373	0.00359
CGM	0.5619	0.5515	-	0.00027	0.00525	0.28798
SGM	0.5515	0.7778	0.9761	-	0.10234	0.00525
YS	0.7778	0.5619	1.0000	0.9761	-	0.00665
LC	0.0716	0.0044	0.1990	0.0015	1.0000	-

$\delta^{15}\text{N}$ values showed a strong latitudinal gradient and significant different among regions ($\chi^2 = 42.723$, $df = 5$, $p = <0.001$, [Table 4](#)). The highest mean $\delta^{15}\text{N}$ values were observed in the NGMc and NGMo ($10.4 \pm 1.2\text{‰}$ and $5.0 \pm 2.2\text{‰}$, respectively; [Fig. 11B](#) and [Table 3](#)) suggesting the assimilation of N from MARS runoff and denitrification. In contrast, the lowest values were for CGM and LC ($1.9 \pm 0.5\text{‰}$ and $2.3 \pm 0.6\text{‰}$, respectively), which suggests the contribution of N_2 fixation. The SGM and YS had significantly higher values ($3.1 \pm 0.8\text{‰}$ and $3.8 \pm 0.9\text{‰}$) than the central gulf. The significant differences in zooplankton isotope ratios among regions support the need of considering regional N sources to estimate contributions.

The $\delta^{13}\text{C}$ -POM values during the XIXIMI-06 cruise ranged from -25.3 to -21.3‰ , but a spatial pattern was not evident ([Fig. 12](#); [Table S2](#)). Mean $\delta^{13}\text{C}$ -POM values did not show statistical differences among CGM, SGM and LC ($F = 0.584$, $p = 0.563$). In contrast, the $\delta^{15}\text{N}$ -POM values ranged from 1.9 to 3.2‰ ([Fig. 12](#)), with lower values in the western GM, in stations with influence by anticyclonic eddy remnant (Poseidon). In the SGM the values were higher compared with the western GM, especially for stations close to the shelf that could reflect cross-shelf transport of DIN from Grijalva-Usumacinta River or subsurface nitrate supply induced by cyclonic circulation.

The linear regression analysis showed a significant and positive correlation ($r = 0.62$, $p = 0.0065$) between $\delta^{15}\text{N}$ -POM and $\delta^{15}\text{N}$ values of zooplankton ([Fig. 13](#)). Also, there was a positive correlation ($r = 0.63$, $p = 0.0065$) between $\delta^{15}\text{N}$ -POM and NO_3^- concentration integrated to 200 m ([Fig. 13](#)), which suggests fluxes of NO_3^- from the subsurface led to higher $\delta^{15}\text{N}$ values of POM.

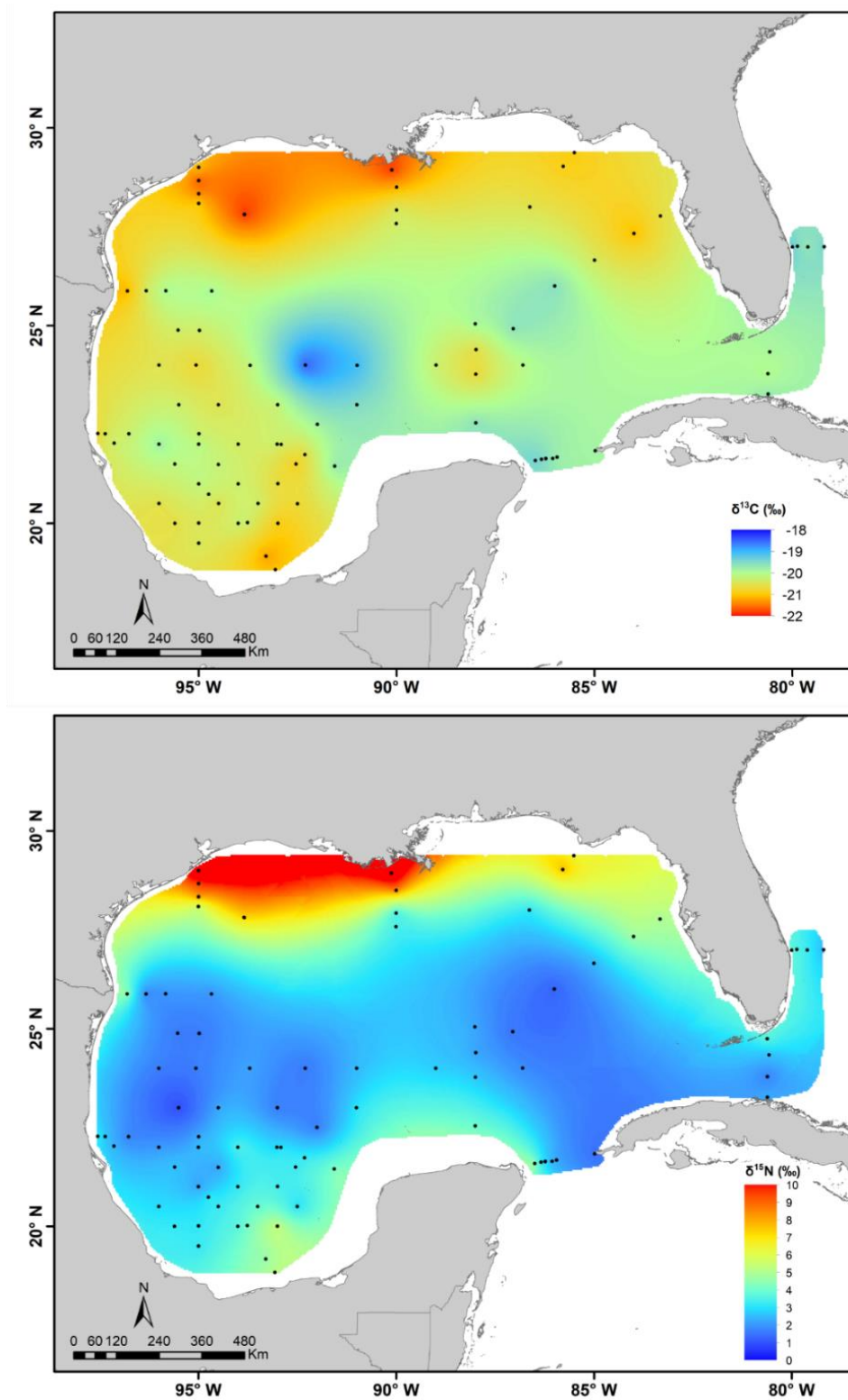


Figure 11. $\delta^{13}\text{C}$ and $\delta^{15}\text{N}$ isoscapes of zooplankton < 1000 μm sampled in the Gulf of Mexico during the summer of 2017. Dots indicate sampling stations. Maps adapted from Le-Alvarado et al. (2021).

Table 5. Dinitrogen fixation rates in oligotrophic waters and Gulf of Mexico.

Organism	N ₂ fixation rate	Region	Method	Season	Study
<i>Trichodesmium</i> Unicellular fixers	2.1 a 9.2 nmol N col ⁻¹ d ⁻¹ 3.3 a 20.5 nmol N col ⁻¹ d ⁻¹ 0.27 to 5.62 nmol N L ⁻¹ d ⁻¹	Western Florida shelf	¹⁵ N ₂ uptake method acetylene reduction method	Jul 2001 and 2002, Jun and Nov 2003	Mulholland et al. (2006)
Unicellular fixers	0 to 13.6 nmol N L ⁻¹ d ⁻¹	Western Florida shelf	¹⁵ N ₂ uptake method	October 2006-2010	Mulholland et al. (2014)
<i>Trichodesmium</i>	84.5 ± 17.7 μmol N m ⁻² d ⁻¹	Western GM	¹⁵ N ₂ uptake method	Jul 2000	Holl et al. (2007)
<i>Trichodesmium</i>	90 ±40 μmol N m ⁻² d ⁻¹	Eastern GM	Estimated based on δ ¹⁵ N values of nitrate and POM	May 2017, 2018	Knapp et al. (2021)
<i>Trichodesmium</i>	0.4-2.5 μmol N m ⁻² d ⁻¹	Eastern GM	Estimated based on acetylene reduction method published by Breitbarth et al., (2008)	May 2017, 2018	Kelly et al. (2021)
<i>Trichodesmium</i> Unicellular fixers	~200 μmol N m ⁻² d ⁻¹ ~ 52 μmol N m ⁻² d ⁻¹	Tropical North Atlantic	¹⁵ N ₂ uptake method acetylene reduction method	April 1996, Oct 1996, Feb 2001, Aug 2001, Oct 2002	Montoya et al. (2007)
<i>Trichodesmium</i>	850 μmol N m ⁻² d ⁻¹ ~125 μmol N m ⁻² d ⁻¹ ~478 μmol N m ⁻² d ⁻¹ ~ 300 μmol N m ⁻² d ⁻¹	Tropical North Atlantic	¹⁵ N ₂ uptake method acetylene reduction method	Jan-Feb Apr-May Jun-Ago Oct	Capone et al. (2005)
<i>Trichodesmium</i>	~ 41 μmol N m ⁻² d ⁻¹	BATS	¹⁵ N ₂ uptake method acetylene reduction method	Annual average	Orcutt et al. (2001)

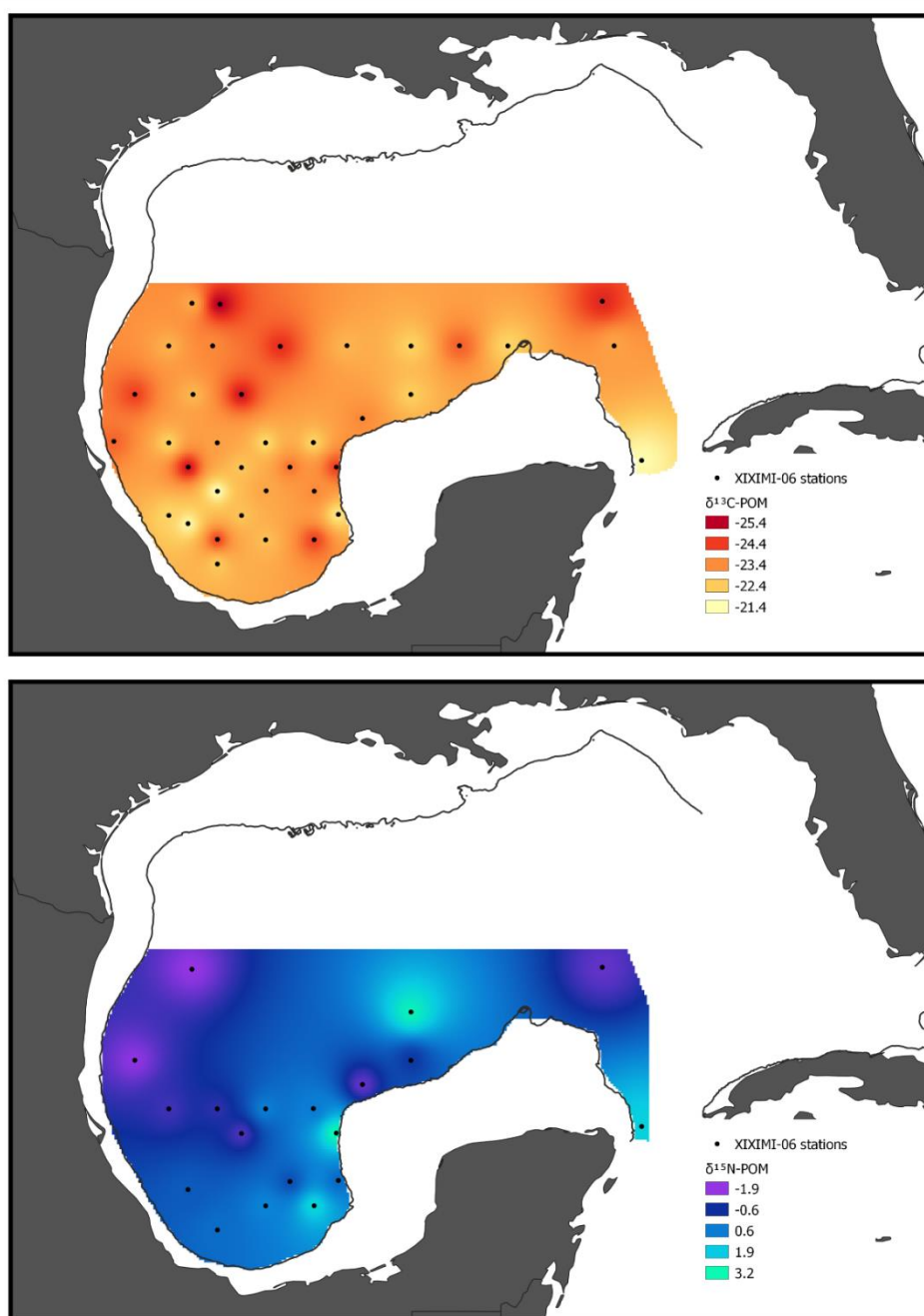


Figure 12. $\delta^{13}\text{C}$ and $\delta^{15}\text{N}$ isoscapes of surface layer POM sampled in the Gulf of Mexico during the XIXIMI-06 cruise during the summer of 2017. Dots indicate sampling stations.

3.3.2 Bayesian mixing model

In the NGMc, the largest contribution was attributed to N from denitrification, with a mean value of 60% (38-80% CI; [Figs. 14D](#) and [15A](#)). Nitrogen from MARS contributed with a mean of 17% (2-51% CI; [Figs. 14C](#) and [15A](#)); in the most coastal stations (E12 and E20) denitrification contributed $\sim 80\%$ of the N ([Fig. 14D](#)).

In the NGMo, the highest contribution was from N_2 fixation, with 45% (23-91% CI; Fig. 14A), although at some stations (E08, E09 and E10) fixation contributed up to $\sim 60\%$. The contribution of nitrate was estimated at 20%, with a broad confidence interval (2-53% CI; Fig. 14B), and MARS, denitrification and WFS contributed less than 15% (Fig. 14C, 14D, 14E). In the CGM and LC, N_2 fixation was the most important N source supporting zooplankton production, with mean contribution of 73% (45-95% CI; Figs. 14A and 15A); a contribution as high as 80% was estimated for some stations (B14 and C21; Fig. 14A). Nitrate was the most important N source in the YS with an estimated mean contribution of 45.5% and a broad confidence interval (8-76%; Fig. 14B).

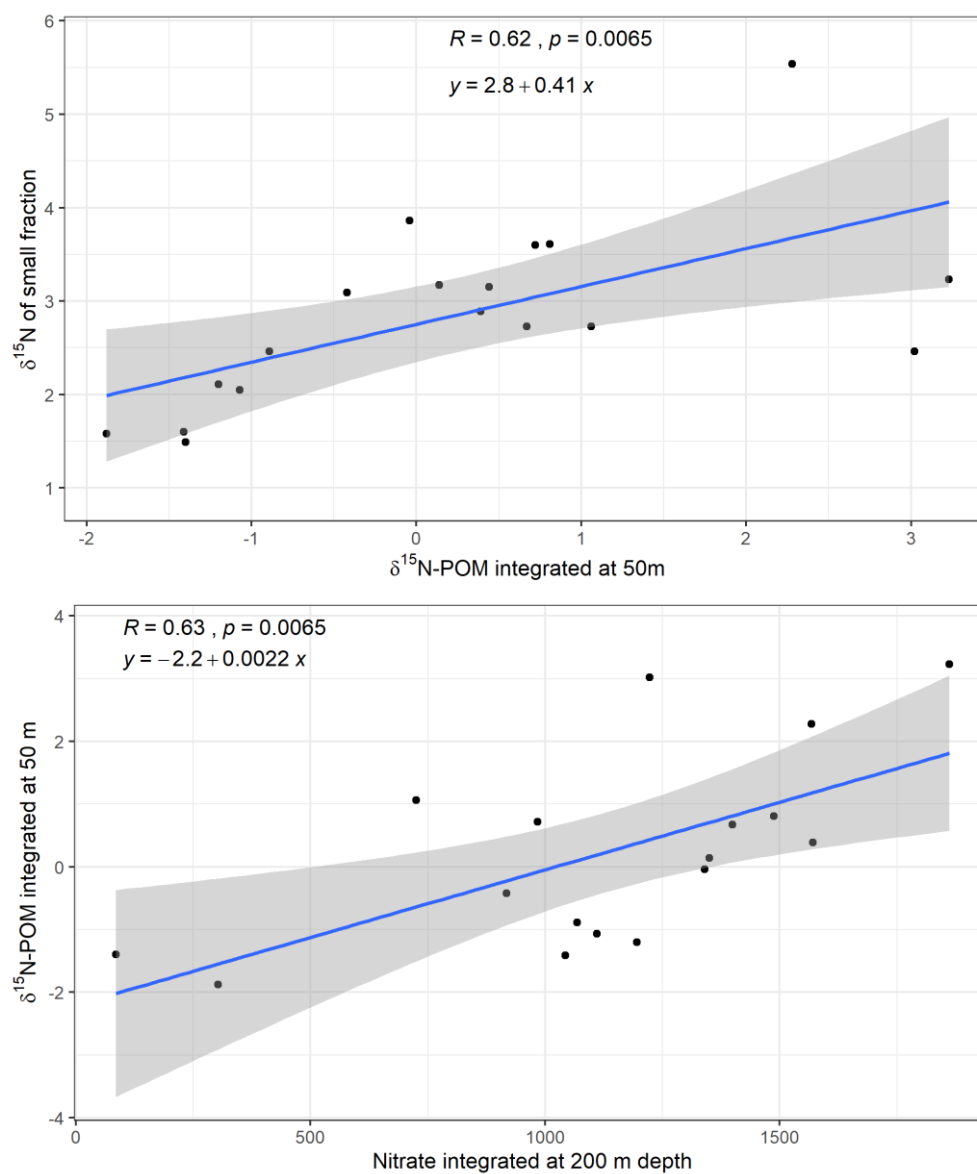


Figure 13. Correlation analysis between $\delta^{15}N$ -POM and $\delta^{15}N$ values of zooplankton (top) and nitrate concentration integrated between 0-200 m at XIXIMI-06 stations (bottom). Grey areas indicate confidence interval.

In the SGM, N_2 fixation was also the most important source with 65% (31-86% CI; Figs. 14A and 15A), and nitrate showed about half the contribution of fixed N_2 , with a mean of 24.5% (3-56% CI). On the other hand, the N associated with the GUS discharge had a contribution of 19% (3-47% CI; Fig. 14F), although the contribution at some stations on the inner shelf was as high as $\sim 30\%$.

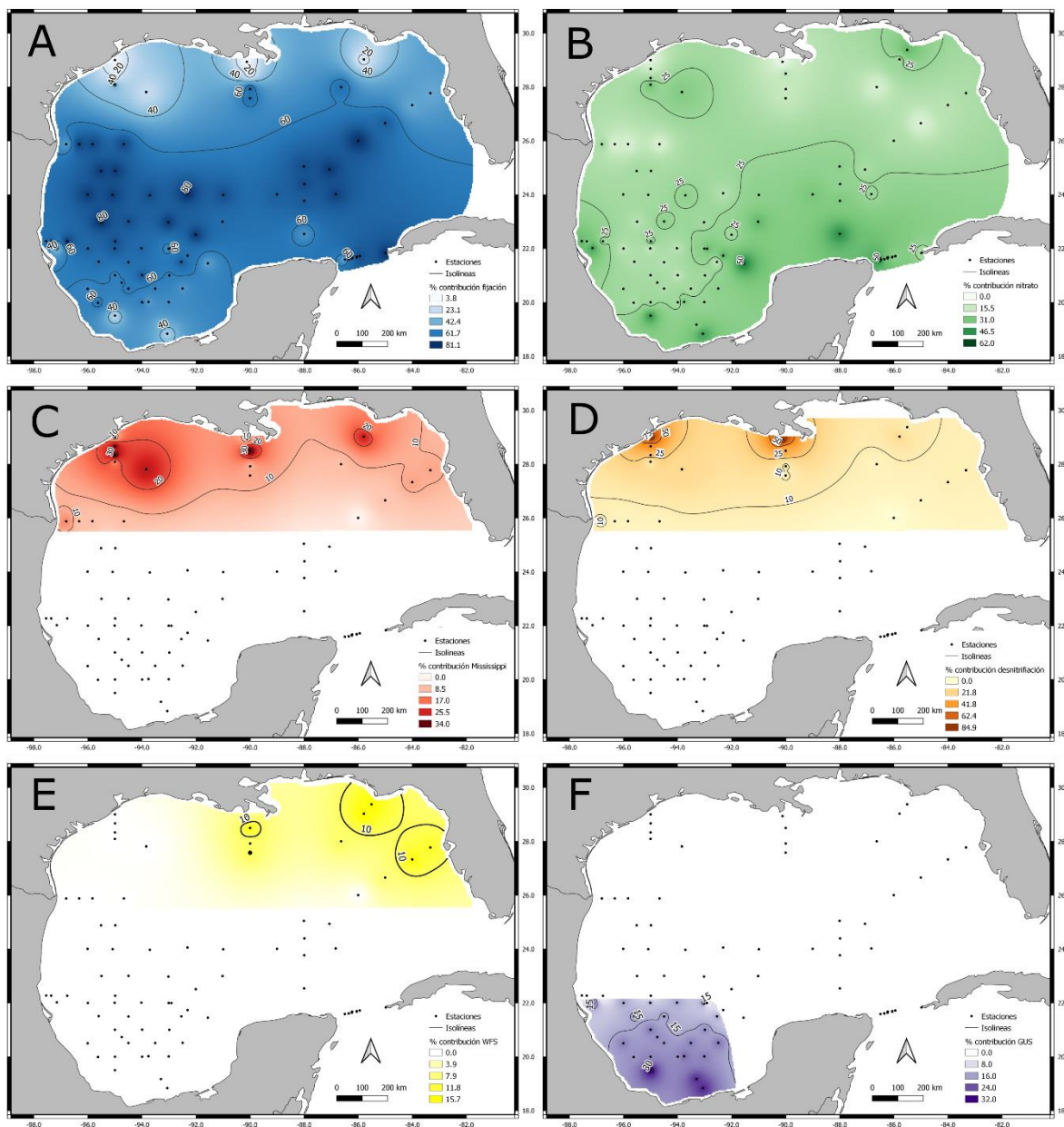


Figure 14. Percent contribution of (A) N_2 fixation, (B) nitrate, (C) Mississippi-Atchafalaya River System "MARS", (D) denitrification, (E) Western Florida shelf "WFS" and (F) Grijalva-Usumacinta System "GUS" for different regions of in the Gulf of Mexico. Black dotted lines represent the isolines of fractional contributions and numbers show the percent contribution. White areas indicate a particular source was not considered important in the region and was thereby not included in isotope mixing models.

3.3.3 Effect of variations in $\delta^{15}\text{N-NO}_3$ in N source contribution calculations

In general, the calculations with scenario 2 resulted in similar N source contributions compared with those obtained with scenario 1 for all regions, which is consistent with the limited difference in nitrate isotope ratios. In other words, a difference in $\delta^{15}\text{N-NO}_3$ values of 0.5‰ between scenario 1 and 2 was too small to substantially change the source contribution estimates. The largest changes (22%) were found between scenario 1 and scenario 3, and mainly for the CGM, SGM, YS and LC. In scenario 2, considering all station for the six regions, the mean gulf-wide contributions of N_2 fixation decreased from 58.1% to 52.1% as compared with scenario 1. In turn, the mean gulf-wide contribution of subsurface nitrate increased from 25.2% to 31.0%. For the other N sources, the mean gulf-wide contributions range 1.4 to 5.6% and the changes were only around <1% in the scenario 2 compared with scenario 1 (Fig. 15A, 15B).

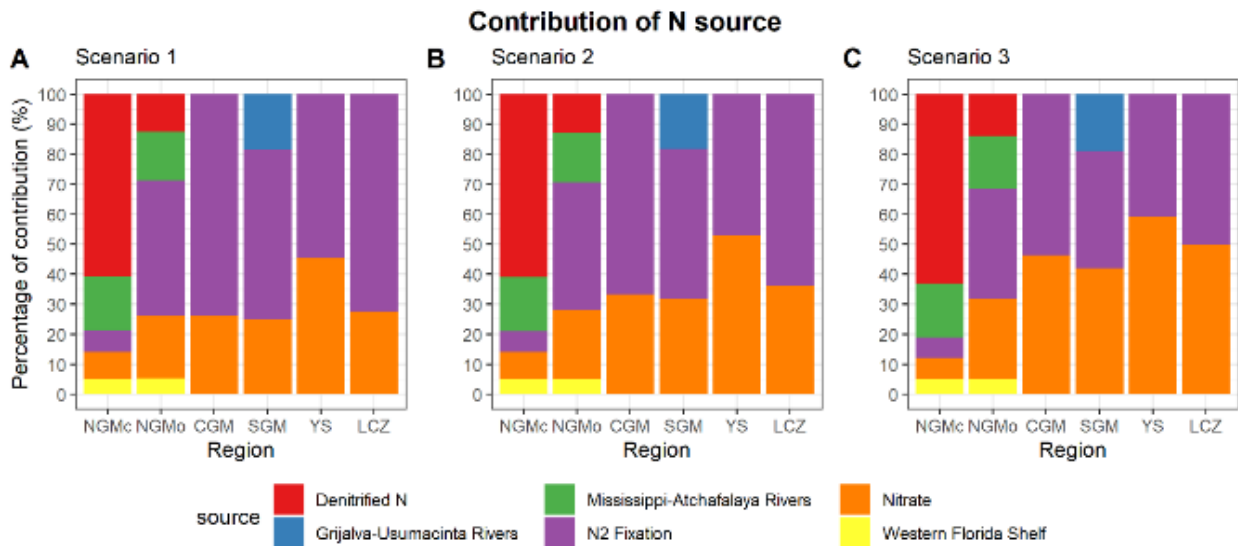


Figure 15. Percent contribution of N sources calculated by varying the isotopic composition of nitrate. (A) Scenario 1: $\delta^{15}\text{N-NO}_3 = 4.0 \pm 0.3\text{‰}$ of subsurface waters for the western Atlantic, (B) Scenario 2: $\delta^{15}\text{N-NO}_3 = 3.5 \pm 1.1\text{‰}$ from Howe et al. (2020), (C) Scenario 3: $\delta^{15}\text{N-NO}_3 = 1.9 \pm 0.8\text{‰}$ from Holl et al. (2007). NGMc: Coastal Northern Gulf of Mexico; NGMo: Oceanic Northern Gulf of Mexico; CGM: Central Gulf of Mexico; SGM: Southern Gulf of Mexico, LC: Loop Current region; YS: Yucatan Shelf.

On the other hand, under scenario 3, in which $\delta^{15}\text{N-NO}_3$ was 2.1 ‰ lower than the value for the western Atlantic, the mean gulf-wide contribution of fixed N_2 decreased from 58.1 to 42.1% compared with the scenario 1, while considering the mean gulf-wide contributions contribution of nitrate increased from 25.2 to 40.3%. The N sources that were limited to regional contributions changed by 1-3% between scenario 1 and 3. The regions with the highest decrease in the contribution of N_2 fixation were the LC (72.2 to 50.0%),

CGM (74.0 to 53.5%), SGM (56.6 to 39.1%), and YS (54.5 to 40.6%). In contrast, the contribution of subsurface nitrate increased in all of these regions, but decreased slightly in the NGMc (from 9.1 to 7.0%; [Fig. 15C](#)).

3.4 Discussion

The gulf-wide isoscapes of $\delta^{13}\text{C}$ and $\delta^{15}\text{N}$ values based on zooplankton that were presented by Le-Alvarado et al. (2021) were used to examine the spatial pattern and the relative contribution of nitrogen sources throughout the GM during summer conditions using a Bayesian isotope mixing model. In addition, the effect of the variations in $\delta^{15}\text{N}\text{-NO}_3^-$ values reported for the subsurface waters of the GM on source contributions was examined.

3.4.1 Regional patterns in zooplankton isoscapes

I found a broad range of $\delta^{15}\text{N}$ values for zooplankton sampled throughout the GM (0.9 to 11.6‰), which indicates that differences in regional source contributions strongly controls the isotopic baseline and therefore $\delta^{15}\text{N}$ values of zooplankton. The isotopic composition of zooplankton showed a strong latitudinal pattern, with the highest $\delta^{15}\text{N}$ values (8.9 to 11.6‰) at the stations of the coastal northern GM. This is the region of influence of the Mississippi and Atchafalaya Rivers, and is the so-called “dead zone,” where suboxic and anoxic conditions are prevalent and caused by high nutrient inputs and stratification (Rabalais et al., 2001; Bianchi et al., 2010). The northern shelf is known for isotopically heavy N inputs, with $\delta^{15}\text{N}\text{-NO}_3^-$ values of 7.3 ± 0.3 ‰ (BryantMason et al., 2013) as well as regional denitrification (Ledford et al., 2020). In contrast, the lowest values were found in the central gulf and in the region of influence of the Loop Current (0.9 to 3.6‰), which have well-described oligotrophic conditions (Biggs et al., 1992; Pasqueron de Fommervault et al., 2017). These lower nitrogen isotope ratios are consistent with inputs of N_2 fixation (see below).

A basin-wide isoscape for the Atlantic Ocean based on a meta-analysis of $\delta^{15}\text{N}$ values of zooplankton showed a marked regional pattern, with low $\delta^{15}\text{N}$ values (0 to 2‰) in the subtropical western region that has been attributed to N_2 fixation by diazotrophic organisms (Montoya et al., 2002; Landrum et al., 2011), compared with higher values (6 to 8‰) for the temperate and arctic regions, where NO_3^- is the major source

of DIN for phytoplankton (McMahon et al., 2013). The $\delta^{15}\text{N}$ values for the central and Loop Current in my study are consistent with those reported by McMahon et al., (2013) for the subtropical northwestern Atlantic Ocean. However, in their meta-analysis there were very limited data for the GM, and the interpolation was based on a few measurements in the northwestern GM. In the meta-analysis, $\delta^{15}\text{N}$ values of zooplankton were estimated as 5-7‰ for the northern and central GM and 2-4‰ for the Yucatan Channel and Strait of Florida, and the northern and central region of GM was interpolated. In contrast, the results of this study indicate that the extrapolation of McMahon et al. (2013) for the GM did not reflect the low isotope ratios of the oligotrophic conditions of the central gulf and Loop Current regions.

However, a zooplankton-based isoscape for the subtropical southwestern Atlantic Ocean reported by Troina et al. (2020) found a strong latitudinal pattern in $\delta^{15}\text{N}$ values, similar to what was found in this study. They found a north to south gradient, with lower $\delta^{15}\text{N}$ values (2.9 ± 1.0 ‰) in the more oligotrophic northern region that was attributed to the influence of N fixed by *Trichodesmium*, compared with higher $\delta^{15}\text{N}$ values (4.0 ± 1.5 ‰) in the southern region, where there are higher fluxes of subsurface NO_3^- and inputs from continental runoff.

In contrast to what was observed for the isotopic composition of nitrogen, in this study the carbon isotope ratios of zooplankton did not show a clear spatial pattern. The range of values (-22 to -14‰) are generally consistent with those of marine phytoplankton (-25 to -18‰, Fry and Sherr, 1984). However, at shelf stations close to the discharge of rivers, there was a gradient toward lower values inshore. Carbon isotope ratios in the coastal northern GM (-21.7‰) and the Grijalva-Usumacinta rivers plume (-21.3‰) were ca. 1‰ lower than for the deep water region of the GM (-20.4‰). This likely reflects the input of C_3 terrestrial organic matter (-27 to 30‰) that is typical of freshwater systems and river runoff, as well as low DIC $\delta^{13}\text{C}$ values due to remineralization of terrestrial organic matter (Ohkouchi et al., 2015). Troina et al. (2020) also reported an inshore-offshore gradient, with low $\delta^{13}\text{C}$ values (ca. 21.8‰) for the shelf-break region compared with offshore stations (ca. -20.5‰), which they attributed to inputs of terrestrial organic matter, riverine water and upwelling of subsurface DIC depleted in ^{13}C . Hence, in my study the $\delta^{13}\text{C}$ values of zooplankton largely reflect phytoplankton, and limited but detectable inputs of C_3 terrestrial carbon in coastal areas close to river plumes.

3.4.2 Regional source contributions

The Bayesian isotope mixing model based on POM and zooplankton C and N ratios indicated that, excluding the coastal northern Gulf of Mexico region, nitrogen fixation was the most important source

supporting secondary production, during the summer, with an estimated mean contribution between 45 and 74%. The lowest nitrogen isotope ratios were found in the CGM, LC and SGM, with mean values of $1.9 \pm 0.5\text{‰}$, $2.3 \pm 0.6\text{‰}$ and $3.1 \pm 0.9\text{‰}$, respectively. These values led to high estimates of the contribution of fixed N_2 (mean 56-74%, Figs. 14A and 15A). Low $\delta^{15}\text{N}$ values have been associated with inputs of nitrogen from N_2 fixation in different regions of the tropical and subtropical Atlantic (Montoya et al., 2002; Holl et al., 2007; Landrum et al., 2011; Kürten et al., 2016), as well as in temperate oceans (Loick-Wilde et al., 2019). For example, for the western tropical and subtropical Atlantic Ocean, the contribution of diazotrophs to POM and zooplankton has been estimated as high as 65% within the mixed layer (Landrum et al., 2011), and where high N_2 rates of nitrogen fixation (150 to $850 \mu\text{mol N m}^{-2} \text{d}^{-1}$) have been reported (Capone et al., 2005; Montoya et al., 2007; Table 5). Also, these contributions are consistent with the findings of Holl et al. (2007), who measured N_2 fixation rates (mean $85 \pm 17 \mu\text{mol N m}^{-2} \text{d}^{-1}$) along a transect running from the continental shelf to the deep water region in the northwestern GM, and used an isotope mixing model to estimate that 60% of the C and N supporting zooplankton production during the summer in the deep water region were from *Trichodesmium*. Hernández-Sánchez et al. (submitted) also reported low $\delta^{15}\text{N}$ values of copepods ($3.7 \pm 1.0\text{‰}$) and mesozooplankton ($<1000 \mu\text{m}$; $2.8 \pm 0.8\text{‰}$) for the CGM and SGM sampled during 4 cruises held between 2010 and 2016, and estimated a 50-63% contribution of fixed N_2 during the summer, which is consistent with my estimates for those regions based on sampling in 2017 (56-74%). Low $\delta^{15}\text{N}$ values (ca. 1.8 to 2.8‰) of zooplankton have also been reported within the northern GM in anticyclonic eddies and the Loop Current, and attributed to the presence of fixed N by *Trichodesmium* during the summer (Dorado et al., 2012; Wells et al., 2017).

Subsurface NO_3^- was the second most important N source to the euphotic layer of the GM, with mean contributions between 25-27% in the deep water regions (CGM, LC and SGM). The moderate contribution of nitrate during the summer is likely due to the strong stratification and shallowing of the mixed layer ($<30 \text{ m}$), that prevents or limits the vertical flux of subsurface NO_3^- to the euphotic zone (Muller-Karger et al., 2015; Damien et al., 2018). Anticyclonic eddies and the Loop Current show a deepening of the nitracline, which is consistent with limited transport of subsurface nitrate toward the euphotic layer, and a higher proportional contribution of fixed N. However, transport of nitrate to the euphotic layer can occur in cyclonic eddies, in which there is a shallowing of the nitracline that drives subsurface waters to the upper layers, resulting in higher $[\text{NO}_3^-]$ available for assimilation by primary producers (Biggs and Muller-Karger, 1994; Seki et al., 2001). The semipermanent cyclonic eddy found in the SGM (Pérez-Brunius et al., 2013) should therefore enhance the nitrate availability in the upper layer (see Fig. 20). Also, in the Bay of Campeche, convergent currents over the shelf during September-October could increase $[\text{NO}_3^-]$ near the surface due to cross-shelf transport (Martínez-López and Zavala-Hidalgo, 2009), while coastal upwelling in

the Tamaulipas-Veracruz shelf in the western GM during the summer and cross-shelf transport in the southwestern LATEX shelf during May would increase the transport of subsurface nitrate to the euphotic zone in the western gulf close to the slope (Martínez-López and Zavala-Hidalgo, 2009; Mateos-Jasso et al., 2012; Zavala-Hidalgo et al., 2014).

Although nitrate was estimated to have a moderate contribution (~25%) to the nitrogen in zooplankton in the deep water regions of the gulf during the summer, a deepening of the mixed layer during the winter could be an important process increasing the nitrate supply to the euphotic zone (Damien et al., 2018). Hernández-Sánchez et al. (2022) reported $\delta^{15}\text{N}$ values ($4.3\pm 0.6\text{‰}$) of copepods sampled during the winter in the CGM and SGM, and estimated a $56\pm 2\%$ contribution of subsurface NO_3^- , which was attributed to fluxes from the deeper layers to the euphotic layer. Hence, there is a seasonal pattern of the relative contribution of subsurface nitrate in the deep water region of the Gulf.

For the Yucatan Shelf, mixing model estimates indicated that in average 50% of the N was from subsurface nitrate, although values as high as 60% were calculated for some stations. This higher contribution is due to upwelling of water from depths of 200-250 m that occurs in the eastern Yucatan shelf due to the interaction of the intense western boundary Yucatan Current with the slope of the Yucatan Channel, as well as the westward winds that can contribute to upwelling of water with high NO_3^- concentrations (8 to 14 μmol ; Merino, 1997; Reyes-Mendoza et al., 2016; Jouanno et al., 2018). This regional upwelling produces positive anomalies in surface chl a concentrations, which has been reported along the inner shelf of YS during the summer months due the transport by the westward current over the shelf (Zavala-Hidalgo et al., 2006).

Denitrified N was the most important N source in the coastal northern GM, contributing 60% of the nitrogen supporting zooplankton (Fig. 15A). Hypoxic conditions have been reported in the Mississippi-Atchafalaya Rivers delta during the spring and summer (Rabalais et al., 2001; 2002; Bianchi et al., 2010), due to two dominant conditions: high nutrient and organic matter loads of the Mississippi-Atchafalaya Rivers that lead to phytoplankton blooms and high water column respiration, and stratification of the water column during the summer months, which exacerbates hypoxia close to the bottom along the coast and shelves off Louisiana and Texas (Bianchi et al., 2010, McCarthy et al., 2015). Under these conditions, denitrification leads to remnant NO_3^- enriched in ^{15}N , since it favors discrimination against ^{15}N with fractionation values as high as ~30-35‰ (Heaton et al., 1986; Kritee et al., 2012). A high contribution of denitrified N was estimated for the NGMc stations, mainly for the inner most stations (E11, E12, E19 and E20), which showed the highest $\delta^{15}\text{N}$ values of zooplankton measured in this study ($10.4\pm 1.2\text{‰}$) as well as

proportional source contributions of 81-85%. Likewise, high $\delta^{15}\text{N}$ values of zooplankton have been reported for the northern GM shelf ($8.9\pm 0.9\text{‰}$; Macko et al., 1984) and high $\delta^{15}\text{N}$ values (between 8.2‰ and 9.9‰) have also been reported for phytoplankton and POM in the Mississippi Sound (Chanton and Lewis, 1999; Sullivan and Moncreiff, 2001). These values are indicative of inputs of denitrified N, and are higher than the mean $\delta^{15}\text{N}$ -POM values from MARS (6.5 to 7.2‰; Wissel and Fry, 2003; Cai et al., 2015). Taken together, these measurements indicate that denitrified N is the most important source of N for zooplankton in the coastal stations of the northern GM.

My results indicate that nitrogen inputs of the Mississippi-Atchafalaya Rivers have a moderate contribution only in the northern shelf, despite the fact that their discharge is the major source of terrestrial organic matter and nutrient inputs to the entire northern GM. The contribution of N from MARS (mean 17%), was lower compared with denitrified N in the NGMc and NGMo, and I estimated moderate contributions for the NGMc and the inner NGMo stations (26-34%; Fig. 14C). Higher $\delta^{15}\text{N}$ - NO_3^- values (7.0‰) and $\delta^{15}\text{N}$ -POM values (6.5-7.2‰) from the Mississippi-Atchafalaya Rivers have been associated with different N sources, including manure, treated waste water in the upper Mississippi River and tributaries and denitrification (Chang et al., 2002; BryantMason et al., 2013). If NO_3^- with these higher $\delta^{15}\text{N}$ values was the main N source supporting the food web in the NGM, the $\delta^{15}\text{N}$ values of zooplankton would be $\sim 8\text{-}9\text{‰}$ (considering a TDF $\sim 2\text{‰}$). However, at two of the inner stations of the NGMc (E12 and E20), the $\delta^{15}\text{N}$ values were 11.6‰, which is almost 3‰ higher than what would be expected if MARS were the main N source. One reason for the low contribution of MARS N to the deep water stations sampled in this study is that the river discharge is transported mainly along the northern shelf. This transport is mostly toward the Texas-Louisiana shelf during the autumn, winter and early spring, while eastward transport can occur during the late spring and summer months (Schiller et al., 2011). In addition, Schiller et al. (2011) reported offshore transport of the low salinity water from MARS due to interactions with mesoscale eddies. The highest discharge of MARS occurs during the spring and early summer, and decrease in the late summer and autumn (Walker et al., 2005) when the zooplankton samples were collected. Hence, MARS was only important in the inner shelf stations of NGMc and NGMo, and limited in the deep water stations of the oceanic northern gulf (5-15%; see Fig. 14C).

The inputs of Grijalva-Usumacinta River system only had moderate contributions at stations relatively close to the river mouths, with $\sim 30\%$. In the coastal southern GM, these rivers are the most important in terms of freshwater inflow and nutrient inputs, and mean $\delta^{15}\text{N}$ values of POM $4.6 \pm 0.5\text{‰}$ have been reported for their lower reaches (Sepulveda-Lozada et al., 2015). The maximum discharge from Grijalva-Usumacinta rivers is during the summer months (August-October; Muñoz-Salinas and Castillo, 2015), and

the chl *a* produced by this discharge is transported toward the SGM due to the cross-shelf transport (Martínez-López and Zavala-Hidalgo, 2009). Zavala-García et al. (2016) evaluated the relationship between zooplankton biomass on the shelf and deep water region of the southern Bay of Campeche and river discharge from rivers in the states of Veracruz, Tabasco and Campeche during an annual cycle and based on data from 14 cruises (1984-2004). They found a positive relationship between zooplankton biomass and the river discharge. Also, these authors used regression tree analysis to examine the relationship, and found that zooplankton biomass was low in samples from the deep water region (6.5 g m^{-3}), intermediate during spring, autumn and winter at inner and outer shelf region ($14 \text{ to } 20 \text{ g m}^{-3}$), and that the highest biomass occurred during the season of high discharge (summer) and along the inner shelf (36.9 g m^{-3} ; depths $<33 \text{ m}$). This is consistent with the contributions estimated with the Bayesian isotope mixing model, which indicated that POM from the Grijalva-Usumacinta River has moderate contributions only at the stations closest to the coast of Campeche.

The N source from WSF rivers had a low N contributions. The zooplankton isotope ratios showed a latitudinal pattern within the WFS, with higher values at the northern stations and intermediate values in the central that the mixing model indicated were due to denitrified N and N fixation, respectively. The N from inputs from WFL rivers had low contribution to the region (mean $\sim 5\%$), although they reached 15-16% at the northern Florida shelf stations. Radabaugh et al. (2013) evaluated the isotopic composition of POM, primary producers and fish along a gradient from eutrophic to oligotrophic waters on the WFS. They also reported a latitudinal pattern in $\delta^{15}\text{N}$ -POM values that was reflected along the food web, with higher values for the northernmost stations ($\sim 6\text{-}7\text{‰}$) compared with those from the southern extent of the shelf ($\sim 3\text{-}5\text{‰}$). Del Castillo et al., (2001) evaluated river runoff, dissolved and particulate carbon organic matter and chl *a* concentrations using multispectral fluorescence and satellite sensing in the eastern GM. They found that high chl *a* was associated with relative low salinities in the inner shelf of the WFS, and that there were lower surface chl *a* concentrations in the central region due to the more limited extent of the area of influence of runoff from WFS rivers. This is consistent with my results, in which the river contribution to the WFS was relatively low (8-15%). Del Castillo et al., (2001) also reported high chl *a* concentrations that were transported eastward from MARS toward the outer shelf of west Florida by LC anticyclonic eddies or a high intrusion of the Loop Current, and which in my data are reflected in a 15-25% contribution of MARS N to the WFS. On the other hand, high fixation rates ($1.32 \text{ to } 8.2 \mu\text{mol N m}^{-2} \text{ d}^{-1}$) of *Trichodesmium* have been reported for the central region of the western Florida shelf considering a 20 colonies L^{-1} (Mulholland et al., 2006; 2014). These authors reported that N fixed by blooms of *Trichodesmium* could support large blooms of the toxic dinoflagellate *Karenia brevis*. The N fixed by

Trichodesmium in the central region of WFS could be a fraction (45-68%) that is reflected by the $\delta^{15}\text{N}$ values of zooplankton (2.4 to 4.8‰) in this study.

3.4.3 Variation in $\delta^{15}\text{N-NO}_3^-$

For the regional mixing models, I used a mean $\delta^{15}\text{N-POM}$ value for subsurface NO_3^- of $4.0 \pm 0.3\text{‰}$ reported for the western Atlantic, and a $\delta^{15}\text{N-POM}$ value of $-1.2 \pm 1.2\text{‰}$ of fixed N (Table 2; Scenario 1). To explore the effect of variations in the isotopic composition of the subsurface NO_3^- that reaches the euphotic zone within the gulf, I compared those results with the $\delta^{15}\text{N-NO}_3^-$ values ($3.5 \pm 1.1\text{‰}$) reported by Howe et al. (2020) for the deep water region of the northern GM (Scenario 2), as well as the value reported by Holl et al. (2007) for the northwestern gulf ($1.9 \pm 0.8\text{‰}$; Scenario 3).

The estimates of the surface nitrate contribution increased with the decrease in to the $\delta^{15}\text{N-NO}_3^-$ values, and this was more marked in the western GM. Under scenario 3, the contribution of N_2 fixation decreased in all regions, and its fractional contribution was similar to that of nitrate (Fig. 15C). In the YS region, the major N source changed from N_2 fixation to subsurface NO_3^- , although a $\delta^{15}\text{N-NO}_3^-$ value of $1.9 \pm 0.8\text{‰}$ measured in the western gulf is not a realistic values to use for the Yucatan Channel, since it is the source region of waters from the Caribbean Sea and ultimately the western Atlantic. Although the fractional contribution of nitrate did increase under scenario 2 and 3, the contribution of N_2 fixation remained important for all regions (37 to 53%), except for NGMc (7%) under scenario 3.

The subsurface nitrate isotope ratios measured to date become lower westward within the GM. Hence, a source of low $\delta^{15}\text{N}$ values of organic matter sinking out the euphotic zone is needed, and there are two possible explanations: (1) the remineralization of organic matter that is supported by subsurface NO_3^- and that results in inorganic nitrogen depleted in ^{15}N , or (2) the remineralization of organic matter that reflects the uptake of fixed N. To address the possible explanations that would produce lower $\delta^{15}\text{N-NO}_3^-$ values below the euphotic layer in the GM compared with the Atlantic, I discuss the following.

A study by Capone et al. (1998) evaluated the importance of *Trichodesmium* in the upper water column and the dynamics of organic matter of C and N during the spring in the Arabian Sea. These authors measured the abundance of *Trichodesmium*, N_2 fixation rates, $\delta^{15}\text{N-POM}$ in the first 100 m and sinking $\delta^{15}\text{N-POM}$ collected with sediment traps deployed at 100-130 m. They reported high rates of fixed N

($129 \pm 23 \mu\text{mol N m}^{-2} \text{d}^{-1}$) during a bloom in which the abundance of the cyanobacteria was high (2000-4000 trichomes L^{-1}). They also found that the $\delta^{15}\text{N}$ -POM values for the upper water column were similar to that of sinking POM during the *Trichodesmium* bloom, demonstrating that N_2 fixation was an important N source to the vertical fluxes out the euphotic zone. They also estimated that 60% of the suspended POM and 20% of the POM sinking was attributed to the *Trichodesmium* blooms. Hence, when blooms of *Trichodesmium* occur, they drive high N_2 fixation rates and the production of organic matter with relatively low nitrogen isotope ratios. Meanwhile, the abundance of *Trichodesmium* have been reported in the western GM range 10 to 1×10^4 trichomes L^{-1} , and the eastern GM range 300 to $\sim 10^6$ trichomes L^{-1} during the summer months (Lenes and Heil, 2010; Holl et al., 2007). Assuming that colony of *Trichodesmium* has 200 trichomes (Lenes and Heil, 2010; Carpenter, 1983) and average fixation rate of $8.8 \text{ nmol N col}^{-1} \text{d}^{-1}$ (Mulholland et al., 2014), could estimate $260 \text{ nmol N m}^{-2} \text{d}^{-1}$ to $880 \mu\text{mol N m}^{-2} \text{d}^{-1}$, this is its range for N_2 fixation rates measured in the western Atlantic Ocean (Capone et al., 2005, see Table 5). Hence, fixation could represent the largest N source that supported the food web for the euphotic layer and moderate source of N fluxes out the euphotic layer in the GM during the summer.

On the other hand, low $\delta^{15}\text{N}$ values of suspended particle organic matter for the GM have been attributed to the remineralization of organic matter in the euphotic zone, which produces discrimination against ^{15}N ($\sim 3\text{‰}$). Knapp et al. (2021) used a box model approach that included a $\delta^{15}\text{N}$ budget to evaluate the relative importance of N_2 fixation and subsurface NO_3^- to the exported production in the deep, eastern GM. They reported $\delta^{15}\text{N}$ -POM values 1.2 to 3 ‰ for the upper 100 m, and argued that these relatively low $\delta^{15}\text{N}$ values were produced by regenerated production supported by remineralized DON or zooplankton excretion, leading to subsurface NO_3^- with values between 2.0 to 3.8‰. Also, they estimated N_2 fixation based on $\delta^{15}\text{N}$ - NO_3^- and $\delta^{15}\text{N}$ values of POM collected in sediment traps drifting below the euphotic zone. When the isotope ratios of sinking POM were similar or higher than that of subsurface nitrate ($> 0.1\text{‰}$), the model indicated that the contribution of N_2 fixation absent or limited. They found that $\delta^{15}\text{N}$ -POM were similar or higher compared with the $\delta^{15}\text{N}$ - NO_3^- values below the euphotic layer in 4 of 5 of their experiments traps, which they interpreted as an absence of fixed N. They reported one sediment trap with $\delta^{15}\text{N}$ -POM values lower than $\delta^{15}\text{N}$ - NO_3^- values, and estimated fixation rates were $90 \pm 40 \mu\text{mol m}^{-2} \text{d}^{-1}$, representing a contribution of only 10-18% of the exported N. Hence, they concluded that subsurface NO_3^- was the dominant N source supporting exported production in the GM.

In addition, Kelly et al. (2021) developed a C and N budget using a biogeochemical model, remote-sensing observations and *in situ* measurements of *Trichodesmium* abundance, and also estimate fixation rates to evaluate the importance N_2 fixation, lateral N transport and upwelled NO_3^- to N exported out of the

euphotic zone in the Loop Current region of the GM. They estimated N_2 fixation rates based on *Trichodesmium* abundance (range 0-19 trichomes L^{-1} ; Selph et al., 2021) and reported low N_2 fixation rates ($<0.4-2.8 \mu\text{mol N m}^{-2} \text{d}^{-1}$). In addition, they estimated that between 90-100% of the particulate N exported out of the euphotic layer (which they considered extends to 130 m of depth) was supported by lateral transport, and that N_2 fixation and subsurface NO_3^- fluxes do not play an important role as a source for particulate N exported during the summer. However, their N_2 fixation rate estimates were lower than reported for the northwestern GM ($85 \pm 18 \mu\text{mol N m}^{-2} \text{d}^{-1}$; Holl et al., 2007) and the Loop Current region ($<20 \mu\text{mol N m}^{-2} \text{d}^{-1}$; Knapp et al., 2021). Also, higher *Trichodesmium* abundance has been reported for the deep water region of the GM (a mean \pm SD of 360 ± 157 trichomes L^{-1} by Holl et al. 2007), and they measured 1,000 to 10,000 trichomes L^{-1} at the surface, and relatively low $\delta^{15}\text{N}$ -values of POM (-2 to 1‰) and zooplankton (1.6 to 2.2‰) in stations in the deep water region. They used two-end members mixing model and estimated that $\sim 60\%$ of the secondary production during summer for the offshore stations in the northwestern GM was attributed to *Trichodesmium*, and suggested that N_2 fixation major importance in the euphotic zone.

The radical difference in the estimated contribution of N_2 fixation between Knapp et al.'s (2021) approach and the approach used in this study is that they evaluated the flux and isotopic composition of POM that sank from the euphotic zone, while I estimated nitrogen sources based on zooplankton isotope ratios that integrate that of phytoplankton. Knapp's (2021) estimations were based on the particle that could sink. The organic matter that sinks tends to be higher $\delta^{15}\text{N}$ values than suspended POM due to the remineralization process favors the discrimination against the ^{15}N (Sigman and Fripiat, 2019). This suggests the N_2 fixation rate could be underestimated. Another difference could be the sampling season and regions covered; Knapp et al., (2021) sampled during late spring (May) in the eastern region of GM, and reported low *Trichodesmium* abundance (0-19 trichomes L^{-1}), and some of the sediment traps drifted relatively close to the MARS delta, which could producing high $\delta^{15}\text{N}$ values of POM and nitrate. In contrast, I sampled during late summer (August and September) during which the abundance of *Trichodesmium* has been reportedly higher (360 ± 157 trichomes L^{-1} ; Holl et al., 2007) and the fixation rates higher ($85 \pm 17 \mu\text{mol N m}^{-2} \text{d}^{-1}$) compared with eastern GM (Knapp et al., 2021). Additionally, the N_2 fixation by unicellular diazotrophs has been omitted for the estimations. Mulholland et al. (2014) measured the N_2 fixation by unicellular diazotrophs during annual October sampling 2006 to 2010 using the $^{15}\text{N}_2$ uptake method and reported N_2 fixation rate range 0 to 272 $\text{nmol N m}^{-2} \text{d}^{-1}$. The high estimation of fixed N in this study could be supported by the high abundance of *Trichodesmium* during the summer months with high N_2 fixation rates in the euphotic layer.

To explore the possible contribution of remineralization of organic matter to the nitrogen isotope ratio of POM and zooplankton, I considering the following. If subsurface NO_3^- fluxes reach the euphotic zone with a $\delta^{15}\text{N}\text{-NO}_3$ value of 3.5‰ in the GM (Howe et al., 2020), I would expect phytoplankton to have a $\delta^{15}\text{N}$ value of 3.5‰. Assuming subsurface nitrate is the only N source to the euphotic layer and that there is no isotopic discrimination due to the assimilation of NO_3^- since it behaves as a closed system, herbivorous zooplankton would have a $\delta^{15}\text{N}$ value of 5.5‰ with a TEF $\sim 2\%$ (Fig. 16A). However, the values reported here for the central GM and LC regions are at least 3‰ lower, which implies that subsurface nitrate did not the major N sources that support the secondary production. Subsequently, the remineralization of organic matter (supported by subsurface nitrate) with an isotopic discrimination factor $\leq 3\%$, would support the food web (Sigman and Fripiat, 2019), thus $\delta^{15}\text{N}$ values of phytoplankton 2-3‰ would be expected (Fig. 16B). However, in this study, the mean \pm SD value of $\delta^{15}\text{N}\text{-POM}$ in the CGM, LC, and SGM was $0.2 \pm 1.4\%$ (range -1.8 to 3.5 ‰; Fig. 12). These low $\delta^{15}\text{N}\text{-POM}$ values cannot be explained only by remineralization of organic matter supported by subsurface NO_3^- , and an additional source of POM with low $\delta^{15}\text{N}$, such as N_2 fixation is required (Fig. 16C; -2 to 0‰; Carpenter et al., 1997). Assuming a $\delta^{15}\text{N}\text{-NO}_3$ value of 2.0‰ reported by Holl et al. (2007), the $\delta^{15}\text{N}$ values of phytoplankton supported by remineralization would be $\sim 1.0\%$, which is 1‰ higher than $\delta^{15}\text{N}\text{-POM}$ measure in this study (Fig. 16D, 16E, 16F), but almost 3‰ higher than $\delta^{15}\text{N}\text{-POM}$ collected in the western GM. This supports the importance of N_2 fixation as an N source in the deep water region of the GM.

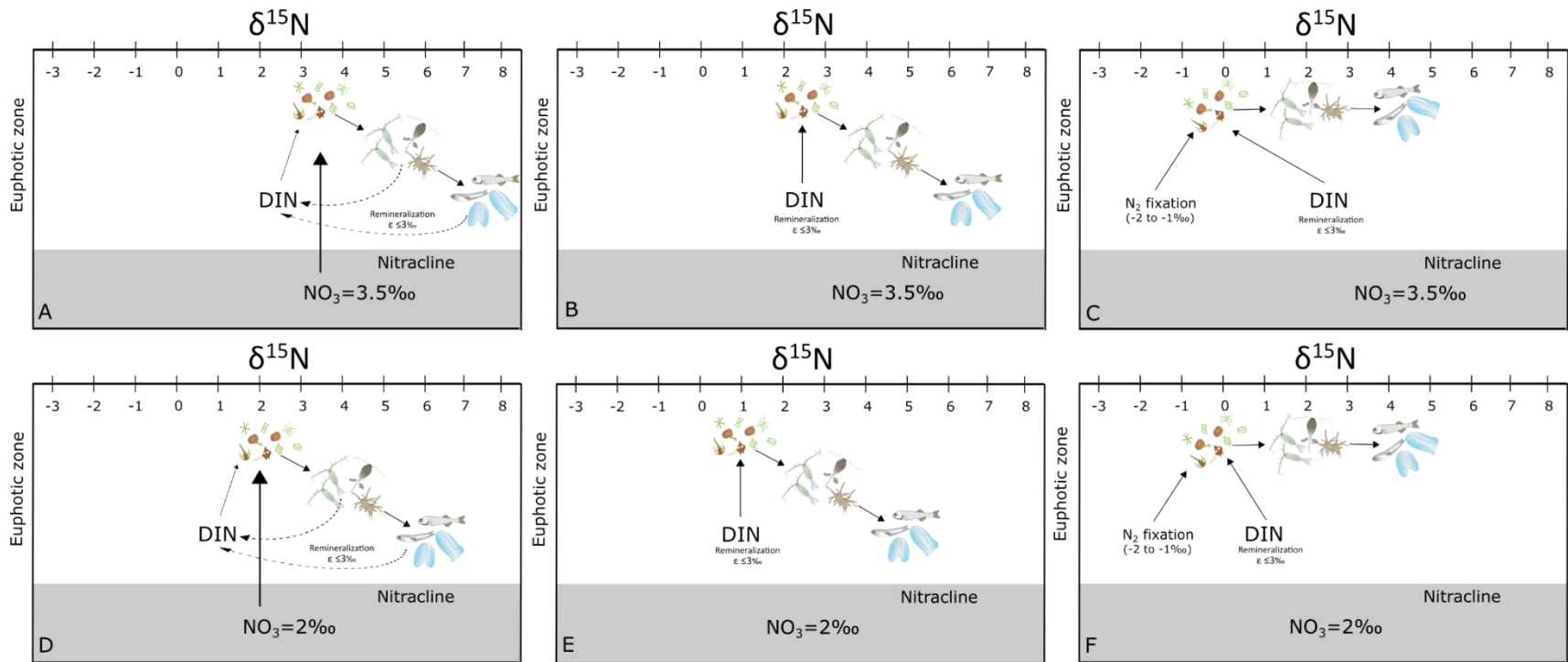


Figure 16. Schematic of the isotopic composition of nitrate, dissolved inorganic nitrogen (DIN), phytoplankton, and zooplankton based on measurement of $\delta^{15}\text{N}$ - NO_3 values within different regions of Gulf of Mexico. The $\delta^{15}\text{N}$ - NO_3 values of 3.5‰ reported by Howe et al. (2020) for the northern Gulf of Mexico (A, B, C), and $\delta^{15}\text{N}$ - NO_3 values of 2.0‰ reported by Holl et al. (2007) for the northwestern Gulf of Mexico (D, E, F). Scenarios when the subsurface nitrate is the major N source (A, D), scenarios when the subsurface nitrate fluxes are limited or absent (B, E), and scenarios with isotopic composition of particulate organic matter (phytoplankton) measured in this study (C, F). Arrows represent only flux direction.

Chapter 4. General conclusions

- My results denote the importance of N_2 fixation supporting the food web in the GM, especially during the summer months and within ACEs due the strong stratification prevent or limited the fluxes of subsurface nitrate.
- During the winter, higher $\delta^{15}N$ values of zooplankton and the mixing model results indicated that 60% of the N assimilated by zooplankton derived from subsurface nitrate due the deeper mixing layer depth supported by the northern winds call “nortes”.
- My findings indicate that mesoscale eddies play a more important role driving the spatial variation in N sources than regional patterns, due to mesoscale modify the water column structure limiting or promoting the fluxes of subsurface nitrate to the euphotic layer. Also, the differences between regions were limited.
- Although I consider that the estimates of source contributions based on zooplankton groups (copepods and euphausiids) is not directly comparable to those based on size fractions (SF and LF), a specific study centered on a comparison of bulk and CSIA-AA $\delta^{15}N$ values of dominant copepods or euphausiids species with known feeding habits (preferably herbivores or filter feeders), the small size fraction we analyzed, and the isotopic composition of POM could help define the extent of the coupling between food web components, and further support their use as indicators of oceanic nitrogen sources.
- Based on Bayesian isotope mixing model, my results indicate that the regional sources contributions strongly controls the isotopic baseline and therefore zooplankton isotope nitrogen values during the XIXIMI-06/GOMECC-3 cruises.
- The low $\delta^{15}N$ values of zooplankton (1-3‰) was indicative of N source with low $\delta^{15}N$ values, and the Bayesian isotope mixing model indicated the N_2 fixation was the most important source that supported secondary production during summer 2017, with a mean contribution of 45-74%, only excluding the coastal northern Gulf of Mexico region.

- On the other hand, the highest $\delta^{15}\text{N}$ values of zooplankton (8-11‰) found in the coastal northern Gulf of Mexico has been supported mainly by denitrified N and the mixing model estimated an average of 60% but raised up 80% in the inner stations. Despite the MARS is the major source of terrestrial organic matter and nutrient inputs in the northern Gulf of Mexico, the estimates were low with an average of 17% for the northern Gulf of Mexico, including the coastal area.
- Although low $\delta^{15}\text{N}$ values of POM could be result of remineralization process, the lower $\delta^{15}\text{N}$ values of POM (-2 to 0‰), especially in the western Gulf of Mexico, where the N_2 fixation has been reported in the deep water region, emphasize and support that N_2 fixation as the important N source in the Gulf of Mexico.
- Under scenarios 2 and 3, the Bayesian isotope mixing model was used lower $\delta^{15}\text{N}\text{-NO}_3$ values that increases the estimates of subsurface nitrate compared with N_2 fixation. Despite that, the N_2 fixation had a moderate contribution between 37 to 53% in all regions.

Literature cited

- Aldeco, J., Monreal-Gómez, M. A., Signoret, M., Salas-de León, D. A., and Hernández-Becerril, D. U. 2009. Occurrence of a subsurface anticyclonic eddy, fronts, and *Trichodesmium* spp. over the Campeche Canyon Region, Gulf of Mexico. *Ciencias Marinas*, **35**, 333–344.
- Alexander, R. B., Smith, R. A., Schwarz, G. E., Boyer, E. W., Nolan, J. V., and Brakebill, J. W. 2008. Differences in phosphorus and nitrogen delivery to the Gulf of Mexico from the Mississippi River Basin. *Environmental Science & Technology*, **42**(3), 822–830. <https://doi.org/10.1021/es0716103>
- Altabet, M. A. 2005. Isotopic Tracers of the Marine Nitrogen Cycle: Present and Past. In *Marine Organic Matter: Biomarkers, Isotopes and DNA*. Springer, Berlin, Heidelberg. **2**, 251–293. https://doi.org/10.1007/698_2_008
- Anderson, W. T. and Fourqurean, J. W. 2003. Intra- and interannual variability in seagrass carbon and nitrogen stable isotopes from south Florida, a preliminary study. *Organic Geochemistry*, **34**, 185–194.
- Bănanu, D., Carlotti, F., Barani, A., Grégori, G., Neffati, N., and Harmelin-Vivien, M. 2014. Seasonal variation of stable isotope ratios of size-fractionated zooplankton in the Bay of Marseille (NW Mediterranean Sea). *Journal of Plankton Research*, **36**, 145–156.
- Benedetti, F., Gasparini, S., and Ayata, S. D. 2016. Identifying copepod functional groups from species functional traits. *Journal of Plankton Research*, **38**, 159–166.
- Berman-Frank, I., Bidle, K. D., Haramaty, L., and Falkowski, P. G. 2004. The demise of the marine cyanobacterium, *Trichodesmium* spp., via an autocatalyzed cell death pathway. *Limnology and Oceanography*, **49**, 997–1005.
- Berthelot, H., Bonnet, S., Grosso, O., Cornet, V., and Barani, A. 2016. Transfer of diazotroph-derived nitrogen towards non-diazotrophic planktonic communities: A comparative study between *Trichodesmium erythraeum*, *Crocospaera watsonii* and *Cyanothece* sp. *Biogeosciences*, **13**, 4005–4021.
- Biggs, D. C. 1992. Nutrients, plankton, and productivity in a warm-core ring in the western Gulf of Mexico. *Journal of Geophysical Research*, **97**, 2143–2154.
- Biggs, D. C., Fargion, G. S., Hamilton, P., and Leben, R. R. 1996. Cleavage of a Gulf of Mexico Loop Current eddy by a deep water cyclone. *Journal of Geophysical Research, C: Oceans*, **101**, 20629–20641.
- Biggs, D.C., and Ressler, P.H. 2001. Distribution and abundance of phytoplankton, zooplankton, ichthyoplankton, and micronekton in the deepwater Gulf of Mexico. *Gulf of Mexico Science*, **1**, 7–29.

- Bianchi, T. S., DiMarco, S. F., Cowan, J. H., Hetland, R. D., Chapman, P., Day, J. W., and Allison, M. A. 2010. The science of hypoxia in the northern Gulf of Mexico: A review. *Science of the Total Environment*, 408(7), 1471–1484. <https://doi.org/10.1016/j.scitotenv.2009.11.047>
- Bianchi, T. S., Wysocki, L. A., Stewart, M., Filley, T. R., and McKee, B. A. 2007. Temporal variability in terrestrially-derived sources of particulate organic carbon in the lower Mississippi River and its upper tributaries. *Geochimica et Cosmochimica Acta*, 71(18), 4425–4437. <https://doi.org/10.1016/j.gca.2007.07.011>
- Bombar, D., Paerl, R. W., and Riemann, L. 2016. Marine Non-Cyanobacterial Diazotrophs: Moving beyond Molecular Detection. *Trends in Microbiology*, 24, 916–927.
- Bonnet, S., Baklouti, M., Gimenez, A., Berthelot, H., and Berman-Frank, I. 2016a. Biogeochemical and biological impacts of diazotroph blooms in a low-nutrient, low-chlorophyll ecosystem: synthesis from the VAHINE mesocosm experiment (New Caledonia). *Biogeosciences*, 13, 4461–4479.
- Bonnet, S., Berthelot, H., Turk-Kubo, K., Cornet-Barthaux, V., Fawcett, S., Berman-Frank, I., ... and Capone, D. G. 2016. Diazotroph derived nitrogen supports diatom growth in the South West Pacific: A quantitative study using nanoSIMS. *Limnology and Oceanography*, 61(5), 1549-1562.
- Boxshall, G.A., Halsey, S.H. 2004. An Introduction to Copepod Diversity. Ray Society Monographs. 166, 966.
- Brault, E. K., Koch, P. L., McMahon, K. W., Broach, K. H., Rosenfield, A. P., Sauthoff, W., ... Smith, W. O. 2018. Carbon and nitrogen zooplankton isoscapes in West Antarctica reflect oceanographic transitions. *Marine Ecology Progress Series*, 593(April), 29–45. <https://doi.org/10.3354/meps12524>
- Brinton, E., M. D. Ohman. A. W. Townsend, M. D. Knight and Bridgeman, A. L. 2000. Euphausiids of the World Ocean (cd-room Expert System). Springer-Verlag.
- Bryantmason, A., Xu, Y. J., and Altabet, M. 2013. Isotopic signature of nitrate in river waters of the lower Mississippi and its tributary, the Atchafalaya. *Hydrological Processes*, 27(19), 2840–2850. <https://doi.org/10.1002/hyp.9420>
- Cai, Y., Guo, L., Wang, X., and Aiken, G. 2015. Abundance, stable isotopic composition, and export fluxes of DOC, POC, and DIC from the Lower Mississippi River during 2006-2008. *Journal of Geophysical Research G: Biogeosciences*, 120(11), 2273–2288. <https://doi.org/10.1002/2015JG003139>
- Cai, Y., Guo, L., Wang, X., Mojzic, A. K., and Redalje, D. G. 2012. The source and distribution of dissolved and particulate organic matter in the Bay of St. Louis, northern Gulf of Mexico. *Estuarine, Coastal and Shelf Science*, 96(1), 96–104. <https://doi.org/10.1016/j.ecss.2011.10.017>
- Callejas-Jimenez, M., Santamaria-del-Angel, E., Gonzalez-Silvera, A., Millan-Nuñez, R., and Cajal-Medrano, R. 2012. Dynamic Regionalization of the Gulf of Mexico based on normalized radiances (nLw) derived from MODIS-Aqua. *Continental Shelf Research*, 37(February 2012), 8–14. <https://doi.org/10.1016/j.csr.2012.01.014>

- Capone, D. G., Burns, J. A., Montoya, J. P., Subramaniam, A., Mahaffey, C., Gunderson, T., Michaels A F. and Carpenter E. J. 2005. Nitrogen fixation by *Trichodesmium* spp.: An important source of new nitrogen to the tropical and subtropical North Atlantic Ocean. *Global Biogeochemical Cycles*, 19, 1–17.
- Capone, D. G., Subramaniam, A., Montoya, J. P., Voss, M., Humborg, C., Johansen, A. M., ... Carpenter, E. J. 1998. An extensive bloom of the N₂-fixing Cyanobacterium *trichodesmium erythraeum* in the central Arabian Sea. *Marine Ecology Progress Series*, 172, 281–292. <https://doi.org/10.3354/meps172281>
- Casey, J. R., Lomas, M. W., Mandecki, J., and Walker, D. E. 2007. *Prochlorococcus* contributes to new production in the Sargasso Sea deep chlorophyll maximum. *Geophysical Research Letters*., 34, 1–5.
- Carpenter, E. J., Harvey, H. R., Brian, F., and Capone, D. G. 1997. Biogeochemical tracers of the marine cyanobacterium *Trichodesmium*. *Deep-Sea Research Part I: Oceanographic Research Papers*, 44(1), 27–38. [https://doi.org/10.1016/S0967-0637\(96\)00091-X](https://doi.org/10.1016/S0967-0637(96)00091-X)
- Carpenter, E., Montoya, J., Burns, J., Mulholland, M., Subramaniam, A., and Capone, D. 1999. Extensive bloom of a N₂-fixing diatom/cyanobacterial association in the tropical Atlantic Ocean. *Marine Ecology Progress Series*, 185(1977), 273–283. <https://doi.org/10.3354/meps185273>
- Castellanos, I. A., and Gasca, R. 1999. Epipelagic euphausiids (Euphausiacea) and spring mesoscale features in the Gulf of Mexico. *Crustaceana*, 72, 391-404.
- Cervantes-Díaz, G. Y., Hernández-Ayón, J. M., Zirino, A., Herzka, S. Z., Camacho-Ibar, V., Norzagaray, O., ... and Delgado, J. A. 2022. Understanding upper water mass dynamics in the Gulf of Mexico by linking physical and biogeochemical features. *Journal of Marine Systems*, 225, 103647.
- Chambers, D. P., Wahr, J., and Nerem, R. S. 2004. Preliminary observations of global ocean mass variations with GRACE. *Geophysical Research Letters*., 31, 1–4.
- Chang, C. C. Y., Kendall, C., Silva, S. R., Battaglin, W. A., and Campbell, D. H. 2002. Nitrate stable isotopes: Tools for determining nitrate sources among different land uses in the Mississippi River Basin. *Canadian Journal of Fisheries and Aquatic Sciences*, 59(12), 1874–1885. <https://doi.org/10.1139/f02-153>
- Chanton, J. P. and Lewis, F. G. 1999. Plankton and Dissolved Inorganic Carbon Isotopic Composition in a River-Dominated Estuary: Apalachicola Bay, Florida. *Estuaries*, 22(3), 575. <https://doi.org/10.2307/1353045>
- Chen, M., Kim, D., Liu, H., and Kang, C. K. 2018. Variability in copepod trophic levels and feeding selectivity based on stable isotope analysis in Gwangyang Bay of the southern coast of the Korean Peninsula. *Biogeosciences*, 15(7), 2055-2073.

- Conroy, B. J., Steinberg, D. K., Song, B., Kalmbach, A., Carpenter, E. J., and Foster, R. A. 2017. Mesozooplankton graze on cyanobacteria in the Amazon River plume and western tropical North Atlantic. *Frontiers in Microbiology*, 8, 1–15.
- Damien, P., Pasqueron de Fommervault, O., Sheinbaum, J., Jouanno, J., Camacho-Ibar, V. F., and Duteil, O. 2018. Partitioning of the Open Waters of the Gulf of Mexico Based on the Seasonal and Interannual Variability of Chlorophyll Concentration. *Journal of Geophysical Research, C: Oceans.*, 123, 2592–2614.
- Daudén-Bengoá, G., Jiménez-Rosenberg, S. P. A., Compaire, J. C., del Pilar Echeverri-García, L., Pérez-Brunius, P., and Herzka, S. Z. 2020. Larval fish assemblages of myctophids in the deep water region of the southern Gulf of Mexico linked to oceanographic conditions. *Deep Sea Research Part I: Oceanographic Research Papers*, 155, 103181.
- Davenport, S. R. and Bax, N. J. 2002. A trophic study of a marine ecosystem off southeastern Australia using stable isotopes of carbon and nitrogen. *Canadian Journal of Fisheries and Aquatic Sciences*, 59, 514–530.
- Dickey-Collas, M., Gowen, R. J., and Fox, C. J. 1996. Distribution of larval and juvenile fish in the western Irish Sea: Relationship to phytoplankton, zooplankton biomass and recurrent physical features. *Oceanographic Literature Review*, 47, 169–181.
- Del Castillo, C. E., Coble, P. G., Conmy, R. N., Müller-Karger, F. E., Vanderbloemen, L., and Vargo, G. A. 2001. Multispectral in situ measurements of organic matter and chlorophyll fluorescence in seawater: Documenting the intrusion of the Mississippi River plume in the West Florida Shelf. *Limnology and Oceanography*, 46(7), 1836–1843. <https://doi.org/10.4319/lo.2001.46.7.1836>
- Dorado, S., Rooker, J. R., Wissel, B., and Quigg, A. 2012. Isotope baseline shifts in pelagic food webs of the Gulf of Mexico. *Marine Ecology Progress Series*, 464, 37–49.
- Durán-Campos, E., Salas-de-León, D. A., Monreal-Gómez, M. A., and Coria-Monter, E. 2017. Patterns of chlorophyll-a distribution linked to mesoscale structures in two contrasting areas Campeche Canyon and Bank, Southern Gulf of Mexico. *Journal of Sea Research*, 123, 30–38.
- El-Sabaawi, R., Trudel, M., and Mazumder, A. 2013. Zooplankton stable isotopes as integrators of bottom-up variability in coastal margins: A case study from the Strait of Georgia and adjacent coastal regions. *Progress in Oceanography*, 115, 76–89.
- Elliott, D. T., Pierson, J. J., and Roman, M. R. 2012. Relationship between environmental conditions and zooplankton community structure during summer hypoxia in the northern Gulf of Mexico. *Journal of Plankton Research*, 34, 602–613.
- Figueiredo, G. G. A. A. de, Schwamborn, R., Bertrand, A., Munaron, J. M., and Le Loc'h, F. 2020. Body size and stable isotope composition of zooplankton in the western tropical Atlantic. *Journal of Marine Systems*, 212, 103449.

- Fry, B., and Sherr, E. B. 1989. $\delta^{13}\text{C}$ measurements as indicators of carbon flow in marine and freshwater ecosystems. *Stable isotopes in ecological research*, 196-229.
- Gaona-Hernández, A. 2019. Estructura de la comunidad de copépodos calanoides en dos zonas contrastantes del golfo de México, en función de condiciones oceanográficas. Master's Thesis. Centro de Investigación Científica y de Educación Superior de Ensenada, Baja California.
- García-Sanz, T., Ruiz, J. M., Pérez, M., and Ruiz, M. 2011. Assessment of dissolved nutrients dispersal derived from offshore fish-farm using nitrogen stable isotope ratios ($\delta^{15}\text{N}$) in macroalgal bioassays. *Estuarine, Coastal and Shelf Science*, 91, 361–370.
- Gasca, R., Castellanos, I., and Biggs, D. C. 2001. Euphausiids (Crustacea, Euphausiacea) and summer mesoscale features in the Gulf of Mexico. *Bulletin of Marine Science*, 68, 397-408.
- Gorbatenko, K. M., Lazhentsev, A. E., and Kiyashko, S. I. 2015. Seasonal dynamics of the trophic status of zooplankton in the Sea of Okhotsk (based on data from stable carbon- and nitrogen-isotope analysis). *Russian Journal of Marine Biology*, 40, 519–531.
- Gordon, L. I., Jennings Jr, J. C., Ross, A. A., and Krest, J. M. 1993. A suggested protocol for continuous flow automated analysis of seawater nutrients (phosphate, nitrate, nitrite and silicic acid) in the WOCE Hydrographic Program and the Joint Global Ocean Fluxes Study. WOCE Hydrographic Program Office, Methods Manual WHPO, (68/91), 1-52.
- Gorokhova, E., and Hansson, S. 1999. An experimental study on variations in stable carbon and nitrogen isotope fractionation during growth of *Mysis mixta* and *Neomysis integer*. *Canadian Journal of Fisheries and Aquatic Sciences*, 56(11), 2203–2210. <https://doi.org/10.1139/f99-149>
- Gurney, L. J., Froneman, P. W., Pakhomov, E. A., and McQuaid, C. D. 2001. Trophic positions of three euphausiid species from the Prince Edward Islands (Southern Ocean): Implications for the pelagic food web structure. *Marine Ecology Progress Series*, 217, 167–174.
- Hamilton, P., Leben, R., Bower, A., Furey, H., and Pérez-Brunius, P. 2018. Hydrography of the Gulf of Mexico using autonomous floats. *Journal of Physical Oceanography*, 48, 773–794.
- Hannides, C. C. S., Popp, B. N., Anela Choy, C., and Drazen, J. C. 2013. Midwater zooplankton and suspended particle dynamics in the North Pacific Subtropical Gyre: A stable isotope perspective. *Limnology and Oceanography*, 58, 1931–1946.
- Hawser, S. P., O'Neil, J. M., Roman, M. R., and Codd, G. A. 1992. Toxicity of blooms of the cyanobacterium *Trichodesmium* to zooplankton. *Journal of Applied Phycology*, 4, 79–86.
- Henschke, N., Everett, J. D., Suthers, I. M., Smith, J. A., Hunt, B. P. V. V, Doblin, M. A., and Taylor, M. D. 2015. Zooplankton trophic niches respond to different water types of the western Tasman Sea: A stable isotope analysis. *Deep Sea Research Part I: Oceanographic Research Papers*, 104, 1–8.

- Hernández-Sánchez, O. G., Camacho-Ibar, V. F., Fernández Álamo, M. A., and Herzka, S. Z. 2022. Nitrogen sources (NO_3^- vs N_2 fixation) inferred from bulk $\delta^{15}\text{N}$ values of zooplankton from the deep water region of the Gulf of Mexico. *Journal of Plankton Research*.
- Herzka, S. Z. 2021. Comunidades marinas. In S. Z. Herzka, Zaragoza Álvarez, R. A., Peters, E.M. and Hernández-Cárdenas, G. (Coordinators) Atlas de línea base ambiental del golfo de México (Tomo III, segunda parte), México: Consorcio de Investigación del Golfo de México. pp. 1-209.
- Heaton, T. H. E. 1986. Isotopic studies of nitrogen pollution in the hydrosphere and atmosphere: A review. *Chemical Geology: Isotope Geoscience Section*, 59(C), 87–102. [https://doi.org/10.1016/0168-9622\(86\)90059-X](https://doi.org/10.1016/0168-9622(86)90059-X)
- Henschke, N., Everett, J. D., Suthers, I. M., Smith, J. A., Hunt, B. P. V. V, Doblin, M. A., and Taylor, M. D. 2015. Zooplankton trophic niches respond to different water types of the western Tasman Sea: A stable isotope analysis. *Deep-Sea Research Part I: Oceanographic Research Papers*, 104, 1–8. <https://doi.org/10.1016/j.dsr.2015.06.010>
- Holl, C. M., Villareal, T. A., Payne, C. D., Clayton, T. D., Hart, C., and Montoya, J. P. 2007. *Trichodesmium* in the western Gulf of Mexico: stable isotope evidence. 52, 2249–2259.
- Hopkins, T. L. 1982. The vertical distribution of zooplankton in the eastern Gulf of Mexico. *Deep Sea Research Part A. Oceanographic Research Papers*, 29, 1069–1083.
- Hou, W., Gu, B., Zhang, H., Gu, J., and Han, B. P. 2013. The relationship between carbon and nitrogen stable isotopes of zooplankton and select environmental variables in low-latitude reservoirs. *Limnology*, 14, 97–104.
- Howe, S., Miranda, C., Hayes, C. T., Letscher, R. T., and Knapp, A. N. 2020. The Dual Isotopic Composition of Nitrate in the Gulf of Mexico and Florida Straits. *Journal of Geophysical Research, C: Oceans.*, 125, 1–17.
- Huang, P. Q., Lu, Y. Z., and Zhou, S. Q. 2018. An objective method for determining ocean mixed layer depth with applications to WOCE data. *Journal of Atmospheric and Oceanic Technology.*, 35, 441–458.
- Hunt, B. P. V., Bonnet, S., Berthelot, H., Conroy, B. J., Rachel, A. F., and Pagano, M. 2016. Contribution and pathways of diazotroph-derived nitrogen to zooplankton during the VAHINE mesocosm experiment in the oligotrophic New Caledonia lagoon. *Biogeosciences*, 13, 3131–3145.
- Hydes, D., Aoyama, M., Aminot, A., Bakker, K., Becker, S., Coverly, S....and Zhang, J. 2010. Determination of dissolved nutrients (N, P, Si) in seawater with high precision and inter-comparability using gas-segmented continuous flow analysers. In The GO-SHIP repeat hydrography manual: A collection of expert reports and guidelines (IOCCP Report 14, ICPO Publication Series 134). UNESCO-IOC, Paris, France. Retrieved from www.go-ship.org/HydroMan.htm

- Jouanno, J., Pallàs-Sanz, E., and Sheinbaum, J. (2018). Variability and Dynamics of the Yucatan Upwelling: High-Resolution Simulations. *Journal of Geophysical Research: Oceans*, 123(2), 1251–1262. <https://doi.org/10.1002/2017JC013535>
- Kelly, T. B., Knapp, A. N., Landry, M. R., Selph, K. E., Shropshire, T. A., Thomas, R. K., and Stukel, M. R. (2021). Supplemental - Lateral advection supports nitrogen export in the oligotrophic open-ocean Gulf of Mexico. *Nature Communications*, 12(1). <https://doi.org/10.1038/s41467-021-23678-9>
- Kinsey, S. T. and Hopkins, T. L. 1994. Trophic strategies of euphausiids in a low-latitude ecosystem. *Marine Biology*, 118, 651–661.
- Klein, P. and Lapeyre, G. 2009. The Oceanic Vertical Pump Induced by Mesoscale and Submesoscale Turbulence. *Annual review of marine science*, 1, 351–375.
- Knapp, A. N., Thomas, R. K., Stukel, M. R., Kelly, T. B., Landry, M. R., Selph, K. E., ... Lamkin, J. 2021. Constraining the sources of nitrogen fueling export production in the Gulf of Mexico using nitrogen isotope budgets. *Journal of Plankton Research*, 1–19. <https://doi.org/10.1093/plankt/fbab049>
- Knapp, A. N., McCabe, K. M., Grosso, O., Leblond, N., Moutin, T., and Bonnet, S. 2018. Distribution and rates of nitrogen fixation in the western tropical South Pacific Ocean constrained by nitrogen isotope budgets. *Biogeosciences*, 15, 2619–2628.
- Knapp, A. N., DiFiore, P. J., Deutsch, C., Sigman, D. M., and Lipschultz, F. 2008. Nitrate isotopic composition between Bermuda and Puerto Rico: Implications for N₂ fixation in the Atlantic Ocean. *Global Biogeochemical Cycles*, 22, 1–14.
- Knapp, A. N., Sigman, D. M., and Lipschultz, F. 2005. N isotopic composition of dissolved organic nitrogen and nitrate at the Bermuda Atlantic Time-series study site. *Global Biogeochemical Cycles*, 19, 1–15.
- Kurle, C. M., and McWhorter, J. K. 2017. Spatial and temporal variability within marine isoscapes: Implications for interpreting stable isotope data from marine systems. *Marine Ecology Progress Series*, 568, 31–45. <https://doi.org/10.3354/meps12045>
- Kürten, B., Painting, S. J., Struck, U., Polunin, N. V. C., and Middelburg, J. J. 2013. Tracking seasonal changes in North Sea zooplankton trophic dynamics using stable isotopes. *Biogeochemistry*, 113(1–3), 167–187. <https://doi.org/10.1007/s10533-011-9630-y>
- Kürten, B., Al-Aidaros, A. M., Kürten, S., El-Sherbiny, M. M., Devassy, R. P., Struck, U., ... and Sommer, U. 2016. Carbon and nitrogen stable isotope ratios of pelagic zooplankton elucidate ecohydrographic features in the oligotrophic Red Sea. *Progress in Oceanography*, 140, 69–90.
- Lamb, K., and Swart, P. K. 2008. The carbon and nitrogen isotopic values of particulate organic material from the Florida Keys: A temporal and spatial study. *Coral Reefs*, 27(2), 351–362. <https://doi.org/10.1007/s00338-007-0336-5>

- Landrum, J. P., Altabet, M. A., and Montoya, J. P. 2011. Basin-scale distributions of stable nitrogen isotopes in the subtropical North Atlantic Ocean: Contribution of diazotroph nitrogen to particulate organic matter and mesozooplankton. *Deep Sea Research Part I: Oceanographic Research Papers.*, 58, 615–625.
- Layman, C. A., Araujo, M. S., Boucek, R., Hammerschlag-Peyer, C. M., Harrison, E., Jud, Z. R., ... Bearhop, S. 2012. Applying stable isotopes to examine food-web structure: An overview of analytical tools. *Biological Reviews*, 87(3), 545–562. <https://doi.org/10.1111/j.1469-185X.2011.00208.x>
- Le-Alvarado, M., Romo-Curiel, A. E., Sosa-Nishizaki, O., Hernández-Sánchez, O., Barbero, L., and Herzka, S. Z. 2021. Yellowfin tuna (*Thunnus albacares*) foraging habitat and trophic position in the Gulf of Mexico based on intrinsic isotope tracers. *PLoS one*, 16, e0246082.
- Ledford, T. C., Mortazavi, B., Tatariw, C., and Mason, O. U. 2020. Elevated nutrient inputs to marshes differentially impact carbon and nitrogen cycling in two northern Gulf of Mexico saltmarsh plants. *Biogeochemistry*, 149(1), 1–16. <https://doi.org/10.1007/s10533-020-00656-9>
- Lenes, J. M., and Heil, C. A. 2010. A historical analysis of the potential nutrient supply from the N₂ fixing marine cyanobacterium *Trichodesmium spp.* to *Karenia brevis* blooms in the eastern Gulf of Mexico. *Journal of plankton research*, 32(10), 1421–1431.
- Lévy, M. 2008. The modulation of biological production by oceanic mesoscale turbulence. *Lecture Notes in Physics*. Springer Berlin Heidelberg, 1, 219–261.
- Linacre, L., Lara-Lara, R., Camacho-Ibar, V., Herguera, J. C., Bazán-Guzmán, C., and Ferreira-Bartrina, V. 2015. Distribution pattern of picoplankton carbon biomass linked to mesoscale dynamics in the southern gulf of Mexico during winter conditions. *Deep Sea Research Part I: Oceanographic Research Papers*, 106, 55–67.
- Loick-Wilde, N., Fernández-Urruzola, I., Eglite, E., Liskow, I., Nausch, M., Schulz-Bull, D., ... and Mohrholz, V. 2019. Stratification, nitrogen fixation, and cyanobacterial bloom stage regulate the planktonic food web structure. *Global change biology*, 25(3), 794–810.
- Lorrain, A., Graham, B. S., Popp, B. N., Allain, V., Olson, R. J., Hunt, B. P. V., ... Ménard, F. 2015. Nitrogen isotopic baselines and implications for estimating foraging habitat and trophic position of yellowfin tuna in the Indian and Pacific Oceans. *Deep-Sea Research Part II: Topical Studies in Oceanography*, 113, 188–198. <https://doi.org/10.1016/j.dsr2.2014.02.003>
- Macko, S. A., Entzeroth, L., and Parker, P. L. 1984. Regional differences in nitrogen and carbon isotopes on the continental shelf of the Gulf of Mexico. *Naturwissenschaften*, 71, 374–375.
- Marconi, D., Alexandra Weigand, M., Rafter, P. A., McIlvin, M. R., Forbes, M., Casciotti, K. L., and Sigman, D. M. 2015. Nitrate isotope distributions on the US GEOTRACES North Atlantic cross-basin section: Signals of polar nitrate sources and low latitude nitrogen cycling. *Marine Chemistry*, 177, 143–156. <https://doi.org/10.1016/j.marchem.2015.06.007>

- Marconi, D., Sigman, D. M., Casciotti, K. L., Campbell, E. C., Alexandra Weigand, M., Fawcett, S. E., ... Haug, G. H. 2017. Tropical Dominance of N₂ Fixation in the North Atlantic Ocean. *Global Biogeochemical Cycles*, 31(10), 1608–1623. <https://doi.org/10.1002/2016GB005613>
- Martinetto, P., Teichberg, M., and Valiela, I. 2006. Coupling of estuarine benthic and pelagic food webs to land-derived nitrogen sources in Waquoit Bay, Massachusetts, USA. *Marine Ecology Progress Series*, 307, 37–48.
- Martinez, M. A., Hereu, C. M., Arteaga, M. C., Jiménez-Rosenberg, S., Herzka, S. Z., Saavedra-Flores, A., ... and Galindo-Sánchez, C. E. 2021. Epipelagic zooplankton diversity in the deep water region of the Gulf of Mexico: a metabarcoding survey. *ICES Journal of Marine Science*.
- Martínez-López, B. and Zavala-Hidalgo, J. 2009. Seasonal and interannual variability of cross-shelf transports of chlorophyll in the Gulf of Mexico. *Journal of Marine Systems*, 77, 1–20.
- Martinez-Perez, C., Mohr, W., Löscher, C. R., Dekaezemacker, J., Littmann, S., Yilmaz, P., ... and Kuypers, M. M. 2016. The small unicellular diazotrophic symbiont, UCYN-A, is a key player in the marine nitrogen cycle. *Nature Microbiology*, 1(11), 1-7.
- Mateos-Jasso, A., Zavala-Hidalgo, J., Romero-Centeno, R., and Allende-Arandía, M. E. 2012. Variability of the thermohaline structure in the northern Veracruz Coral Reef System, Mexico. *Continental Shelf Research*, 50–51, 30–40. <https://doi.org/10.1016/j.csr.2012.10.001>
- Mauchline, J. and Fisher, L. R. 1969. The Biology of Euphausiids. *Advances in Marine Biology*. 7, 1-454.
- McCarthy, M. J., Newell, S. E., Carini, S. A., and Gardner, W. S. 2015. Denitrification Dominates Sediment Nitrogen Removal and Is Enhanced by Bottom-Water Hypoxia in the Northern Gulf of Mexico. *Estuaries and Coasts*, 38(6), 2279–2294. <https://doi.org/10.1007/s12237-015-9964-0>
- McClelland, J. W., Holl, C. M., and Montoya, J. P. 2003. Relating low $\delta^{15}\text{N}$ values of zooplankton to N₂-fixation in the tropical North Atlantic: Insights provided by stable isotope ratios of amino acids. *Deep Sea Research Part I: Oceanographic Research Papers*, 50, 849–861.
- McClelland, J. W. and Montoya, J. P. 2002. Trophic relationships and the nitrogen isotopic composition of amino acids in plankton. *Ecology*, 83, 2173–2180.
- McCutchan, J. H., Lewis, W. M., Kendall, C., and McGrath, C. C. 2003. Variation in trophic shift for stable isotope ratios of carbon, nitrogen, and sulfur. *Oikos*, 102(2), 378–390. <https://doi.org/10.1034/j.1600-0706.2003.12098.x>
- McMahon, K. W., and McCarthy, M. D. 2016. Embracing variability in amino acid $\delta^{15}\text{N}$ fractionation: mechanisms, implications, and applications for trophic ecology. *Ecosphere*, 7, e01511
- McMahon, K. W., Hamady, L. L., and Thorrold, S. R. 2013. A review of ecogeochemistry approaches to estimating movements of marine animals. *Limnology and Oceanography*, 58(2), 697–714. <https://doi.org/10.4319/lo.2013.58.2.0697>

- Merino, M. 1997. Upwelling on the Yucatan Shelf: Hydrographic evidence. *Journal of Marine Systems*, 13(1–4), 101–121. [https://doi.org/10.1016/S0924-7963\(96\)00123-6](https://doi.org/10.1016/S0924-7963(96)00123-6)
- Moisander, P. H., Zhang, R., Boyle, E. A., Hewson, I., Montoya, J. P., and Zehr, J. P. 2012. Analogous nutrient limitations in unicellular diazotrophs and *Prochlorococcus* in the South Pacific Ocean. *ISME Journal*, 6, 733–744.
- Mompeán, C., Bode, A., Latasa, M., Fernández-Castro, B., Mouriño-Carballido, B., and Irigoien, X. 2016. The influence of nitrogen inputs on biomass and trophic structure of ocean plankton: A study using biomass and stable isotope size-spectra. *Journal of Plankton Research*, 38, 1163–1177.
- Moncreiff, C., and Sullivan, M. 2001. Trophic importance of epiphytic algae in subtropical seagrass beds: evidence from multiple stable isotope analyses. *Marine Ecology Progress Series*, 215, 93–106. <https://doi.org/10.3354/meps215093>
- Montoya, J. P., Voss, M., and Capone, D. G. 2007. Spatial variation in N₂-fixation rate and diazotroph activity in the Tropical Atlantic. *Biogeosciences*, 4(3), 369–376. <https://doi.org/10.5194/bg-4-369-2007>
- Montoya, J. P., Carpenter, E. J., and Capone, D. G. 2002. Nitrogen fixation and nitrogen isotope abundances in zooplankton of the oligotrophic North Atlantic. *Limnology and Oceanography*, 47, 1617–1628.
- Mulholland, M. R., Bernhardt, P. W., Ozmon, I., Procise, L. A., Garrett, M., O’Neil, J. M., ... Bronk, D. A. 2014. Contribution of diazotrophy to nitrogen inputs supporting *Karenia brevis* blooms in the Gulf of Mexico. *Harmful Algae*, 38(C), 20–29. <https://doi.org/10.1016/j.hal.2014.04.004>
- Mulholland, Margaret R., Bernhardt, P. W., Heil, C. A., Bronk, D. A., and O’Neil, J. M. 2006. Nitrogen fixation and release of fixed nitrogen by *Trichodesmium spp.* in the Gulf of Mexico. *Limnology and Oceanography*, 51, 1762–1776.
- Mulholland, M R, Heil, C. A., Bronk, D. A., O’Neil, J. M., and Bernhardt, P. 2004. Does nitrogen regeneration from the N₂ fixing cyanobacteria *Trichodesmium spp.* fuel *Karenia brevis* blooms in the Gulf of Mexico? *Harmful Algae*, 47–49.
- Muller-Karger, F. E., Smith, J. P., Werner, S., Chen, R., Roffer, M., Liu, Y., ... and Enfield, D. B. 2015. Natural variability of surface oceanographic conditions in the offshore Gulf of Mexico. *Progress in Oceanography*, 134, 54-76.
- Muller-Karger, F. E., Walsh, J. J., Evans, R. H., and Meyers, M. B. 1991. On the seasonal phytoplankton concentration and sea surface temperature cycles of the Gulf of Mexico as determined by satellites. *Journal of Geophysical Research*, 96, 12,645-12,665.
- O’Neil, J. M. and Roman, M. R. 1994. Ingestion of the cyanobacterium *Trichodesmium spp.* by pelagic harpacticoid copepods *Macrosetella*, *Miracia* and *Oculosetella*. *Hydrobiologia*, 292–293, 235–240.

- Oey, L. Y., Ezer, T., and Lee, H. C. 2013. Loop Current, rings and related circulation in the Gulf of Mexico: A review of numerical models and future challenges. *Circulation in the Gulf of Mexico: Observations and Models*, 161, 31–56.
- Ohkouchi, N., Ogawa, N. O., Chikaraishi, Y., Tanaka, H., and Wada, E. 2015. Biochemical and physiological bases for the use of carbon and nitrogen isotopes in environmental and ecological studies. *Progress in Earth and Planetary Science*, 2(1), 1–17. <https://doi.org/10.1186/s40645-015-0032-y>
- Olson, R. J., Popp, B. N., Graham, B. S., López-Ibarra, G. A., Galván-Magaña, F., Lennert-Cody, C. E., ... and Fry, B. 2010. Food-web inferences of stable isotope spatial patterns in copepods and yellowfin tuna in the pelagic eastern Pacific Ocean. *Progress in Oceanography*, 86(1-2), 124-138.
- Ortner, P. B., Hill, L. C., and Cummings, S. R. 1989. Zooplankton community structure and copepod species composition in the northern Gulf of Mexico. *Continental Shelf Research*, 9, 387–402.
- Orcutt, K. M., Lipschultz, F., Gundersen, K., Arimoto, R., Michaels, A. F., Knap, A. H., and Gallon, J. R. 2001. A seasonal study of the significance of N₂ fixation by *Trichodesmium spp.* at the Bermuda Atlantic Time-series Study (BATS) site. *Deep Sea Research Part II: Topical Studies in Oceanography*, 48(8-9), 1583-1608.
- Otis, D. B., Le Hénaff, M., Kourafalou, V. H., McEachron, L., and Muller-Karger, F. E. 2019. Mississippi River and Campeche Bank (Gulf of Mexico) episodes of cross-shelf export of coastal waters observed with satellites. *Remote Sensing*, 11(6), 1–14. <https://doi.org/10.3390/RS11060723>
- Parnell, A. C., Inger, R., Bearhop, S., and Jackson, A. L. 2010. Source partitioning using stable isotopes: Coping with too much variation. *PLoS One*, 5, 1–5.
- Pasqueron De Fommervault, O., Pérez-Brunius, P., Damien, P., Camacho-Ibar, V. F., and Sheinbaum, J. 2017. Temporal variability of chlorophyll distribution in the Gulf of Mexico: Bio-optical data from profiling floats. *Biogeosciences*, 14, 5647–5662.
- Pérez-Brunius, P., García-Carrillo, P., Dubranna, J., Sheinbaum, J., and Candela, J. 2013. Direct observations of the upper layer circulation in the southern Gulf of Mexico. *Deep Sea Research Part II: Topical Studies in Oceanography*, 85, 182–194.
- Perry, R. I., Thompson, P. A., Mackas, D. L., Harrison, P. J., and Yelland, D. R. 1999. Stable carbon isotopes as pelagic food web tracers in adjacent shelf and slope regions off British Columbia, Canada. *Canadian Journal of Fisheries and Aquatic Sciences*, 56(12), 2477–2486. <https://doi.org/10.1139/f99-194>
- Phillips, D. L., Inger, R., Bearhop, S., Jackson, A. L., Moore, J. W., Parnell, A. C., ... Ward, E. J. 2014. Best practices for use of stable isotope mixing models in food-web studies. *Canadian Journal of Zoology*, 92(10), 823–835. <https://doi.org/10.1139/cjz-2014-0127>
- Post, D. M. 2002. Using stable isotopes to estimate trophic position: Models, methods, and assumptions. *Ecology*, 83(3), 703–718.

- Rabalais, N. N., Turner, R. E., and Wiseman, W. J. 2001. Hypoxia in the Gulf of Mexico. *Journal of Environmental Quality*, 30(2), 320–329. <https://doi.org/10.2134/jeq2001.302320x>
- Rabalais, N. N., Turner, R. E., and Wiseman, W. J. 2002. Gulf of Mexico hypoxia, a.k.a. “The dead zone.” *Annual Review of Ecology and Systematics*, 33, 235–263. <https://doi.org/10.1146/annurev.ecolsys.33.010802.150513>
- Raes, E., Waite, A., McInnes, A., Olsen, H., Nguyen, H., Hardman-Mountford, N., and Thompson, P. 2014. Changes in latitude and dominant diazotrophic community alter N₂ fixation. *Marine Ecology Progress Series*, 516, 85–102.
- Reyes-Mendoza, O., Mariño-Tapia, I., Herrera-Silveira, J., Ruiz-Martínez, G., Enriquez, C., and Largier, J. L. 2016. The Effects of Wind on Upwelling off Cabo Catoche. *Journal of Coastal Research*, 32(3), 638–650. <https://doi.org/10.2112/JCOASTRES-D-15-00043.1>
- Roger, C. 1994. The plankton of the tropical western Indian ocean as a biomass indirectly supporting surface tunas (yellowfin, *Thunnus albacares* and skipjack, *Katsuwonus pelamis*). *Environmental Biology of Fishes*, 39, 161–172.
- Rooker, J. R., Turner, J. P., and Holt, S. A. 2006. Trophic ecology of Sargassum-associated fishes in the Gulf of Mexico determined from stable isotopes and fatty acids. *Marine Ecology Progress Series*, 313, 249–259.
- Salas-de-León, D. A., Monreal-Gómez, M. A., Signoret, M., and Aldeco, J. 2004. Anticyclonic-cyclonic eddies and their impact on near-surface chlorophyll stocks and oxygen supersaturation over the Campeche Canyon, Gulf of Mexico. *Journal of Geophysical Research, C: Oceans*, 109, 1–10.
- Salmerón-garcía, O. and Zavala-Hidalgo, J. 2011. Regionalization of the Gulf of Mexico from space-time chlorophyll- a concentration variability. *Ocean Dynamics*, 63, 439–448.
- Schiller, R. V., Kourafalou, V. H., Hogan, P., and Walker, N. D. 2011. The dynamics of the Mississippi River plume: Impact of topography, wind and offshore forcing on the fate of plume waters. *Journal of Geophysical Research*, 116(C6), C06029. <https://doi.org/10.1029/2010JC006883>
- Schmidt, K., McClelland, J. W., Mente, E., Montoya, J. P., Atkinson, A., and Voss, M. 2004. Trophic-level interpretation based on $\delta^{15}\text{N}$ values: Implications of tissue-specific fractionation and amino acid composition. *Marine Ecology Progress Series*, 266, 43–58. <https://doi.org/10.3354/meps266043>
- Schwamborn, R., and Giarrizzo, T. 2015. Stable Isotope Discrimination by Consumers in a Tropical Mangrove Food Web: How Important Are Variations in C/N Ratio? *Estuaries and Coasts*, 38, 813–825.
- Seki, M. P., Polovina, J. J., Brainard, R. E., Bidigare, R. R., Leonard, C. L., and Foley, D. G. 2001. Biological enhancement at cyclonic eddies tracked with GOES thermal imagery in Hawaiian waters. *Geophysical Research Letters*, 28, 1583–1586.

- Selph, K., Swalethorp, R., R Stukel, M., B Kelly, T., N Knapp, A., Fleming, K., ... R Landry, M. 2021. Phytoplankton community composition and biomass in the oligotrophic Gulf of Mexico. *Journal of Plankton Research*, 1–20. <https://doi.org/10.1093/plankt/fbab006>
- Sepúlveda-Lozada, A., Mendoza-Carranza, M., Wolff, M., Saint-Paul, U., and Ponce-Mendoza, A. 2015. Differences in food web structure of mangroves and freshwater marshes: evidence from stable isotope studies in the Southern Gulf of Mexico. *Wetlands Ecology and Management*, 23(2), 293–314. <https://doi.org/10.1007/s11273-014-9382-2>
- Siegel, D. A., McGillicuddy, D. J., and Fields, E. A. 1999. Mesoscale eddies, satellite altimetry, and new production in the Sargasso Sea. *Journal of Geophysical Research, C: Oceans*, 104, 13359–13379.
- Sigman, D. M., Altabet, M. A., McCorkle, D. C., Francois, R., and Fischer, G. 2000. The $\delta^{15}\text{N}$ of nitrate in the Southern Ocean: Nitrogen cycling and circulation in the ocean interior. *Journal of Geophysical Research, C: Oceans*, 105, 19599–19614.
- Sigman, D. M. and Casciotti, K. L. 2001. Nitrogen Isotopes in the Ocean. *Encyclopedia of Ocean Sciences*. Elsevier, 1997. 1884–1894.
- Sigman, D. M., and Fripiat, F. 2019. Nitrogen isotopes in the ocean. *Encyclopedia of Ocean Sciences*, (September 2018), 263–278. <https://doi.org/10.1016/B978-0-12-409548-9.11605-7>
- Somes, C. J., Schmittner, A., Galbraith, E. D., Lehmann, M. F., Altabet, M. A., Montoya, J. P., ... Eby, M. 2010. Simulating the global distribution of nitrogen isotopes in the ocean. *Global Biogeochemical Cycles*, 24(4), 1–16. <https://doi.org/10.1029/2009GB003767>
- Sogawa, S., Sugisaki, H., Tadokoro, K., Ono, T., Sato, E., Shimode, S., and Kikuchi, T. 2017. Feeding habits of six species of euphausiids (Decapoda: Euphausiacea) in the northwestern Pacific Ocean determined by carbon and nitrogen stable isotope ratios. *The Journal of Crustacean Biology.*, 37, 29–36.
- Steinberg, D. K. and Landry, M. R. 2017. Zooplankton and the Ocean Carbon Cycle. *Ann. Annual review of marine science*, 9, 413–444.
- Stock, B. C., Jackson, A. L., Ward, E. J., Parnell, A. C., Phillips, D. L., and Semmens, B. X. 2018. Analyzing mixing systems using a new generation of Bayesian tracer mixing models. *PeerJ*, 6, 1–27. <https://doi.org/10.7717/peerj.5096>
- Strzelecki, J., Koslow, J. A., and Waite, A. 2007. Comparison of mesozooplankton communities from a pair of warm- and cold-core eddies off the coast of Western Australia. *Deep Sea Research Part II: Topical Studies in Oceanography*, 54, 1103–1112.
- Sturges, W. and Leben, R. 2000. Frequency of ring separations from the Loop Current in the Gulf of Mexico: A revised estimate. *Journal of Physical Oceanography*, 30, 1814–1819.

- Suarez-Morales, E., and Lopez-Salgado, I. 1998. Copepod assemblages in surface waters of the western Gulf of Mexico. *Crustaceana*, 71(3), 312-330.
- Tang, W. and Cassar, N. 2019. Data-Driven Modeling of the Distribution of Diazotrophs in the Global *Geophysical Research Letters*, 46, 12258–12269.
- Troina, G. C., Dehairs, F., Botta, S., Tullio, J. C. Di, Elskens, M., and Secchi, E. R. 2020. Zooplankton-based $\delta^{13}\text{C}$ and $\delta^{15}\text{N}$ isoscapes from the outer continental shelf and slope in the subtropical western South Atlantic. *Deep Sea Research Part I: Oceanographic Research Papers*, 159, 103235. <https://doi.org/10.1016/j.dsr.2020.103235>
- Turner, R. E., and Rabalais, N. N. 2019. The Gulf of Mexico. In *World seas: An environmental evaluation* (pp. 445-464). Academic Press.
- Turner, J. T. 2015. Zooplankton fecal pellets, marine snow, phytodetritus and the ocean's biological pump. *Progress in Oceanography*, 130, 205–248.
- Turner, J. T. 2004. The Importance of Small Planktonic Copepods and Their Roles in Pelagic Marine Food *Zoological studies*, 43, 255–266.
- Ursella, L., Pensieri, S., Pallàs-Sanz, E., Herzka, S. Z., Bozzano, R., Tenreiro, M., ... and Sheinbaum, J. 2021. Diel, lunar and seasonal vertical migration in the deep western Gulf of Mexico evidenced from a long-term data series of acoustic backscatter. *Progress in Oceanography*, 195, 102562.
- Vanderklift, M. A. and Ponsard, S. 2003. Sources of variation in consumer-diet $\delta^{15}\text{N}$ enrichment: A meta-analysis. *Oecologia*, 136, 169–182.
- Venkataramana, V., Anilkumar, N., Naik, R. K., Mishra, R. K., and Sabu, P. 2019. Temperature and phytoplankton size class biomass drives the zooplankton food web dynamics in the Indian Ocean sector of the Southern Ocean. *Polar Biology*, 42, 823–829.
- Waite, A. M., Muhling, B. A., Holl, C. M., Beckley, L. E., Montoya, J. P., Strzelecki, J., Thomposn P. A., Pesant, S. 2007. Food web structure in two counter-rotating eddies based on $\delta^{15}\text{N}$ and $\delta^{13}\text{C}$ isotopic analyses. *Deep Sea Research Part II: Topical Studies in Oceanography*, 54, 1055–1075.
- Waite, A. M., Raes, E., Beckley, L. E., Thompson, P. A., Griffin, D., Saunders, M., ... and Jeffs, A. 2019. Production and ecosystem structure in cold-core vs. warm-core eddies: Implications for the zooplankton isoscape and rock lobster larvae. *Limnology and Oceanography*, 64(6), 2405-2423..
- Walker, N. D., Wiseman, W. J., Rouse, L. J., and Babin, A. 2005. Effects of River Discharge, Wind Stress, and Slope Eddies on Circulation and the Satellite-Observed Structure of the Mississippi River Plume. *Journal of Coastal Research*, 216(216), 1228–1244. <https://doi.org/10.2112/04-0347.1>
- Walsh, B. M. and O'Neil, J. M. 2014. Zooplankton community composition and copepod grazing on the West Florida Shelf in relation to blooms of *Karenia brevis*. *Harmful Algae*, 38, 63–72.

- Wells, R. J. D., Rooker, J. R., Quigg, A., and Wissel, B. 2017. Influence of mesoscale oceanographic features on pelagic food webs in the Gulf of Mexico. *Marine Biology*, 164, 1–11.
- Werner, T., and Buchholz, F. 2013. Diel vertical migration behaviour in Euphausiids of the northern Benguela Current: seasonal adaptations to food availability and strong gradients of temperature and oxygen. *Journal of Plankton Research*, 35, 792–812.
- Wissel, B., and Fry, B. 2003. Sources of Particulate Organic Matter in the Mississippi River, USA. *Large Rivers*, 15(1–4), 105–118. <https://doi.org/10.1127/lr/15/2003/105>
- Wissel, B., and Fry, B. 2005. Tracing Mississippi River influences in estuarine food webs of coastal Louisiana. *Oecologia*, 144(4), 659–672. <https://doi.org/10.1007/s00442-005-0119-z>
- Wormuth, J. H., Ressler, P. H., Cady, R. B., and Harris, E. J. 2000. Zooplankton and micronekton in cyclones and anticyclones in the northeast Gulf of Mexico. *Gulf of Mexico Science*, 18, 23–34.
- Yang, G., Li, C., Guilini, K., Wang, X., and Wang, Y. 2017. Regional patterns of $\delta^{13}\text{C}$ and $\delta^{15}\text{N}$ stable isotopes of size-fractionated zooplankton in the western tropical North Pacific Ocean. *Deep Sea Research Part I: Oceanographic Research Papers*, 120, 39–47.
- Zavala-García, F., Flores-Coto, C., and Espinosa-Fuentes, M. de la L. 2016. Relación entre la biomasa zooplanctónica y las descargas de aguas continentales, en el sur del Golfo de México (1984-2001). *Revista de Biología Marina Y Oceanografía*, 51(1), 21–31. <https://doi.org/10.4067/S0718-19572016000100003>
- Zavala-Hidalgo, J., Morey, S. L., O'Brien, J. J., and Zamudio, L. 2006. On the Loop Current eddy shedding variability. *Atmosfera*, 19, 41–48.
- Zavala-Hidalgo, Jorge, Morey, S. L., and O'Brien, J. J. 2003. Seasonal circulation on the western shelf of the Gulf of Mexico using a high-resolution numerical model. *Journal of Geophysical Research, C: Oceans*, 108, 1–19.
- Zehr, J. P. and Capone, D. G. 2020. Changing perspectives in marine nitrogen fixation. *Science*, 368, 729. 1–9.
- Zhang, X., Song, T., Liu, D., Keesing, J., K., Gong, Jun. 2015. Macroalgal blooms favor heterotrophic diazotrophic bacteria in nitrogen-rich and phosphorus-limited coastal surface waters in the Yellow Sea. *Estuaries and Coastal Shelf Sciences*, 163, 75–81.
- Zimmerman, R. A. and Biggs, D. C. 1999. Patterns of distribution of sound-scattering zooplankton in warm- and cold-core eddies in the Gulf of Mexico, from a narrowband acoustic Doppler current profiler survey. *Journal of Geophysical Research, C: Oceans*, 104, 5251–5262.

Supplementary material

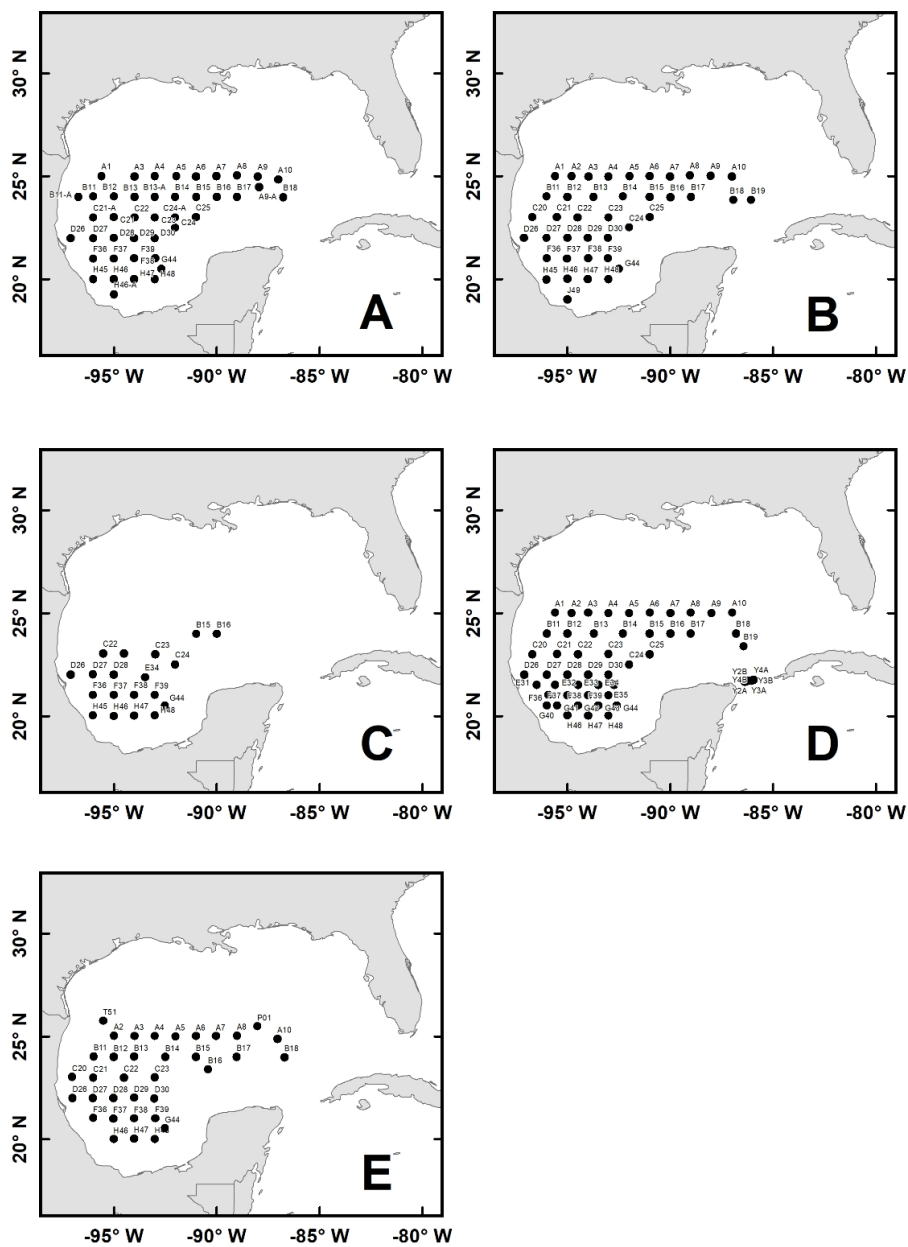


Figure 17. Sampling stations for zooplankton, NO_3^- concentration sampling and CTD cast are indicated by black dots. A) XIXIMI-01, November 2010; B) XIXIMI-02, July 2011; C) XIXIMI-03, Feb-Mar 2013; D) XIXIMI-04, August 2015; E) XIXIMI-05, July 2016. CTD data was no available for XIXIMI-01 due to equipment malfunction. All stations are at depths > 1000m, except for some in the Yucatan Channel.

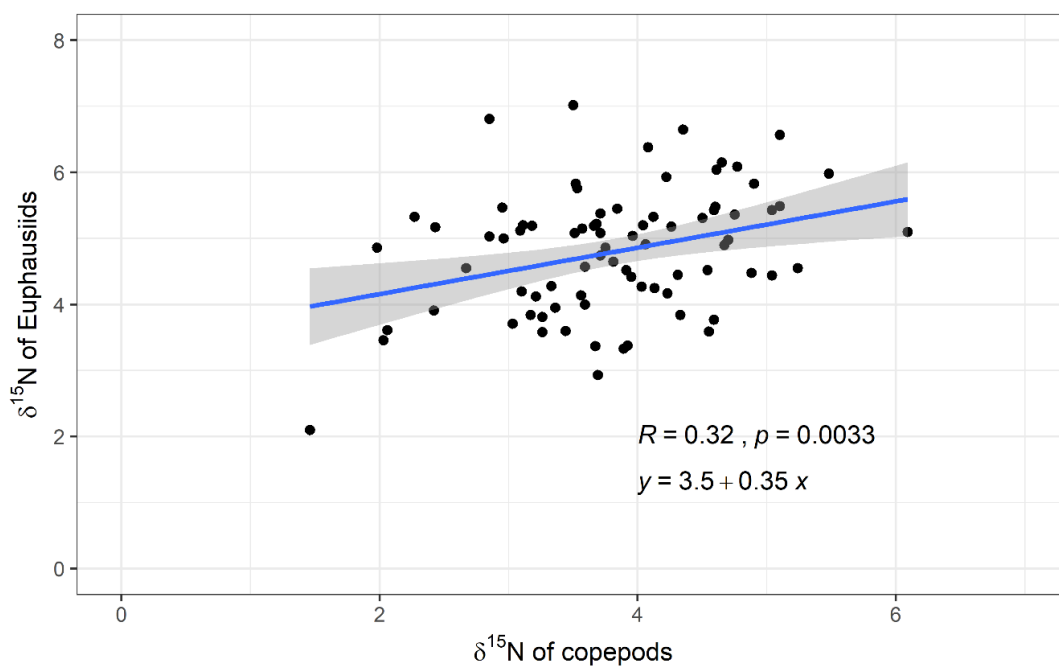


Figure 18. Pearson's correlation between the isotopic composition (in ‰) of copepods and euphausiids for XIXIMI-01, -02 and -03.

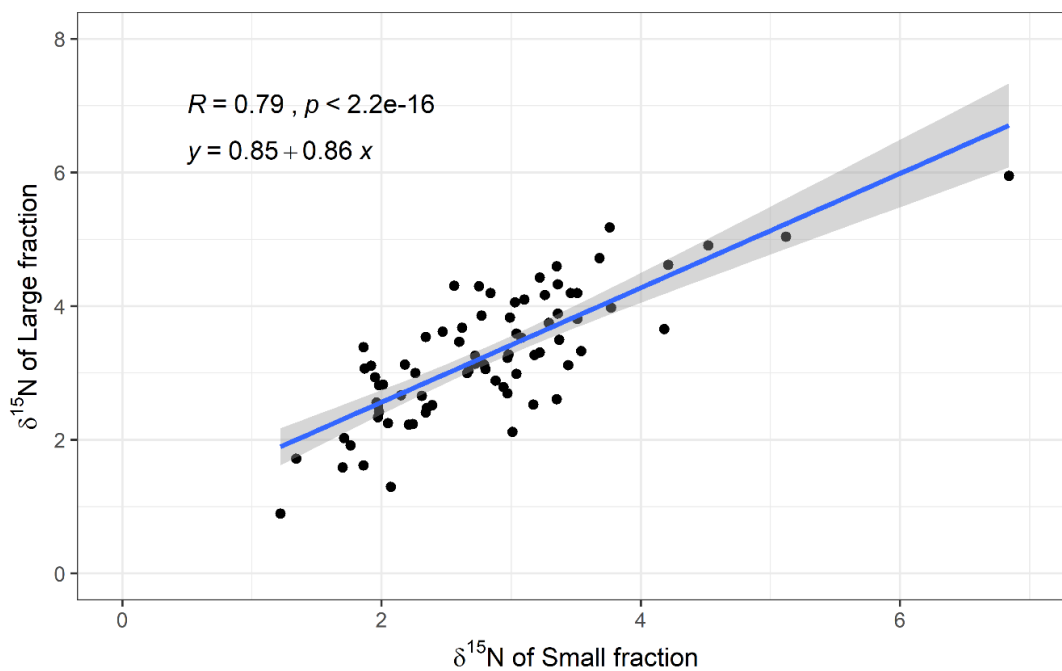


Figure 19. Pearson's correlation between isotopic composition (in ‰) of small and large fraction for XIXIMI-04 and -05.

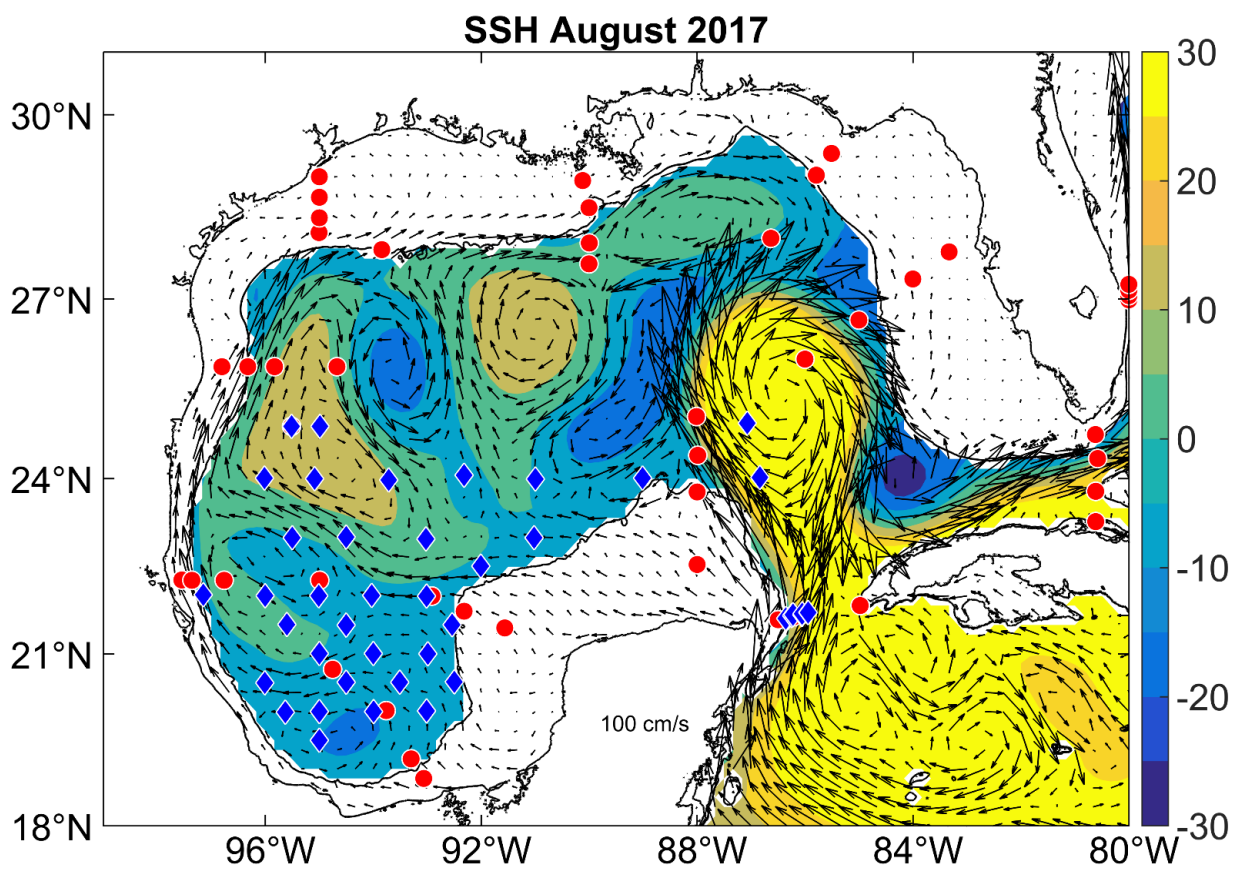


Figure 20. SSHA for August 2017. The red circles and blue diamonds represents the GOMECC-3 and XIXIMI-06 station samples, respectively. Black line represents 200 m isobath. Arrows represent geostrophic velocities.

Table 6. Summary of published stable isotope values of end members used for zooplankton in the upper water column.

Sample	$\delta^{15}\text{N}$ (‰)	SD	Source
<i>Richelia / Hemiaulus</i>	-1.4	0.2	Carpenter <i>et al.</i> , 1999
<i>Trichodesmium</i>	-1.7	0.5	Carpenter <i>et al.</i> , 1999
<i>Trichodesmium</i>	-2 to -1		Holl <i>et al.</i> , 2007
<i>Trichodesmium</i>	-0.7	0.6	Dorado <i>et al.</i> , 2012
<i>Trichodesmium</i>	-1.7	0.4	McClelland <i>et al.</i> , 2003
	-1.3	0.6	Average \pm SD applied in mixing model
NO_3^-	4.8	0.2	Sigman <i>et al.</i> 2000
NO_3^-	5.0	0.5	Knapp <i>et al.</i> 2005
NO_3^-	5.3	0.6	Knapp <i>et al.</i> 2008
NO_3^-	5.0	0.5	Howe <i>et al.</i> 2020
	5.0	0.2	Average \pm SD applied in mixing model

Table 7. Published trophic enrichment factors (TEF) used for zooplankton.

Source	TEF (‰)
Henschke <i>et al.</i> , 2015	1.6
Schwamborn and Giarrizzo, 2015	2.3
McCutchan <i>et al.</i> , 2003	2.2
Vanderklift and Ponsard, 2003	2.1
Average used in this study	2.0 \pm 0.5

Table 8. Mean \pm standard deviations (SD) of $\delta^{15}\text{N}$ values of zooplankton sampled during five cruises that covered the deep water region of the Gulf of Mexico. Ranges presented in parentheses. The n represents the number of stations covered in each cruise.

Cruise	Group	n	Mean \pm SD (‰)
XIXIMI-01 (Nov 2010)	Copepods	35	3.8 \pm 1.1 (1.5-6.4)
	Euphausiids	33	5.0 \pm 1.1 (2.1-7.3)
XIXIMI-02 (Jul 2011)	Copepods	33	3.7 \pm 0.9 (1.9-6.1)
	Euphausiids	34	4.6 \pm 0.9 (2.9-6.8)
XIXIMI-03 (Feb-Mar 2013)	Copepods	21	4.3 \pm 0.6 (3.4-5.5)
	Euphausiids	19	5.0 \pm 0.7 (3.6-6.1)
XIXIMI-04 (Aug 2015)	<1000 μm	45	2.7 \pm 0.7 (1.4-4.5)
	1000-2000 μm	45	3.1 \pm 0.9 (1.3-4.9)
XIXIMI-05 (Jul 2016)	<1000 μm	33	2.9 \pm 1.0 (1.2-6.8)
	1000-2000 μm	33	3.5\pm1.0 (0.9-6.0)

Table 9. Mean \pm standard deviation (SD) of $\delta^{15}\text{N}$ values of copepods, euphausiids, and the small fraction and large size fractions of zooplankton caught within anticyclonic eddies, cyclonic eddies, or outside of eddies during the XIXIMI-02, -03, -04 and -05 cruises in the deep water region of the Gulf of Mexico. The n represents the number of stations (and hence zooplankton samples) classified to each feature. The range of values are reported within parenthesis.

Zooplankton group	ANTICYCLONIC EDDIES		CYCLONIC EDDIES		NO EDDIES	
	n	Mean \pm SD (‰)	n	Mean \pm SD (‰)	n	Mean \pm SD (‰)
Copepods	8	3.5 \pm 1.3 (2.0-6.1)	13	4.7 \pm 0.6 (3.5-5.3)	33	3.9 \pm 0.6 (2.9-5.5)
Euphausiids	8	4.2 \pm 0.7 (3.5-5.1)	14	5.1 \pm 0.6 (4.3-6.1)	31	4.8 \pm 0.9 (2.9-6.1)

Size fraction	ANTICYCLONIC EDDIES		CYCLONIC EDDIES		NO EDDIES	
	n	Mean \pm SD (‰)	n	Mean \pm SD (‰)	n	Mean \pm SD (‰)
Small (<1000 μm)	18	2.1 \pm 0.5 (1.2-2.7)	18	3.3 \pm 0.5 (2.4-4.5)	42	2.9 \pm 0.9 (1.8-6.8)
Large (1000-2000 μm)	18	2.5 \pm 0.9 (0.9-4.3)	18	3.9 \pm 0.7 (0.9-4.9)	42	3.5 \pm 0.9 (1.9-5.9)

Table 10. Results of two-way ANOVAs of $\delta^{15}\text{N}$ values of copepods and euphausiids collected during XIXIMI cruises. ACE: Anticyclonic eddy, CE: Cyclonic eddy, NE: non-eddy.

	F-value	p	Post-hoc test
Copepods			
Mesoscale feature (ACE, CE, NE)	10.63	5.48X10⁻⁰⁵	ACE \neq CE; ACE \neq NE; CE \neq NE
Cruise	10.29	0.000681	XIX-02 \neq XIX-03
Cruise * Mesoscale feature	3.54	0.000863	X2:ACE \neq X2:CE; X2:ACE \neq X2:NE; X2:CE \neq X2:NE; X2:ACE \neq X3:CE; X2:ACE \neq X3:NE; X2:ACE \neq X3:NE
Euphausiids			
Mesoscale feature (ACE, CE, NE)	3.625	0.0353	ACE \neq CE; ACE \neq NE
Cruise	6.062	0.0145	XIX-02 \neq XIX-03
Cruise * Mesoscale feature	0.086	0.9846	N.S.
Small size fraction (<1000 μm)			
Mesoscale feature (ACE, CE, NE)	18.393	5.11x10⁻⁰⁷	ACE \neq CE; ACE \neq NE; CE \neq NE
Cruise	0.261	0.611	N.S.
Cruise * Mesoscale feature	1.691	0.193	N.S.
Large size fraction (1000-2000 μm)			
Mesoscale feature (ACE, CE, NE)	10.591	0.000108	ACE \neq CE; ACE \neq NE
Cruise	0.590	0.445	N.S.
Cruise * Mesoscale feature	0.38	0.612	N.S.

Table 11. Mean \pm standard deviation (SD), minimum and maximum $\delta^{15}\text{N}$ values of copepods, euphausiids, small (<1000 μm) and large (1000-2000 μm) size fractions of zooplankton caught in the central Gulf of Mexico and the Bay of Campeche during the XIXIMI-01, -02, -03, -04 and -05 cruises in the deepwater region of the Gulf of Mexico. Samples were collected in the Yucatan Channel only during XIXIMI-04 and -05.

Zooplankton group	Central region		Bay of Campeche	
	n	Mean \pm SD (range) (‰)	n	Mean \pm SD (range) (‰)
Copepods	29	3.7 \pm 0.9 (2.0-5.5)	22	4.2 \pm 0.8 (2.9-6.1)
Euphausiids	29	4.7 \pm 0.9 (3.4-6.6)	22	4.8 \pm 0.9 (2.9-6.8)

Size fraction	Central region		Bay of Campeche		Yucatan Channel	
	n	Mean \pm SD (range) (‰)	n	Mean \pm SD (range) (‰)	n	Mean \pm SD (range) (‰)
Small (<1000 μm)	38	2.8 \pm 1.0 (1.2-6.8)	34	3.0 \pm 0.6 (1.8-4.5)	6	2.2 \pm 0.3 (1.7-2.6)
Large (1000-2000 μm)	38	3.2 \pm 1.1 (0.9-6.0)	34	3.5 \pm 0.8 (1.2-4.9)	6	3.0 \pm 0.8 (2.0-4.3)

Table 12. Stable isotopes values for POM in the Gulf of Mexico collected at the euphotic layer

Literature	Source	$\delta^{13}\text{C}$ (‰)	$\delta^{15}\text{N}$ (‰)	Study site	Regions
Bianchi et al. (2007)	POM	-25.0 ± 0.8	6.8 ± 1.4	Mississippi River at Baton Rouge	NGMc and NGMo
Wissell and fry (2003)	POM	-24.9 ± 1.4	7.1 ± 1.4	Mississippi River at Baton Rouge	
Chanton and Lewis (1999)	Phytoplankton	-22.4 ± 0.2	6.6 ± 0.7	NGM Shelf	
Rooker et al. (2006)	POM	-20.9 ± 0.8	7.1 ± 1.1	North GM	
Macko et al. (1984)	POM	-21.0 ± 1.4	7.5 ± 0.8	LATEX Shelf	
	Mean	-22.8 ± 1.8	7.0 ± 0.3		
Moncreiff and Sullivan (2001)	Phytoplankton	-21.8 ± 0.7	9.9 ± 0.9	NGM shelf	NGMc and NGMo
Chanton and Lewis (1999)	Phytoplankton	-26.8 ± 2.3	9.6 ± 1.2	Apalachicola Bay	
	Mean	-24.3 ± 2.5	9.8 ± 0.2		
Holl et al. (2007)	POM	-23.3 ± 1.6	-2.3 ± 1.4	West GoM	All regions
Dorado et al. (2012)	POM	-17.1 ± 0.6	0.5 ± 0.8	NGM	
Wells and Rooker. (2009)	POM	-21.5 ± 0.6	2.8 ± 0.7	NGM	
	Mean	-18.1 ± 3.9	-1.2 ± 1.2		
Dorado et al. (2012)	POM	-22.1 ± 1.5	4.0 ± 0.3	NGM	All regions
	Mean	-22.1 ± 1.15	$4.0 \pm 0.3\%$		
Radabaugh et al. (2013)	POM	-23.4 ± 1.1	5.4 ± 1.5	West Florida shelf	NGMc and NGMo
Gu et al. (2001)	POM	-28.7 ± 4.0		West Florida shelf	
	Mean	-26.1 ± 2.7	5.4 ± 1.5		
Sepúlveda-Lozada et al. (2015)	POM	-24.4 ± 2.8	4.6 ± 0.5	Grijalva-Usumacinta River	SGM
	Mean	-24.4 ± 2.8	4.6 ± 0.5		

Table 13. Mean and SD Isotope ratios of carbon and nitrogen of particulate organic matter collected during XIXIMI-06 cruise at different depths

	Central Gulf of Mexico			Southern Gulf of Mexico			Loop Current		
	Mean (SD)	Range	n	Mean (SD)	Range	n	Mean (SD)	Range	n
$\delta^{13}\text{C-POM}$	-23.3 ± 1.0	-25.3 to -22.3	12	-22.9 ± 0.9	-24.9 to -21.4	19	-23.0 ± 1.3	-24.6 to -21.3	3
$\delta^{15}\text{N-POM}$	-0.1 ± 1.2	-1.8 to 3.0	4	0.4 ± 1.2	-1.2 to 3.2	12	-0.1 ± 1.2	-1.4 to 1.0	2
$\delta^{15}\text{N-POM}$ surface	2.0 ± 1.9	0.1 to 5.3	7	1.5 ± 1.6	-0.7 to 4.8	19	1.2	1.2	1